BYPASSING BARRIERS: SURFACE-GROUNDWATER EXCHANGE BETWEEN A WETLAND, SANDUR, AND LAVA FIELD IN SOUTHEASTERN ICELAND

AIESHA AGGARWAL

A THESIS SUBMITTED TO

THE FACULTY OF GRADUATE STUDIES

IN PARTIAL FULFILLMENT OF THE REQUIREMENTS

FOR THE DEGREE OF

MASTER OF SCIENCE

GRADUATE PROGRAM IN GEOGRAPHY

YORK UNIVERSITY

TORONTO, ONTARIO

October 2020

ABSTRACT

Iceland is expected to experience slight increases in temperature, precipitation, glacial melt, and volcanic activity over the next century. The influence this will have on groundwater recharge and discharge in spring-fed ecosystems cannot be predicted without a better understanding of spring geological framework and their hydrological regimes. In May 2019, over 50 springs were identified at a sandur-lava field-wetland complex in Southeast Iceland and a subset was selected for further investigation. Spot measurements of water chemistry during the May 2019 field season revealed that the springs discharged cold (4–5°C), slightly acidic (pH 6.1–6.7) freshwater. The acidic pH may point towards interactions with ash/dust deposits. Between May 2019 and September 2019, springs at the study site had relatively stable water levels and temperatures, although heavy rains (> 10 mm) corresponded with increased water level and/or temperatures at some locations. Together, the water level and chemistry data suggest that the springs at the study site are fed by older groundwater from an aquifer that is recharged by precipitation. Spikes in water level indicated that at least one spring at the edge of the sandur also received floodwater and shallow subsurface flows from the glacial-fed Brunná River. Long-term studies will be needed to gain an improved understanding of seasonal spring vulnerability to climate change.

ACKNOWLEGMENTS

I would like to thank my supervisor Dr. Kathy L. Young for her support and guidance throughout my M.Sc. studies at York University. Both Dr. Young and Patrick Mojdehi (Department of Geography Laboratory Technician) introduced me to various methods to measure hydrological and meteorological variables in the field. Patrick Mojdehi also worked with me to ensure that equipment was in working condition for my field season. I would also like to thank Dr. Jennifer Korosi for teaching me freshwater laboratory techniques. I am thankful to Dr. Young, Dr. Korosi, Dr. Tarmo Remmel and Dr. Nirupama Agrawal for their valuable feedback on my thesis.

I am grateful to Filippus Ström Hannesson, Hannes Jónsson, their families and the rest of the Hvoll Guesthouse staff for their immense kindness and hospitality, and for permitting my research at this beautiful location. Thank you to Marc Isabelle, D'Moi Keen and Elizabeth Perera for their assistance in the field and continued friendship and support. During my time in Iceland, I was thankful for the peace of mind brought by knowing that I could reach out to Kristinn Guðjónsson for assistance if anything went wrong.

This research was supported primarily through research funds from Dr. Kathy L. Young, York University Field Research Cost Fund, and the Government of Canada Northern Student Scientific Training Program. I also received financial support through the York University Enbridge Graduate Student Award, York Graduate Scholarship, and various teaching assistant positions at York University. I am grateful to Yvonne Yim for her patience and help in answering my many questions about the application processes. Finally, I would like to thank my family and friends for their love and support throughout my master's studies. Mom, Dad, Jasmin, Tosh, Omi, Kerrie, Hayley, Lauren, Joe, and Marissa, thank you!

TABLE OF CONTENTS

LIST OF TABLES

LIST OF FIGURES

SECTION ONE: INTRODUCTION

1.1 Introduction

Springs are discrete discharge points where groundwater is delivered to the earth's surface (Woo, 2012). These conduits provide a link in the hydrological cycle by bringing groundwater back to the Earth's surface. Spring water is supplied by groundwater, and groundwater is supplied by melt water, surface waters and precipitation. Due to this inter-connected relationship, studies of spring hydrology can provide insight into groundwater recharge patterns and has hydrological (Levy et al., 2015), chemical (Morgenstern et al., 2015) and ecological (Jansson et al., 2007; Fattorini et al., 2016) implications for the downstream systems they feed. Recently, the sensitivity of springs to changes in short and long-term air temperature and precipitation trends has been a topic of interest for studies looking to understand the vulnerability of spring-fed systems to climate change (Burns et al., 2017).

In Iceland, a country that supplies 95% of its household water from groundwater (via springs, boreholes, and wells), springs can be found feeding rivers and wetlands along the edges of young, tertiary basalt lava fields (Kiernan et al., 2003; Kløve et al., 2017) Spring-fed rivers show little seasonal variability, and little response to precipitation or snowmelt (Jónsdóttir & Uvo, 2009) (Figure 1.1). However, predicting the vulnerability of springs is complex, and many variables influence their longevity. While groundwater springs may exhibit little seasonal variation, long-term studies have found that if groundwater is not replenished, springs may be lost completely (Finger et al., 2013; Levy et al., 2015). Between 1987 and 2012, 97% of the surface area previously covered by the groundwater seeps (springs in unconsolidated sediments) became dry in the northern portion of Skeiðarársandur, Iceland - the world's largest glacial outwash plain. Coincident with this loss was an increase in temperature and glacial margin retreat leading to the decoupling of streams from Vatnajökull glacier (Levy et al., 2015). Icelandic glacial loss in 2019 was one of the highest on record (Veðurstofa Íslands et al., 2020).

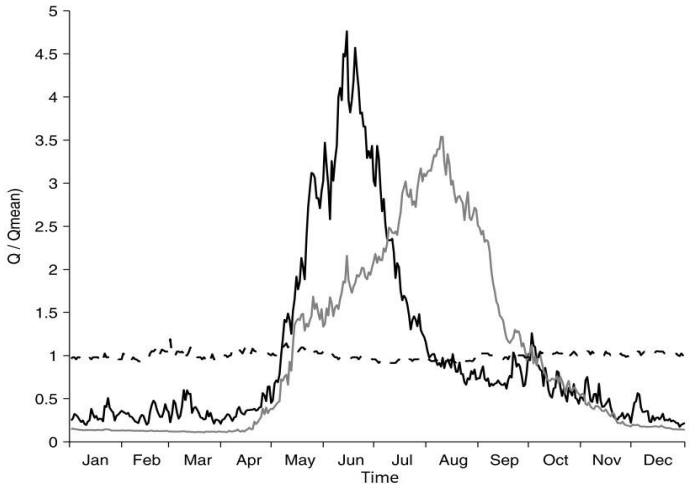

Figure 1.1 Discharge profiles from the runoff river, Fossá (black), glacier fed river, Jökulsá (grey), and spring fed river Brúará (dotted), in Iceland 1945. Modified from Jónsdóttir & Uvo (2009).

Long-term increases in precipitation, annual air temperature, and glacial melt are expected to bring about changes in the hydrology of the landscape (Jóhannesson et al., 2007). The effect that these changes will have on water discharge and chemistry is likely to vary across the landscape. Where some water-bodies, such as glacial fed streams may be lost, springs with reliable discharge may become important in preventing the loss of some wetlands. More immediate changes to the hydrology can be triggered by episodic events. Volcanic eruptions, glacial-outburst floods (jökulhlaup), dust storms, and heavy precipitation events of the near and distant past have had drastic effects on Iceland's hydrology (Old et al., 2005; Scheffel & Young, submitted).

Scheffel & Young (submitted), found that the glacial fed Brunná River, located in Southeast Iceland, experienced an increase in flow during glacial outburst floods (jökulhlaups) and heavy precipitation events. However, water level in adjacent wetland ponds was higher than could be predicted by horizontal Darcian groundwater flow calculations. Springs were suspected to contribute to this difference (Scheffel & Young, submitted). Whether the water supplying these springs came from the highly permeable gravels of the neighbouring Brunná River and Skeiðarársandur or deeper groundwaters flowing beneath the Laki Lava field has implications for the short-term hydrology and long-term longevity of these wetlands.

In 2016 and 2018, multiple springs were observed between where the Brunná River and Skeiðarársandur meet the Laki Lava field and a wetland meadow. This setting provided a unique opportunity to investigate spring discharge regimes in a variety of environments. A total of 13 springs were studied, covering a variety of environments including the edge of a sandur (S1, S2, S3, S4, S5, S6), the center of a grassy wetland (W1, W2, Runoff Spring), the edge between a lava field and wetland (L1, L2, L3), and an oxbow stream (Oxbow Spring).

With changes to groundwater recharge and storage, environments that rely on a balance of hydrological inputs and outputs for their maintenance may be at risk. A better understanding of the sources of water that replenish groundwater stores is required to predict the response of springs to both episodic, seasonal, and long-term events. Short-term fluxes in discharge and water chemistry can provide some insight into these connections.

1.2 Research Objectives

The aim of this study was to determine the role of springs in a sandur-lava field-wetland complex in Southeast Iceland. The objectives were as follows:

1. Identify spring locations, their geometries and subsurface connections in order to predict how they originally formed in the geological framework of the Hvoll farm study site.

2. Determine springs' water quantity, and quality contributions to the sandur-lava field-wetland complex, and;

3. Utilize stable isotopes, hydrograph analysis and water quality changes to assess the effects of hydroclimatic events (i.e. severe weather, jökulhlaups) on spring discharge and source location.

SECTION TWO: LITERATURE REVIEW

2.1 Spring Hydrogeology

Aquifers are saturated below-ground zones that transmit and store more water than the strata that surround them (Woo, 2012). Springs form where water from aquifers are brought to the earth's surface by gravity, hydraulic conductivity, or pressure (Kresic & Stevanovic, 2010). The structure of the aquifer and overlying strata influence how water from the earth's surface is transmitted through the earth to the springs. In Iceland, springs have been found along the edges of basaltic lava fields (Kiernan et al., 2003) and sandar (Robinson et al., 2007; Levy et al., 2015).

Spaces for water flow first form in basaltic rock as the lavas solidify. Such structures include vesicles, lava tubes, tree molds, and columnar joints (Todd, 1980). Secondary porosities such as fractures and fissures may form due to tectonic activity, weathering, and collapse. The permeability of basaltic lavas decreases as they age due to weathering, hydrological activity, structure collapse, and erosion that delivers sediments to fill spaces. Where new lava flows overlay older basaltic rocks, large gaps between the successive flows offer another route for water to travel relatively unimpeded. Alluvial sediments covered by lava flows also offer excellent storage for groundwater (Kiernan et al., 2003). When impounded by rock strata, the water held within aquifers cannot infiltrate further and once saturated, will be forced out of cracks. This is an essential component of many aquifer springs (Mazor, 1990).

Seepage springs can also form in unconsolidated sediments such as those found in sandar. These types of springs have been observed on Skeiðarársandur (Levy et al., 2015). In some springs, discharge may be pushed to the surface by underlying and/or bordering bedrock or a less penetrable layer of material such as clay. Springs with this mechanism of water delivery are classified as barrier or contact springs (Kresic & Stevanovic, 2010).

Springs can be classified based on various properties from their orientation to the intermittency, and chemistry of their waters (Bryan, 1919). Gravity/descending springs discharge in the direction of gravity while rising/ascending springs discharge against it (Figure 2.1). Springs can also form where the

water table meets the surface. Rainfall and snowmelt can raise the water table, forming temporary springs on hillslopes and depressions. Meteoric events can also influence discharge from gravity springs and mesa springs (impervious material with overlying sandstone or lava flows) (Bryan, 1919).

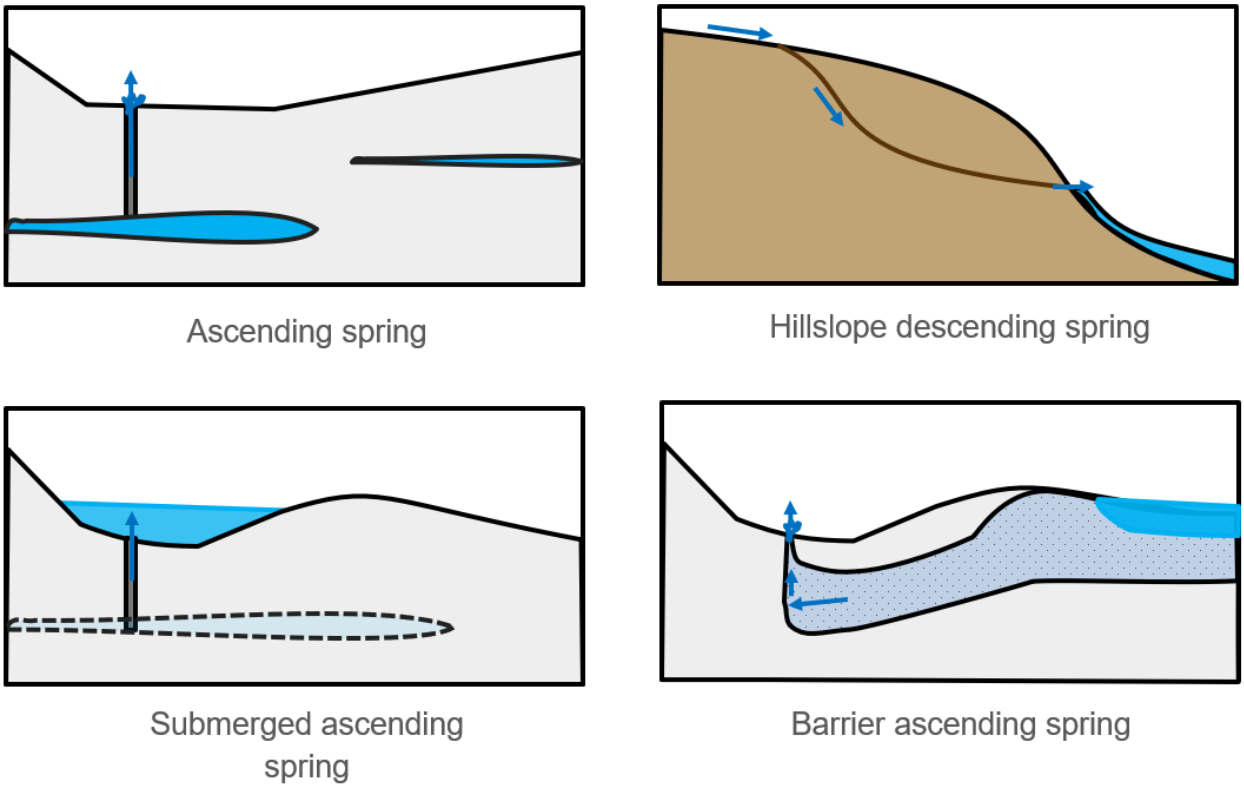

Figure 2.1 Conceptual diagrams of different types of springs and their properties. Blue arrows represent the direction of water flow.

2.2 Hydrological Cycle in Iceland

2.2.1 Groundwater Recharge

In Iceland, groundwater is replenished by precipitation and melt waters that travels over the landscape and percolates through soil and rock into deeper groundwater stores. Recharge of groundwater mostly comes from precipitation in Iceland, as the island has a particularly wet climate (Thien et al., 2015). Other sources of recharge include glacial melt water, snowmelt water, and older surface waters (Figure 2). Some of this water will infiltrate into the ground and become groundwater.

The porosity and composition of the surface of the ground, and layers below will influence the rate and volume of surface water that is able to become groundwater (Faybishenko et al., 2003). Young, tertiary basalts, such as those of the Laki lava field have high permeability (0.086 – 8.6 m/day) as they have many large cracks and voids that water can quickly pass through to reach deeper into the earth (Sigurdsson & Stefansson, 2002). Older Tertiary and quaternary lavas have reduced permeability (4.3×10^{-4} to $^{-6}$ m/day) and a larger portion of precipitation flows off their surface as runoff (Gíslason et al., 1996; Sigurdsson & Stefansson, 2002).

Surface waters that move over sandar are easily exchanged with groundwater through the loose gravels and sediments. Liljedahl et al. (2017) found that for a creek in Delta Junction, Alaska, approximately 41-56% of stream flow was lost to groundwater through the coarse sediments of a glacial stream. Borehole studies of the of the Virkisjökull sandur (63.95° N, -16.84° W), Iceland indicated that the shallow aquifer of loose glacialfluvial sediments or sand, gravel, and cobbles here were at least 15 m deep, and had high transmissivity (median of 600 m^2/day) and hydraulic conductivity (median of 35 m/day). The waters were easily transmitted to lower elevations where springs were found discharging from otherwise dry portions of the sandur (Dochartaigh et al., 2019).

Water chemistry has been used to determine recharge locations with mixed results. The quality of water will change as it interacts with rock and surface waters, dissolving anions, cations, and trace elements. The isotopic composition of the water will also change as water travels along various pathways. Differences in isotopic composition between precipitation and surface waters were identified over 59 years ago (Craig, 1961).Water isotopomers ($^1H_2{}^{16}O$, $^1H^2H^{16}O$, $^1H_2{}^{18}O$) are differentially evaporated, with lower molecular weights evaporating more easily. Fresh rainwater therefore has low ^{18}O and ^2H content compared to older surface water that has experienced evaporation. The chemistry and stable isotope composition will shift towards the chemistry and stable isotope composition of the largest contributing source of recharge (Jefferson et al., 2006).

Both short- and long-term changes in recharge can result in altered spring discharge. Manga (1999) found that basaltic springs at Big Springs and Crystal Lake Springs California experienced a 2-fold decrease in discharge during a 1987 to 1993 drought. Monitoring spring discharge and hydrology of groundwater-fed streams can provide more information about groundwater recharge when the location of recharge areas is not known.

2.2.2 Groundwater Discharge

In Iceland, streams are categorized by their water sources including surface runoff, glacial, and groundwater-fed waters (Kjartansson, 1945). The temperature, volume and timing of groundwater discharge can provide insight into the hydrology and geology of the aquifer. Cold and continuous groundwater flow is an indicator of a deep aquifer with old groundwater. It can take days to years for surface waters to reach these aquifers, so their discharge is unaffected by local changes in temperature and precipitation (Kresic & Stevanovic, 2010). In contrast, springs fed by shallow aquifers with low storage capacity would have a periodicity that is more-strongly linked with groundwater-recharge events such as rainfall and snow melt (McDonnell et al., 2007; Kresic & Stevanovic, 2010) .

Gauging groundwater-fed streams for discharge (volume of water per unit time), is a useful method of monitoring groundwater fluxes in surface waters. Discharge (or water level as a proxy) is then plotted against time, to create a time-series called a hydrograph (Arnold & Allen, 1999). While not as widely utilized, water temperature offers an inexpensive alternative to understanding groundwater fluxes. Stallman (1965) was the first to use temperature as a marker of groundwater in surface streams. Like a hydrograph, temperature can be plotted in a time series called a thermograph. (Anderson, 2005). Precipitation data is commonly displayed along with hydrograph data, as runoff, overland flow and subsurface flows can be initiated and/or enhanced by rainfall.

Various techniques can be used to identify the relative proportions of groundwater and runoff (glacial, snowmelt, and precipitation) contributing to a gauged water feature. Arnold et al. (1995) were

able to mathematically separate baseflow (water contributed by groundwater and high water table flows), from the hydrograph.

Hydrograph separations are commonly supplemented by ^{18}O and ^{2}H, precipitation, discharge, and solute data (McDonnell et al., 2007). One of the first studies to use isotopes tracers to supplement hydrograph data was performed in Quebec by Sklash & Farvolden (1979). Groundwater was found to contribute 60-80% of the discharge during rainfall events across multiple sub-basins. The identification of pre-existing groundwater as a significant source of stormflow was an important discovery. Previously overland flow of rainfall was considered to be the dominant process governing stormflow while groundwater's primary role was in "sustaining streams during low-flow period between rainfall and snow-melt events" (Freeze, 1974).

Hydrographs and thermographs can be displayed with hyetographs (precipitation time series) to identify components of streamflow coming from these different sources. The lag between the peak in the recharge event (precipitation, glacial melt, snow melt) and change in spring discharge or chemistry is related to various factors such recharge volume, intensity, flow paths, and residence times (McNamara et al., 1998). The height of the resulting peak can also be an indicator of the importance of runoff to the water supply. Streams with peaks in flow occurring during spring melt and rainy seasons are runoff dominated. Glacial rivers can be identified by a large peak in discharge from spring to autumn when higher air temperature and radiation increases snow and ice melt. If discharge is steady with a slight and delayed increase in discharge following a precipitation event, it is more likely to be a groundwater-dominated spring/stream (Jónsdóttir & Uvo, 2009). The steadier the discharge, the deeper the groundwater aquifer is likely to be (McDonnell et al., 2010).

Recession limb analyses are also useful tools in hydrograph analyses. The recession limb is the part of the hydrograph starting from a peak in spring/stream discharge and ending when the discharge returns to baseflow conditions. The rate of return to baseflow conditions is related to the size of the catchment, meteorological conditions, and properties of storage and transfer (Tallaksen, 1995).

2.3 Episodic Events in Iceland

Episodic events due to volcanic activity, glacial flooding, and heavy precipitation cause rapid and drastic changes in water availability and water quality. Volcanic activity can have profound implications for the climate and hydrological regimes of Iceland. Above- and below-ground hydrological flow paths are altered when molten hot lava melts the earth surface and solidifies as rock (Guilbaud et al., 2005). Pyroclastic material released during eruptions can spread 100s of kilometers, creating a blanket of hot ash and particles on the ground, infrastructure, and glaciers (Arnalds et al., 2016). This causes a sudden increase in surface water turbidity while deposited fine sediments slow infiltration and smother groundwater seeps (Old et al., 2005; Levy et al., 2015).

When volcanic activity occurs beneath glaciers, it often triggers glacial outburst floods (jökulhlaups) (Thordarson & Larsen, 2007). This has been observed with Grimsvötn, an active volcano beneath the Vatnajökull ice cap. It erupted in November 1996, causing an estimated 3.2 km^3 of water to be released over 40 hours (Björnsson, 2002). Jökulhlaups can also occur when an ice-dammed lake suddenly drains, as occurred in the August 5, 2018 jökulhlaup that flooded Skaftá, Iceland with discharge rates as high as 2,000 m^3/s (IMO, 2018). Highly permeable lavas are often present beside glacial-streams and when jökulhlaups occur, the floodwaters may quickly enter the groundwater system (Old et al., 2005). The Grimsvötn volcanic system, which experiences cycles of 50–80 years of low activity followed by 50–80 years of high activity, is entering a period of high volcanic activity, with a peak expected from 2030–2040 (Thordarson & Larsen, 2007). Increased volcanic activity from this subglacial volcano will result in rapid influxes of glacial meltwaters and sediments being delivered to downstream systems.

Rapid changes to water availability also occur during precipitation events. In Iceland, single precipitation events can contribute significantly to monthly totals. A precipitation event on a single day in August 2016 measured at Höfn, Southeast Iceland constituted 42% of the total precipitation for that month (Scheffel & Young, submitted). Wang et al. (2015) found that when precipitation exceeded 45 mm/h, more than 50% of the precipitation became surface water, while a smaller proportion became soil moisture and groundwater. Compaction of soil and/or soil saturation can often limit infiltration, leading to

a lower proportion of the rainfall becoming groundwater in higher intensity events (Wang et al., 2015). However, for environments where precipitation falls on surfaces such as glaciers and porous lava fields, a different relationship between rainfall events and groundwater recharge may be expected.

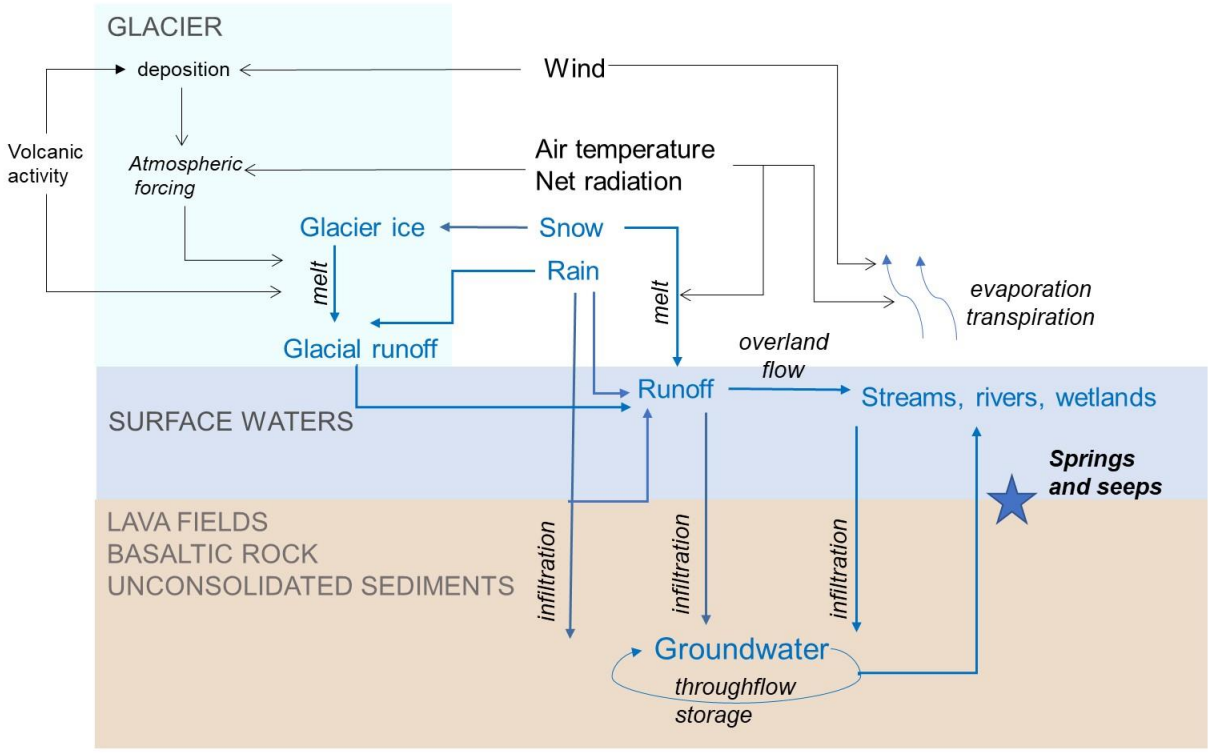

Figure 2.2 Representation of the hydrological cycle in Iceland. Dotted boxes encapsulate locations where processes take place. Glaciers store water in the form of ice and meltwaters. Climatological variables such as wind and air temperature directly and indirectly influence melt of snow and ice. Water is delivered to the earth as rain, which travels as runoff, and infiltrates into the earth. Groundwater may travel horizontally or vertically by throughflow. Springs and seeps return water to the earth's surface (see star).

2.4 Climate Change in Iceland

Fall and winter precipitation is expected to increase in the decades to come (Jónsdóttir, 2008). Climate models for Iceland predict that 2071–2100 will be 2.8°C warmer than 1962–1990 (Björnsson & Pálsson, 2008). Based on current projections and measured melt rates, Vatnajökull, the largest glacier in Iceland, is expected to lose 25% of its volume within 100 years (Björnsson & Pálsson, 2008). This may lead to decoupling of glacier-fed systems from their water source, while creating new glacial-fed systems

in other locations (Liljedahl et al., 2017). Newly revealed landscapes will also increase surface area for the deposition of sands, gravels, and its erosion, driving a positive feedback loop of aeolian-radiative forcing leading to enhanced glacier melt (Wittmann et al., 2017).While initial runoff is expected to increase from 2071–2100 in comparison to 1961–1990, Iceland's glaciers are projected to disappear completely within the next 200 years, eliminating the glacial-fed portion of the islands' hydrology (Aðalgeirsdóttir et al., 2006; Jónsdóttir, 2008). To better predict changes in surface water flows and temperatures, the roles of groundwater recharge and discharge in this complex system needs to be better understood (Burns et al., 2017).

SECTION THREE: STUDY REGION

3.1 Iceland

3.1.1 Geographic Setting

Iceland is a 103,000 km^2 island country located in the North Atlantic Ocean, just south of the Arctic Circle extends from (63.38 N to 66 .53 N and 13.50 W to 24.53 W). Iceland is geologically active and formed due to volcanic activity occurring at the Mid Atlantic Ridge (the spreading boundary between the North American and Eurasian tectonic plates). In the past 1100 years, ~87 km^3 of magma erupted from Iceland's volcanoes (Thordarson & Larsen, 2007). The 1783–1784 Laki flood lavas and the Eldgjá eruptions were the greatest contributors to new lava fields in this time frame. Glaciers cover nearly 11% of Iceland's total land area (Björnsson & Pálsson, 2008). Long-term trends and annual cycles in glacial retreat play an important role in shaping the geology and hydrology of the landscape. Landscapes influenced by glaciers experience erosion of rock walls and mantle slopes, and deposition of large volumes of sediments in valleys by fluvial and aeolian activity (Figure 3.1 D). Further from the glacial margins, alluvial fans and valleys of debris deposits form and spread by fluvial reworking, wind, waves, and currents (Mercier, 2008). These processes are accelerated by glacial outburst floods (jökulhlaup) (Björnsson & Pálsson, 2008; Duller et al., 2014).

3.1.2 Climate

Oceanic and atmospheric circulations are important determinants of Iceland's climate. The Irminger Current, part of the North Atlantic Current transports warm Gulf Stream water to the southwest and northwest coasts of Iceland (Jónsson, 1999) (Figure 3.2). This current has a moderating effect on the island's air temperatures (Björnsson et al., 2013). Along the coasts, the annual air temperature range has been reported as low as 9 to 11ºC (Einarsson, 1984). Mean annual temperatures in lowland Iceland are ~4ºC and can reach above 5ºC along the southern coast (Einarsson, 1984).

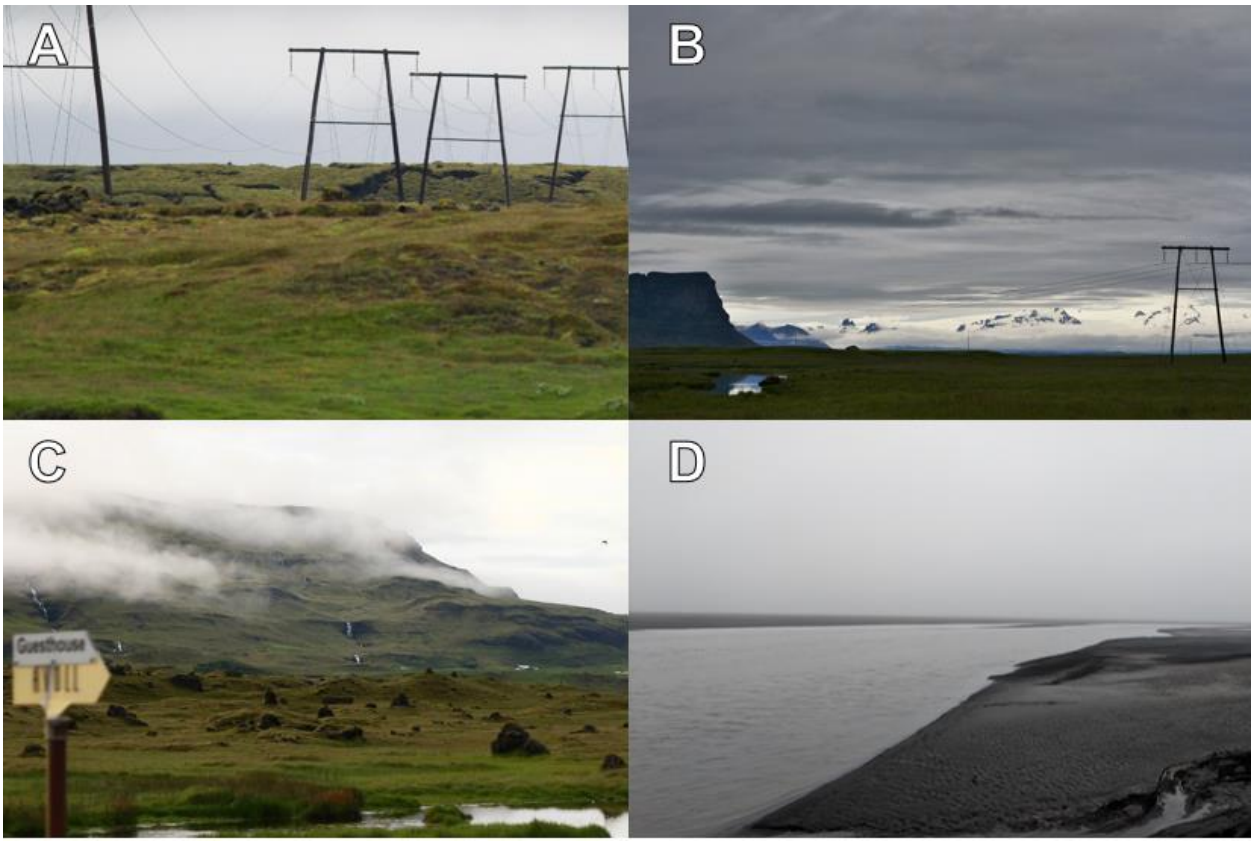

Figure 3.1 Landscapes in Iceland. A. Laki lava field, seen in background, has large fissures and cracks. B. Mountains and glaciers in Iceland. C. Older lava fields are smoother and less permeable than the younger lava field observed in A. Spring-fed wetland is seen in the foreground and a waterfall recharged by surface waters can be observed in the background. D. Skeiðarásandur on a foggy evening. The Brunná river delivers sediment and is involved in fluvial reworking of the landscape.

North of Iceland, cool ocean waters are brought in by the East Iceland Current branch of the East Greenland Current. Temperatures here are generally cooler than other regions of the island (Einarsson, 1984; Jónsson, 1999).

Precipitation and cyclonic activity are driven by the Icelandic Low (IL) low pressure center between southwest Iceland and southern Greenland (Hurrell et al., 2003; Jónsdóttir & Uvo, 2009). This pressure system and its interactions with the Azores High pressure system, drives southeastern winds across the country, picking up moisture and depositing it in the eastern and southeastern regions of the country (Einarsson, 1984; Hurrell et al., 2003). Topography also plays a role in precipitation distribution,

causing large amounts of rain to fall as orographic precipitation on mountains and ice caps (Crochet et al., 2007). Historically, October has been the rainiest month of the year in Iceland (Einarsson, 1984) . Between 1971 and 2000, southeast Iceland was the rainiest region of Iceland (Crochet et al., 2007).

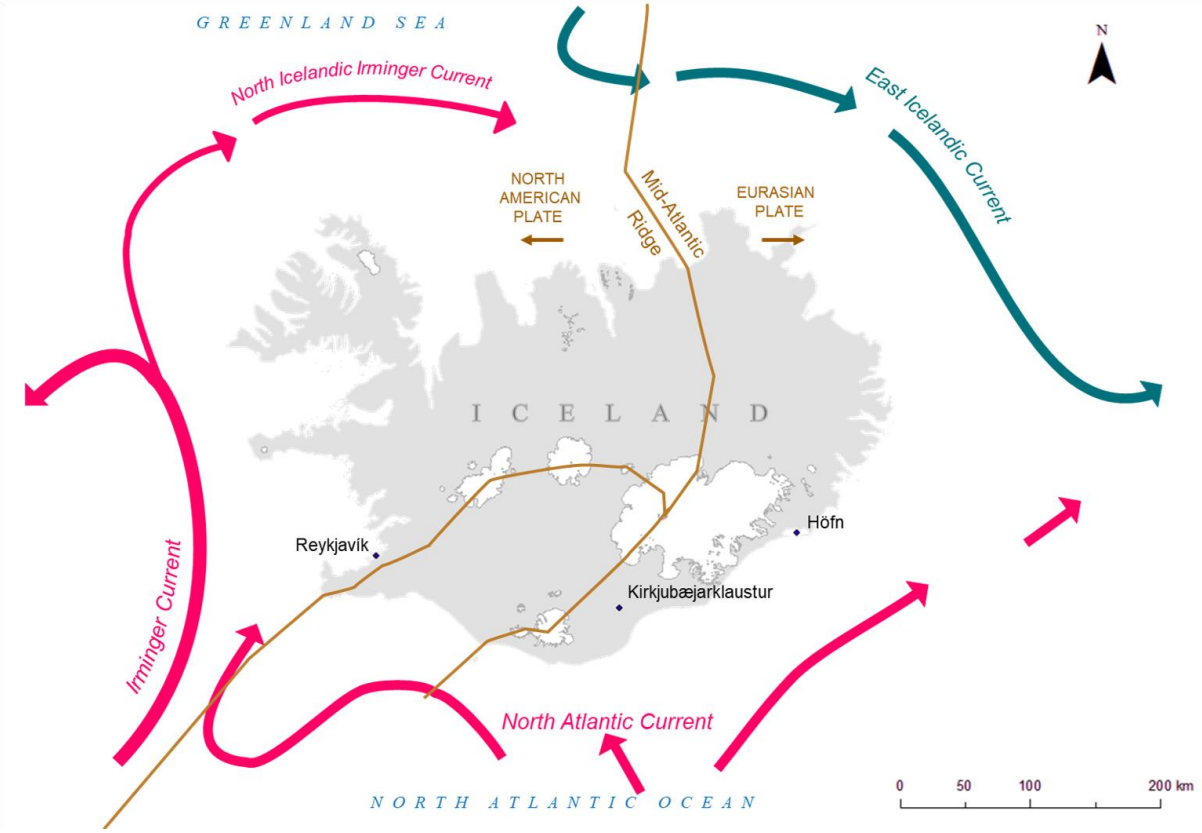

Figure 3.2 Conceptual diagram showing key oceanic currents surrounding Iceland. The Irminger current and North Atlantic current bring warm water to Iceland's South and West coasts. The East Icelandic Current brings cooler waters from the North. Current locations are approximated based on Óskarsson et al. (2009). The Mid-Atlantic ridge is approximated from Thordarson & Larsen (2007).

3.2 Hvoll Study Site

The study site is at Hvoll farm, located in southeast Iceland (63.91° N, 17.69° W) (Figure 3.3). (Guilbaud et al., 2005). The farm is a mixture of wetland and pasture at the edge of two postglacial basalt, and igneous (volcanic) rock lava fields: the Núpahruan (ca. 4000 BP) to the northwest, and the Brunahraun branch of the Laki lava field (1783–1784 AD) to the southeast (Figure 3.4). Years of

succession have led to the establishment of soils and vegetation on the Núpahruan lavas at Hvoll. The rocks of the wetland lava field have been broken down, possibly by farming activity, erosion and weathering. Originally, it may have had a structure like the Laki lava field, as they both formed from large Holocene age eruptions from basaltic fissures, where lavas travelled down river gorges then broke free at coastal plain. The Laki lava field has a range of morphological structures, from sheet pahoehoe surfaces dotted with lava rise-pits, to rubbly lavas with irregular shapes and fragments (Guilbaud et al., 2005). These types of structures can provide routes for water to quickly penetrate and travel through the lava field (Kiernan et al., 2003).

The Brunná River cuts diagonally through the property, dividing the Laki Lava field in the west, from the older lavas on the northern portion of the property. The Brunná River is fed by glacial melt waters from the Skeiðará lobe of Vatnajökull ice cap (Björnsson & Pálsson, 2008). Sediments carried downstream by the Brunná River contribute to the expansion of Skeiðarársandur glacial outwash plain. The property is located on the Northwest edge of Skeiðarársandur.

Springs have previously been reported along the edges of lava fields and sandurs in Iceland. The study site is no exception. Springs can be found along the edges of the Núpahruan lava field, where the lava field meets the sandur, and where the lava field meets the wetland. These springs vary in size from 0.06 to 3.58 m across. They discharge from various substrates with some springs emerging from macropores in rubbly lavas, while along the sandur, medium sized springs discharge from macropores surrounded by mostly-consolidated sediments. This study aimed to catalog the springs at the study site and determine the quantity and quality of their waters.

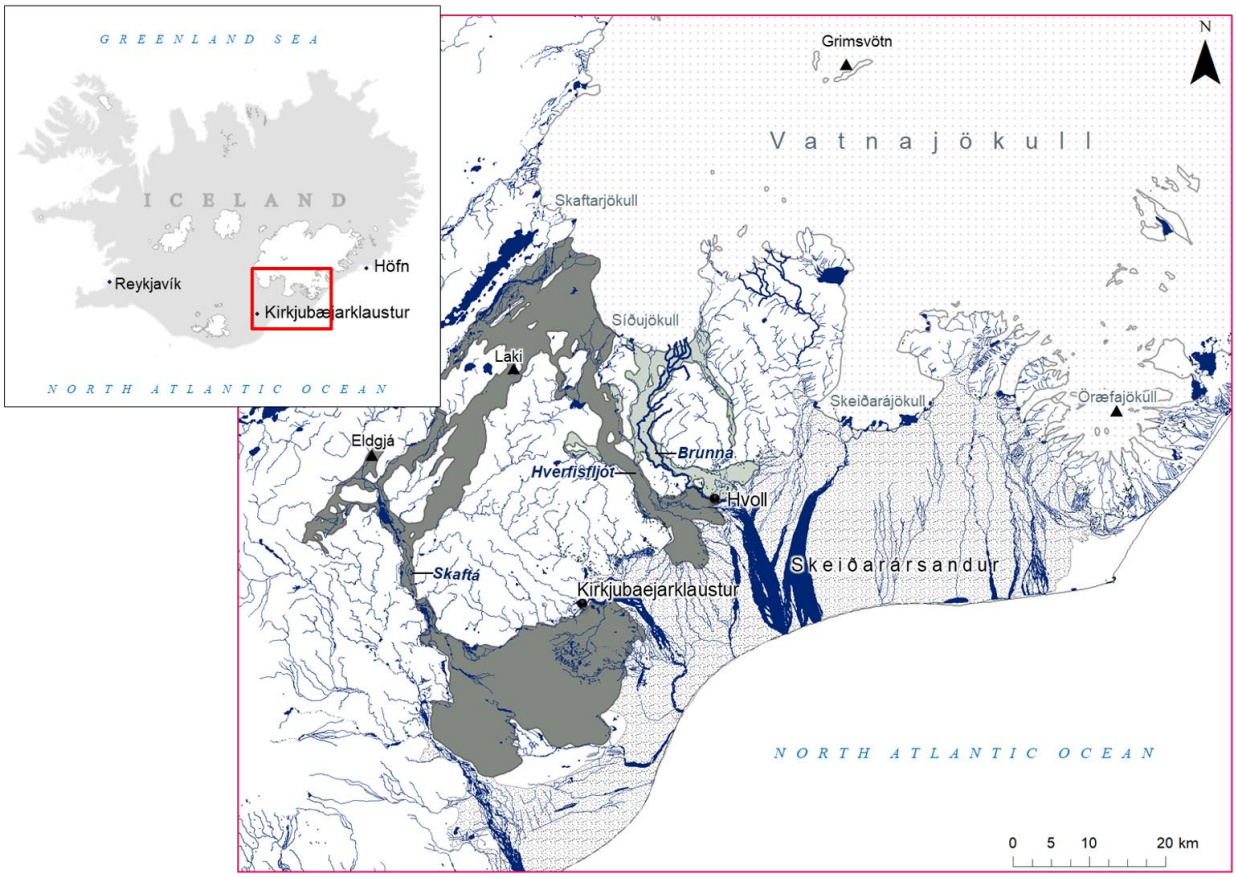

Figure 3.3 Map of the area surrounding the study site at Hvoll. River flow paths, surface cover (glaciers, sandar, lavas) are from the National Land Survey of Iceland. Hvoll is located at the lower lobes of two lavas. Postglacial lavas erupted from the 1783–1784 Laki eruption and are represented by a dark grey, and prehistoric (>871 years), postglacial lavas are shown in light green-grey.

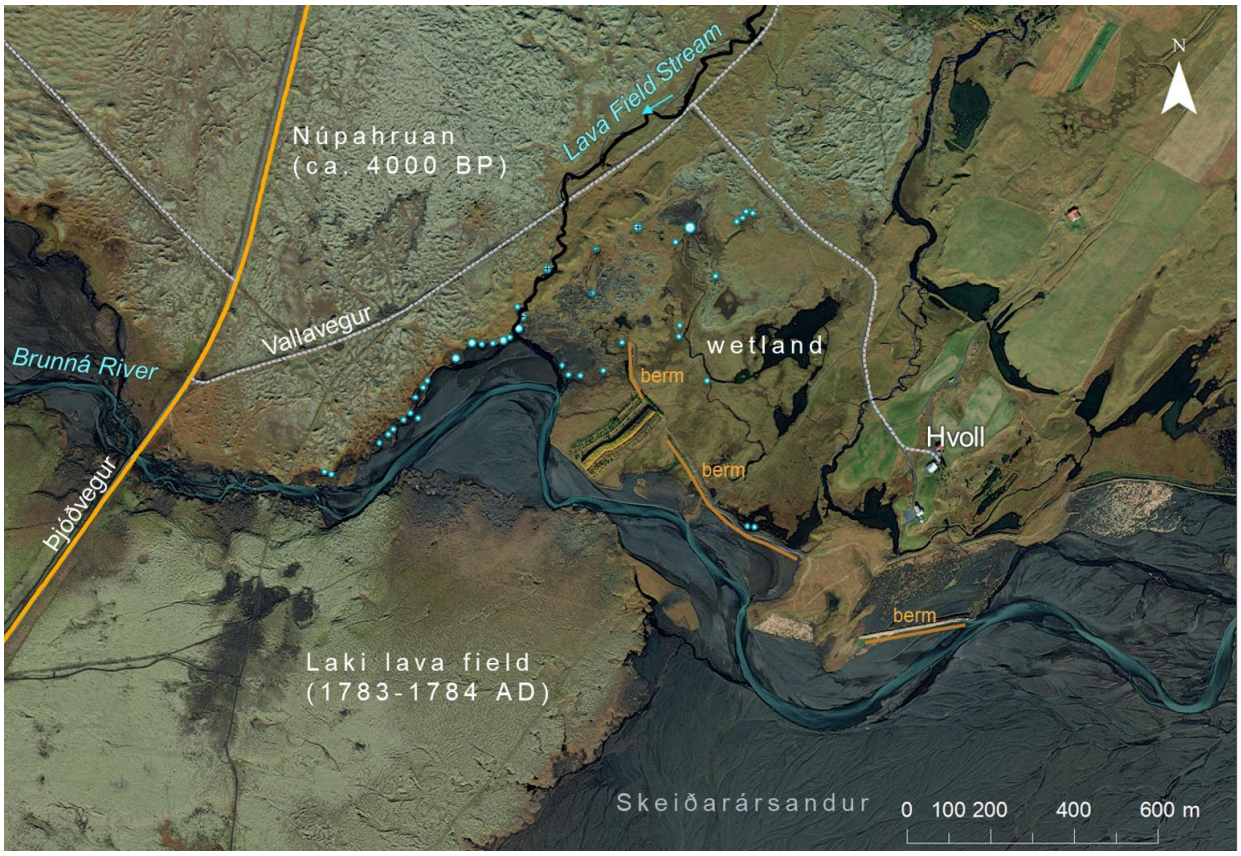

Figure 3.4 Map of Hvoll Study Area. Satellite imagery is from DigitalGlobe, available through ESRI Basemaps (2020). Blue dots show the locations of springs. Blue dots represent springs found at the study site 18-–30 May 2019.

SECTION FOUR: METHODOLOGY

This section of the thesis outlines the theory, methodology, and equipment used to collect data on water quantity and quality from the springs at the study site. Data collection extended from July 2018 to October 2019.

4.1 Catalog of Springs in Study Region

Springs locations were identified by walking upstream along the streams in the study site on 29 June 2018 and 18–30 May 2019. Additional springs were also identified incidentally while walking across the study site during these periods. The coordinates of springs observed in the field were recorded by handheld Garmin GPSMAP 64 (± 3 m). Photographs and/or video footage were obtained. The dimensions of the pore openings were measured with surveyors' tape (± 0.01 m). The spring distribution and variation in pore dimensions and surrounding substrate (rock, alluvial sediments) were also noted. A sub-sample of the different springs were selected for more in-depth study. Springs were selected to include a range of sizes, discharge volumes, and locations. To limit error from mixing of surface waters from other sources, only springs at headwaters were included in the study. Between 1 July 2018 and 18 May 2019 two springs in the wetland were monitored for water level and temperature. Twelve springs across the study site were selected to be monitored for water temperature between 19 May 2019 and 17 October 2019. Two springs from each section of the study area (sandur, lavafield/wetland, and wetland) were selected for daily spot measurements of discharge and water chemistry during the May 2019 field visit.

4.2 Weather Data

Precipitation and air temperature data were collected to explore how water quantity and chemistry changes in relation to local weather and climatic conditions. These data were collected at the Hvoll study site. During times when these data were not available, climate data (precipitation, air temperature, relative humidity, wind speed and direction) were obtained from the closest Icelandic Meteorological Office (IMO) station -Kirkjubæjarklaustur Stjórnarsandur (Station Number 6272, 63.793° N, 18.012° W). These

seasonal data were compared to normal (1961–1990) estimates of monthly total precipitation and average air temperature from 1961 to 1990 obtained for the IMO Kirkjubæjarklaustur station (IMO, 2019), 20 kilometers from the study.

4.2.1 Precipitation

Two ONSET HOBO RG3-M tipping bucket rain gauges (± 0.2 mm/tip) were placed at the study site on 18 May 2019. The two rain gauges were placed 1.4 km apart, with one in the lava field and the other in the wetland. The wetland rain gauge collected data from 19 May 2019, 0000h (12:00 AM) to 30 May 2019, 2230 h (10:30 PM). This set of data was used to verify the data collected by the lava field rain gauge. The Hvoll lava field rain gauge remained at the study site to collect rainfall data from 19 May 2019, 0000h (12:00 AM) to 7 October 2019, 2345 h (11:45 PM). Unfortunately, a field visit to the study site on 7 October 2019 revealed that the lid of the rain gauge had been knocked off over the summer. Precipitation recordings stopped after 30 June 2019. A windy period occurred between 25 July and 30 July 2019. On 25 July 2019, in the nearby town of Kirkjubæjarklaustur, wind gusts of 15.1 m/s and a daily max wind speed of 10.8 m/s were recorded by the IMO weather station. These were the second highest gusts recorded between 19 May and 1 July 2019 and may have loosened the rain gauge lid.

The Hvoll lava field rain gauge collected viable precipitation data from 19 May to 30 June 2019. Due to the loss of rainfall data from the study site, additional rainfall data (from 1 January 2017 to 29 September 2019) were obtained from the Icelandic Meteorological Office (IMO) Kirkjubæjarklaustur Stjórnarsandur (Station Number 6272, 63.793° N, 18.012° W) weather station. The IMO station is approximately 20 kilometers southwest of the study site. With rain falling on only 18 days between 19 May and 30 June 2019, not enough data was available to determine a relationship between the data sets. Therefore, precipitation data from both IMO Kirkjubæjarklaustur and Hvoll were presented where available.

Precipitation data were summarized using the programming language R (R Core Team, 2019) in RStudio (RStudio Team, 2020) to provide hourly, daily, and cumulative rainfall. To reduce skewing of daily averages and totals, days with more than 4 hours of missing data were removed from analyses. To determine if the amount of total precipitation received in a day has an impact on water levels or temperatures, daily total precipitation was grouped into 4 categories: dry (0 mm), negligible (0.1–1 mm), light (1.1–10 mm), and heavy (> 10 mm). The light and heavy precipitation groupings are frequently used in precipitation studies (Sun et al., 2006; Vincent & Mekis, 2006). The 0.1–1 mm range was not grouped into the "dry" category to cautiously ensure that effects of negligible rainfall were not missed.

4.2.2 Air Temperature and Atmospheric Temperature

An ONSET HOBO U20 Water Level pressure transducer was tied 1-m above the ground, onto a hydro pole at the border of the sandur and wetland. It recorded air temperature and atmospheric pressure hourly, from 1 July 2018 0100 h to 8 October 2019 2000 h. Atmospheric pressure data is required to correct water level data obtained with non-vented HOBO U20 Water level sensors, into units of water depth (m) (see Rosenberry & Hayashi, 2013). Air temperature would be less likely to influence spring water that comes from deep groundwater stores but would have an influence on older surface water and rainwater temperatures. Additionally, air temperature can provide an indication of the energy for warming the waters (Woo, 2012) and for glacial melt (Jónsdóttir & Uvo, 2009).

4.3 Spring Water Discharge

The quantity of water discharged from springs was determined by various methods. Water discharge was measured using a water velocity probe during the field work period in May 2019. Water levels provided a lower-cost method to provide information on the periodicity of spring discharge and response to hydroclimatic events while we were unable to be at the study site. Discharge data from nearby rivers gauged by the IMO were used as a reference for the hydrological behaviour of runoff, spring-fed, and glacier fed rivers in southeast Iceland.

4.3.1 Spring Discharge

Water discharge can be calculated by the velocity-area method (Herschy, 1993). Water velocity (m/s) was measured using a SENSA-RC2 Water Velocity Meter (range 0.000–4.000 m/s, Resolution: 0.001–0.020 m/s, accuracy ± 0.5 % ± 5 mm/s). The probe is unaffected by temperature variation and suspended sediments, making it a good choice for the purpose for a study where changes in water temperature and sediments are of interest.

The volume of water passing through a cross section of a stream per unit time is determined by the speed at which the water moves, and the area of the cross-section. As the stream bed was not uniform, and water moves more quickly at the center of the stream, and at deeper sections, the channel was divided into 10 sections of equal width, w_i , (or 5 sections if stream width was less than 0.5 m). The depth, d_i, was recorded at the center of each section. Velocity, v_i, was obtained at a single depth, $0.6d_i$, below the water surface at the center of each section. This method was selected because it is recommended by Herschy (1993) for streams shallower than 0.75 m, and all streams in the study were less than 0.3 m deep. The velocity of each section was the average of two 1-minute average velocity measurements obtained by the SENSA-RC2 Water Velocity. Following methods from Herschy (1993), the section discharge, q_i , was calculated by multiplying the width, depth, and velocity measured for each section (Equation 1). The sum of discharge, q_i , for each section gave the total channel discharge, Q_{total} (Equation 2).

$$q_i = w_i \times d_i \times v_i \tag{1}$$

$$Q_{total} = \sum_{i=1}^{n} q_i \tag{2}$$

As the streams emerged from the springs and had no other apparent sources (besides rainfall), the discharge of the channel was taken to be the discharge of the spring. The exception was the water emerging from W2, W1, and L2 where multiple small springs are located close together, their waters merging to form a stream where the measurements were taken at each. It was assumed that the discharge measured from the stream should be representative of the discharge from the spring(s) if all discharged water flows to the outlet stream and the outlet stream did not have any interfering surface or subsurface inflows.

Stream discharge was measured in the evening, 20–30 May 2019. Discharge was measured once in the morning and once in the evening, 21–29 May 2019. Due to a technical malfunction of the SENSA-RC2 Water Velocity meter, measurements from the evening 28 May 2019 and the morning of 29 May 2019 were omitted.

Three categories of discharge (Q) were defined: Low discharge springs ($0 < Q \leq 25$ L/s), Medium discharge springs ($0 < Q \leq 50$ L/s), and High discharge springs ($Q > 50$ L/s). An ANOVA test followed by a TukeyHSD test (R Core Team, 2019) was used to determine significant differences between the defined discharge categories.

4.3.2 Icelandic Meteorological Office (IMO) River Discharge Data

Non-vented ONSET HOBO U20 Water Level pressure transducers (± 0.075 % per 0.3 cm water) were installed at Hvoll to monitor hourly Brunná River water levels, 20–30 May 2019. The logger was washed away during the summer and additional data was unable to be recovered. Discharge data were obtained from the IMO (IMO, 2019) for two nearby glacial rivers, the Djúpá (VHM150) and Skaftá (VHM183). Djúpá is fed by the same glacial margin (Síðujökull) as the Brunná River. Skaftá is fed by Skaftárjökull, which is also on the southwest side of Vatnajökull. A regression was used to determine whether these data are a satisfactory approximation of water levels in the Brunná River. Water levels at

the Brunná River were assumed to experience increases when spikes in discharge were recorded at Djúpá and to a lesser extent, Skaftá.

Trends in discharge were used to provide a better understanding of how rivers with different water sources respond to seasonal trends in air temperature and rainfall. In addition to the glacial rivers, IMO discharge data were also obtained for the direct-runoff fed river, Gierlandsá (VHM475), and the spring-fed river Þverárvatn (VHM476). The glacial river and runoff river datasets were composed of hourly discharge measurements from 1 January 2017 to 29 September 2019. Data for Þverárvatn was only available for 1 January 2017 to 6 October 2018.

Daily discharge was calculated for all rivers and plotted against time along with Kirkjubæjarklaustur daily total precipitation and average air temperature. Baseflow was calculated using the EcoHydrology package (Fuka et al., 2018) in R, with a filter parameter of 0.925 (standard) and running 3 passes over the daily average water level. Baseflow is a representation of the groundwater component of the hydrograph, and was used to show how seasonal groundwater contributions vary in different river systems.

The recession limbs following 5 different rainfall events between 30 April and 27 May 2018 were plotted for Djúpá, Gierlandsá, and Þverárvatn to determine how they recover following rainfall events at different times of the year.

4.3.3 Hvoll Spring-fed River Water Levels

Water level data from non-vented ONSET HOBO U20 Water Level pressure transducers (± 0.075 % per 0.3 cm water) were used to visualize changes in spring and stream flows seasonally, and in response to jökulhlaups and precipitation events. These loggers collect data on water temperature and pressure. A water level pressure transducer was also installed at 1.0 m above the ground to gather data on atmospheric air pressure. Water levels were computed by HOBOware Pro Barometric Compensation

Assistant. This software uses the density of freshwater and measured water pressure and water temperature data to calculate water level while correcting for changes in atmospheric pressure.

On 29 June 2018, during a preliminary visit to the Hvoll field site, non-vented HOBO water pressure transducers were installed at two streams in the wetland. One logger was suspended from a horizontal pipe over a low flowing stream emerging from small ascending submerged springs (W2). The other logger was installed at the headwaters of a stream that was fed by a subsurface conduit. This stream will be referred to as the Runoff Spring, as paths created on ground by previous, repeated flows indicated that the conduit receives water from runoff and river overflow from higher ground. This logger was also suspended from a string, tightly secured to rocks on either side of the stream. With the low flow at these sites and the weight of the logger, no drift was observed. These two loggers collected hourly water level data from 1 July 2018 to 18 May 2019.

These loggers were installed at new locations on the study site on 20 May 2019. The wetland spring was moved to a similar wetland steam emerging from a small spring (W1), a few meters north. The top of the logger was secured to the side of a pipe, installed horizontally across the stream, such that the top of the logger was not blocked by the pipe. The other logger was installed directly inside the pore of a medium sized spring (S1) at the edge of the lava field and sandur. The pvc pipe was pushed into the soil beside the spring to serve as an anchor to suspend the water level logger from. No drift was observed. The logger was installed 0.5 m below the surface of the water in 20 May 2019.

While the HOBO U20 logger is supposed to be able to operate at temperatures between -20°C and 50°C with a maximum error less than 0.8%, when temperatures dropped below 0°C, extreme positive increases (up to a meter in a single hour) or negative water levels were often recorded, possibly due to water freezing. All daily water levels occurring on days with a daily average temperature below 0°C were removed from the dataset.

The heights of the stream/spring bank from the logger sensor were recorded for the sandur spring S1 and wetland spring W1 in 2019. A threshold analysis was used to determine when water levels exceed the banks, resulting in flooding. For S1, the height of the lip of the spring pore from the logger was also measured. Water levels that dipped below the opening of the pore (indicating that the spring no longer discharged water to the surface), were identified using simple conditional statements (Equation 3). For W1, where the water level logger was placed in the stream emerging from the spring, the height of the banks was recorded. To identify when flooding occurred at this location, a conditional statement (Equation 4) was used.

x = current water level h = lip height

$$x < h \tag{3}$$

x = current water level b = bank height

$$x < b \tag{4}$$

Water level data between 11 January and 9 March 2019 were removed from the dataset due to freezing conditions (extremely high water levels). The daily average water level, maximum water level, and time of maximum water level were then calculated for each location. Baseflow, low flow of spring discharge can be calculated using an automated digital filter on a curved line that connects the low discharge values in a moving kernel. Baseflow was calculated using the BaseflowSeparation function in the EcoHydrology package (Fuka et al., 2018) in R, with a filter parameter of 0.925 (standard, recommended by Nathan & McMahon, 1990) and running 3 passes over the daily average water level. This function passes a filter over the water level data, to separate baseflow from streamflow data. The timing of seasonal peaks and troughs in baseflow were also noted for each gauged location.

The difference between the measured hourly water level and baseflow water level was calculated to quantify the component of water level that might have occurred from overland flows, or groundwater

store replenished by rainfall, melt, or other sources (collectively referred to as “Recharge”). To standardize the water level increases due to recharge between the gauged locations, it was calculated as the percent increase in daily average water level from the daily baseflow. To determine if springs responded differently to precipitation events, the percent increase due to recharge (PIR) was compared between sandur spring S1 and wetland spring W1, as well as between wetland spring W2 and the runoff spring. The differences between the timing of maximum water levels for each pair of springs was also calculated. ANOVA tests followed by a Tukey HSD test were used to identify significant effects of rainfall categories on the difference in PIR.

Spring water levels and baseflows were plotted with daily Kirkjubæjarklaustur precipitation data and air temperature data. Similar trends between Hvoll and IMO rivers were used to help predict the importance of runoff and glacial water in replenishing the groundwater stores that feed the springs at the study site. Water levels measured at Hvoll were expected to show similar seasonal and episodic (response to rainfall events) trends as the spring-fed river Þverárvatn.

4.4 Water Quality

Water quality data were collected at the 6 main study springs (L1, L2, S1, S2, W1, W2) and the Brunná River, twice a day from 21 May to 30 May 2019. These data were used to understand changes in water chemistry across space and time. Spatially, water quality data were used to assess the influence of spring water on the surrounding surface waters.

Electrical conductivity (µS/cm) is a useful tool for identifying groundwater flows as long-term interactions with bedrock can result in groundwater having a different conductivity from surface waters. High conductivity readings has co-occurred with mineral and ion enrichment in Icelandic springs (Ketilsson et al., 2017).The timing of peaks in specific water quality variables (temperature, electric conductivity, pH, salinity) will also assist in identifying spring recharge sources. Changes that correspond with precipitation events would indicate the respective events as a likely contributing source of water to the springs.

4.4.1 Water Temperature

Water temperature was recorded for twelve springs across the study site. HOBO Pendant MX Temp MX2201 and Temp/Light MX2202 Loggers (± 0.5°C, -20°C–70°C and ± 10% light accuracy for direct sunlight) were placed in the streams emerging from nine springs of various size and locations at the study site. Metal corner braces were zip-tied to rocks to create a platform for the logger to be zip-tied to. The temperature loggers were installed horizontally across the corner braces with the light sensor facing up, toward the surface of the water. The Temp/Light sensors installed at a spring in the sandur, a spring in the lava field, and a spring in the wetland collected data on incoming light intensity. These data were used to indicate decreases in turbidity, and the impact of incoming light on temperatures recorded by the temperature sensor. Hourly water temperature data was also available for S1 and W1 from the HOBO U20 non-vented water level loggers.

An ascending seepage spring located in the oxbow from a glacial-fed river that runs through the study site and joins with the Brunná river was also gauged. Since this spring was not at the headwaters of stream, one HOBO MX2202 Pendant Temperature/Light Data was installed before the spring, and another was installed directly after. The sensors were zip-tied to rocks with the sensors facing directly upward and placed on the streambed. In total, three different types of HOBO water temperature loggers were installed at thirteen locations across the study site from 20 May to 1 October 2019 (see Figure 5.1).

The water temperatures for each location were plotted against time, with daily precipitation and daily air temperature. The timing of peaks in temperature were noted in relation to precipitation events and temperature. When temperatures measured by the logger matched with the air temperature, it was assumed that the water level was below the height of the logger, and the datapoints were removed.

For each logger, the daily average, maximum, minimum, mode was calculated. The time of the daily maximum was also determined. The daily range was used to provide a representation of short-term spikes in water temperature while the daily mode and min (usually the same value), provided a

representation of water temperatures without the influence of incoming solar radiation. For springs with light data, a linear regression was used to determine if water temperature was affected by light intensity.

Daily total precipitation was grouped into different rain categories (0, 0.01–1 mm, 1.1–10 mm, and > 10 mm) defined by the IMO. For the six main study springs an ANOVA and Tukey HSD test was used to determine if the range in water temperature was affected by the amount of precipitation that fell. A linear regression was used to determine if daily average water temperature could be predicted by daily average air temperature at Hvoll. Since hours of daylight changes across time, an ANOVA and Tukey HSD test were used to determine if daily maximum water temperature changed by month.

4.4.2 Water Chemistry

Short-term water chemistry data were collected using a Hanna HI98194 Multimeter Probe that measured temperature, pH and mV, oxidation reduction potential, dissolved oxygen, conductivity, and total dissolved solids (see Appendix A for specifications). The device was programmed to record measurement every 30 seconds during spot tests. An additional Hanna multimeter probe was left at W1 to obtain continuous measurements of spring water quality during the May 2019 field period. These data were used to capture changes in water chemistry that could not be captured by spot measurements. The continuous dataset was also used to confirm the accuracy of the spot data for periods where data was available for W1 from both loggers.

Water chemistry was obtained for six study sites, the Brunná River, and precipitation. The water chemistry from springs was measured by placing the water chemistry probe into the pores of the springs, away from the walls. Chemistry readings for the Brunná River were obtained by wading into the north side of the river, near the sandur springs. The river was deep and fast flowing, so measurements were taken only a few meters from shore. Rainwater was collected by placing a beaker with a small funnel in a hole dug in the soil of the wetland. Placing the beaker in the ground kept the collected rainwater insulated to reduce evaporation. Once enough water was collected to fully immerse the multimeter probe, the

rainwater chemistry was sampled. After sampling the rainwater was dumped and the catcher rinsed and set up again to collect the next rainwater event.

The water chemistry data was collected twice a day at each location between 21–29 May, and once on 20 May and 30 May 2019. The Brunná River chemistry readings were taken once per day between 21–23 May 2019. One rainwater reading was taken on 27 May 2019.

For each session of recordings, the probe was placed in the water and collected 30 second water chemistry readings for at least 10 minutes. The data points often took up to 5 minutes to stabilize, and these points were removed. Extreme anomalous readings were also removed, as they were assumed to be due to the logger accidentally touching the walls of the pore.

The stable water chemistry data were averaged for each session of recordings for each spring. The (bi)daily water chemistry for the springs, Brunná River, and rain were plotted across time, along with precipitation and air temperature data.

4.4.3 Stable Water Isotope Analysis

The isotopic composition of rain has been found to vary across space and time (Lawrence and White, 1991). This can be useful for determining the source (recharge area) of surface and groundwater, assuming that the isotopic composition of the precipitation is different from other possible sources.

The difference in stable isotope composition was examined for water features under baseflow conditions and following rainfall events. Samples were obtained from surface water (the Brunná River), spring water (from the six main study springs) and rainwater. All samples were collected in 30 mL high-density polyethylene (HDPE) sample bottles.

The water sampled from springs were collected from inside the spring pore, before the water mixed with surface waters or could be affected by evaporation. Before the isotope samples could be collected, water quality was assessed to ensure that the sample was representative of the water in the pore

at that point in time. The samples were not obtained until the water quality readings were stable. Surface water samples were obtained by grab samples from the edge of the Brunná River.

A rain collector made of a beaker with a funnel attached to the top was placed in the wetland (see section 4.3.2 for more information on the rain collector). Typically, the rain collector should have been left for at least one-month before collecting the sample. Due to the short field season, the collector could only be left out for 12 days. The Local Meteoric Water Line (LMWL) for South Iceland was defined as $\delta^2H = 6.5\ \delta^{18}O - 3.5$ by Sveinbjörnsdóttir et al. (1995) and was used as the baseline to compare δ^2H and $\delta^{18}O$ compositions obtained in the present study.

The samples were analyzed by the University of Waterloo Environmental Isotope Laboratory using a Los Gatos Research T-LWIA-45-EP Liquid Water Isotope Analyzer (LWAI). The accuracy of these analyses are 0.8 ‰ Vienna Standard Mean Ocean Water (VSMOW) for δ^2H and 0.2 ‰ VSMOW for $\delta^{18}O$.

δ^2H-$\delta^{18}O$ plots were used to visualize the spread of data with the GMWL and LMWL. Waters from similar sources tend to cluster more closely together on a δ^2H-$\delta^{18}O$ plot and may exhibit changes across time and hydrometeorological conditions. For example, plotting lower on the LMWL is an indicator of input from waters that originated inland, at a high-altitude and cooler temperatures (glacial water). This makes δ^2H-$\delta^{18}O$ plots useful for identifying potential sources of water contributing to a sampled water body (see Figure 4.2 for guide to interpreting δ^2H-$\delta^{18}O$ plots). Two-sample *t*-tests were used to investigate differences in δ^2H and $\delta^{18}O$ composition between wet and dry conditions and between May and October 2019.

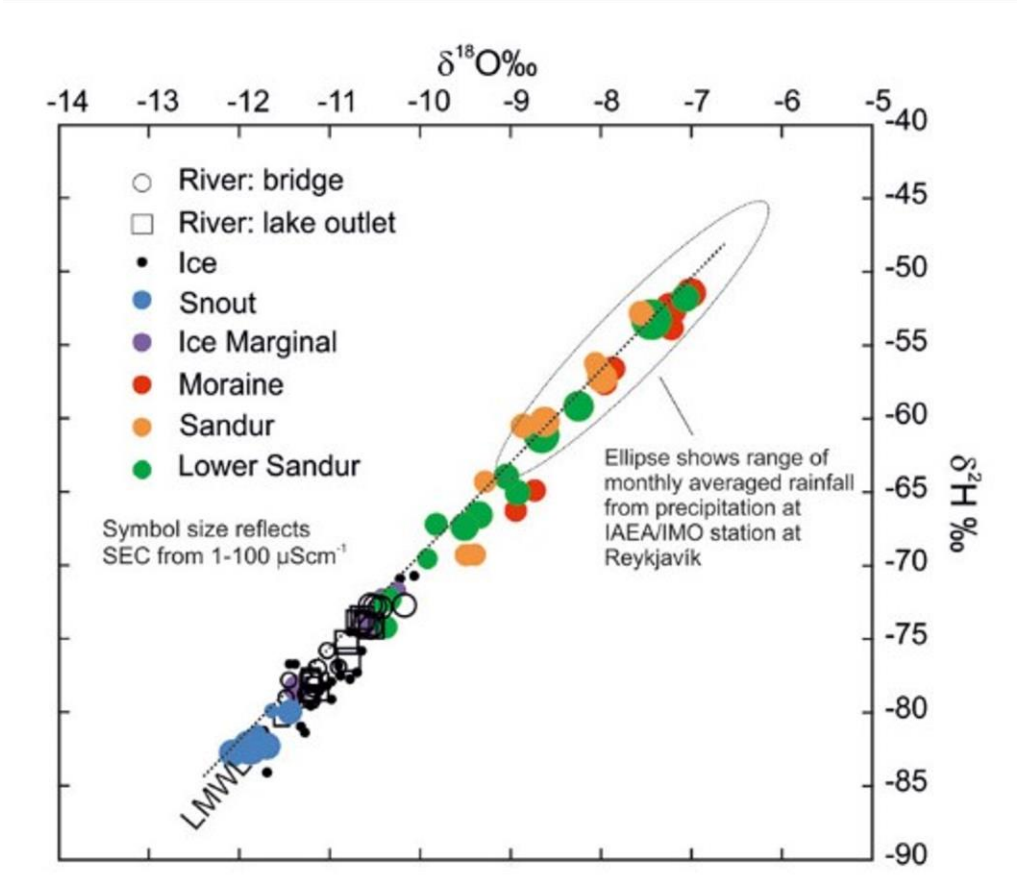

Figure 4.1 An example of how to interpret δ^2H-$\delta^{18}O$ plots. The plot above shows isotopic signatures for various water sources sampled in the Virkisá, Iceland catchment between September 2011 and May 2014. Moraine and sandur waters show significant overlap with the range in δ^2H and $\delta^{18}O$ obtained for rainfall (grey ellipse), and little to no similarity in range is shared with waters collected from glacier (ice, snout, ice margin at Falljökull). This indicates that sandur waters, measured from dug holes and natural springs are fed by rainwater rather than glacial waters. Figure from Macdonald et al. (2016).

SECTION FIVE: RESULTS

5.1 Catalog of Springs in Study Region

Over 50 springs were found at the site, although the true number is likely much higher as safety concerns and nesting birds prevented investigation of some locations. Twenty springs were found where the sandur meets the prehistoric lava field, another 20 were found in the wetland, and at least 10 were found in a stream that runs between the lava field and the wetland (will be referred here as the lava field stream) (Figure 5.1). The springs varied in size, orientation and substrates.

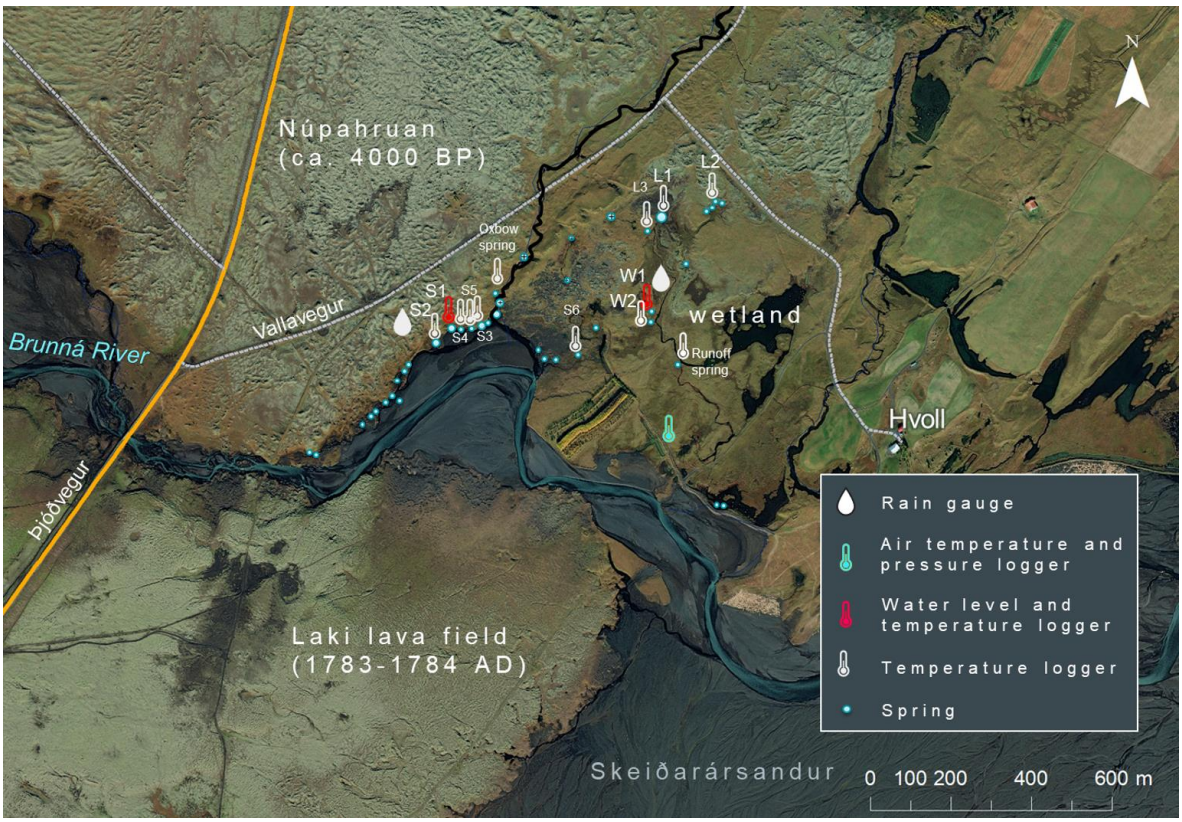

Figure 5.1 The locations of springs discovered at the Hvoll study site in southeast Iceland. Each blue dot represents one or more springs. The main study springs are labelled (S1, S2, L1, L2, W1, and W2). Locations of streams gauged for temperature, and water level are shown, as well as the locations of the two rain gauges, and one air temperature and air pressure logger.

The land in the wetland is composed of broken-down lava rock covered by a thin layer of soil. Water was seen seeping from small slopes at the edge of the lava field and flowing out of small springs that feed the headwaters of small streams at low elevations (Figure 5.2 A, C). The ground around many of these springs was observed to be near saturation, indicating a high water table. The spring-fed streams in the wetland, flowed southeast towards a complex of wetland ponds, and eventually to Skeiðarársandur. Where soil was less developed, spring-fed streams could be seen flowing over lava-rocks then disappearing underground. This description is typical of gravity springs which are fed by a high water table intersecting the ground-surface (Kresic & Stevanovic, 2010).

Various types of springs were found at the border between the sandur and old lava field. Small, seepage springs discharged water from the lava field towards the Brunná River (Figure 5.2 H). Other small springs (having openings less than 0.5 m across) had a similar geomorphology to small springs where the wetland, with waters that emerged horizontally and vertically from porous, broken down lava rocks. Soft sediments lined the bottom of the spring openings, and hard packed sediment lined the bed of the emerging stream. The pore depths of up to 0.2 m were recorded for the springs, but due to their irregular shapes were likely underestimated.

Small submerged, seepage springs were observed in the unconsolidated materials of the lava field river, and in a wetland pond. Sediment was transported through these springs, as large piles of unconsolidated sediment built up beside/inside the pore. Two seepage-springs observed in June 2018 were nearly dry in May 2019. Other seepage-type springs were found on gentle slopes in the wetland, where water seeped out from horizontal flows, saturating the nearby soils and formed surface flows (Figure 5.2 H).

Medium sized springs (having openings between 0.5 and 2 m across) were found along the sandur-lavafield edge, and in the lava field river. The springs in the river were found in complexes, where water welled up from 2–5 *swiss-cheese-like* circular pores in consolidated sediment. Due to the high, fast-flowing waters, they could not be investigated further.

The two medium springs along the sandur were ascending springs with pore depths over 1 m. They fed the headwaters of small streams that flowed into the Brunná River. One large spring (3.58 m width) was found in the wetland, closer to the lava field. The medium and large springs in this study had similar geomorphologies, with smooth, well-defined walls of consolidated sediments.

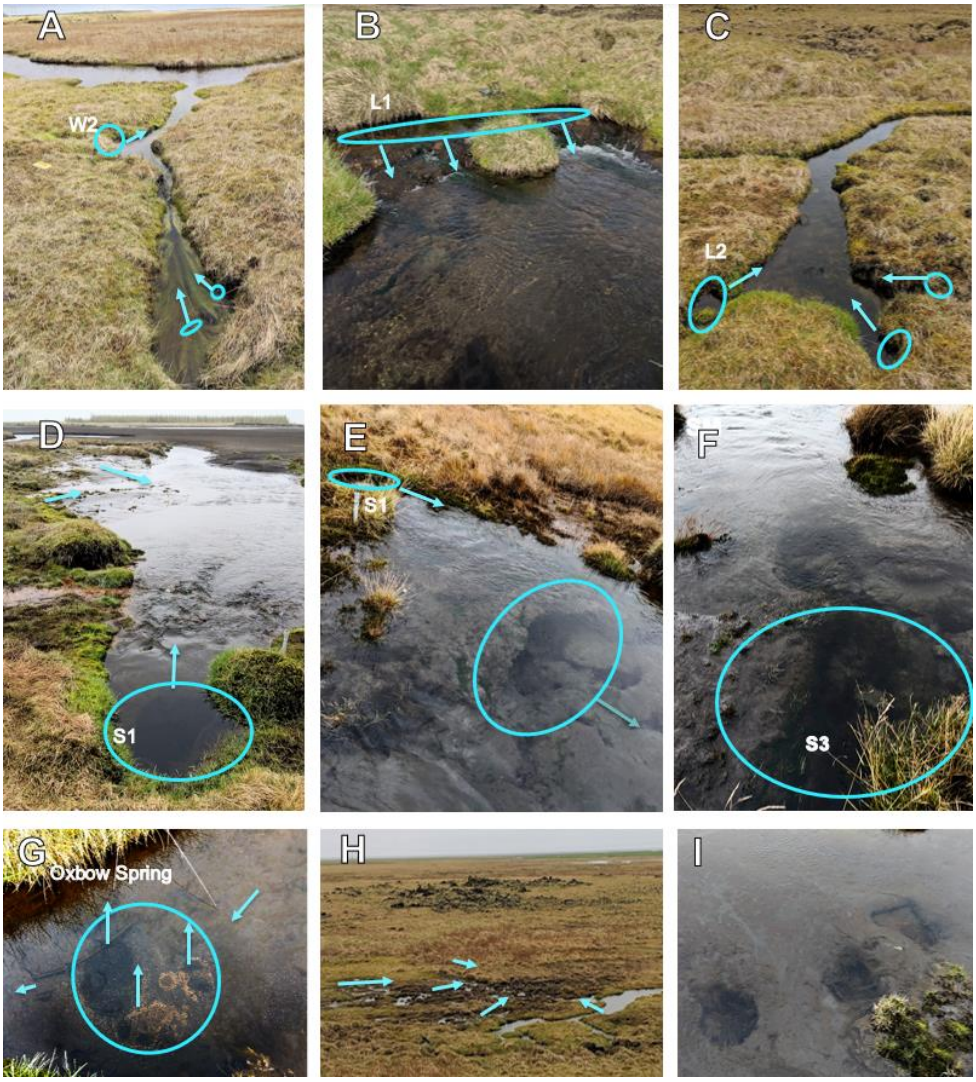

Figure 5.2 Images of springs found across the study sight. A, B, and C show W1, L1, and L2, springs found in the wetland. D and E show medium spring S1, with image E showing the morphology of the end of the tube. F shows SM, a medium sandur spring. The seepage spring at the oxbow stream is shown in G. H shows seepage springs at the bottom of a slope (image taken from top of slope). I indicates 'swiss-cheese'-like springs in the lava field river.

Two medium springs (S1 and S2) from the sandur, two small springs (W1 and W2) from the wetland, and one small and one large spring (L1 and L2) from the lava field/wetland were selected for further study of water discharge and water chemistry (See sections 5.6 and 5.7). Characteristics of the springs are summarized in Table 5.1.

Table 5.1 Characteristics (location, pore size, depth, sediment type, algae) of the six main study springs.

	L1	L2	S1	S2	W1	W2
Location	Lavafield/ wetland	Lavafield/ wetland	Sandur	Sandur	Wetland	Wetland
Pore Size	Large: 3.58 × 0.7 m	Small: 0.17 × 0.21 m	Medium: 1.07 × 0.8 m	Medium: 1.3 × 0.45 m	Small (2): 0.27 × 0.2 m 0.19 × 0.07 m	Small: 0.06 × 0.08 m
Depth	0.28 - 0.42 m	0.18 m	0.59 - 1.17 m	0.90 - 1.03 m	0.2 m	0.16 m
Sediment Type	Light weight "stone", can break off chunks with hands	Irregularly shaped porous, lava rock. Hard packed sediment stream bed.	Hard packed sediments	Hard packed sediments	Irregularly shaped porous, lava rock. Hard packed sediment stream bed.	Irregularly shaped porous, lava rock. Hard packed sediment stream bed.
Algae	Yes, especially in slower flowing parts	Yes. Long and green	Short yellow-green algae bed on packed sediments where stream starts	No large algae	Very long bright green algae	Some short yellow algae. Large green globular algae formed on temperature logger
Spring Type	At the edge of the lava field, feeding water into the edge of the wetland.	Water comes up through lavas	Water comes horizontally from lava field then flows up and out towards the sandur	Water comes horizontally then flows up and out, flowing to the sandur	Water emerges from below, through lava rocks.	Water emerges vertically, through lava rocks.

5.2 Weather Data

5.2.1 Precipitation

Precipitation (rainfall) measured at the study site lava field and wetland was similar (cumulative precipitation $R^2 = 1.0$, Fig. 1) during the May field season between 19–30 May 2019. This demonstrated that the lava field rain gauge, which collected precipitation data on the study site from 19 May to 30 June 2019 provided a reasonable representation of precipitation falling at the study site. The Hvoll lava field

rain gauge was disturbed, rendering data past 30 June 2019 unusable. A regression indicated that the weather station followed a similar (R^2 = 0.97) trend in cumulative precipitation to that measured at the Hvoll lava field, though some precipitation events delivered more rain to one region than the other (Figure 5.2). For example, on 20 June 2019 15.6 mm total daily precipitation was measured at Hvoll and only 3.5 mm were recorded in Kirkjubæjarklaustur. The highest daily rainfall (20 mm) recorded at Hvoll during the May field season (18 May and 30 May) occurred on 28 June. Ninety-two percent of this precipitation occurred over 5 hours. The highest intensity for rainfall occurred on 20 June, when 7.2 mm of precipitation fell in a single hour.

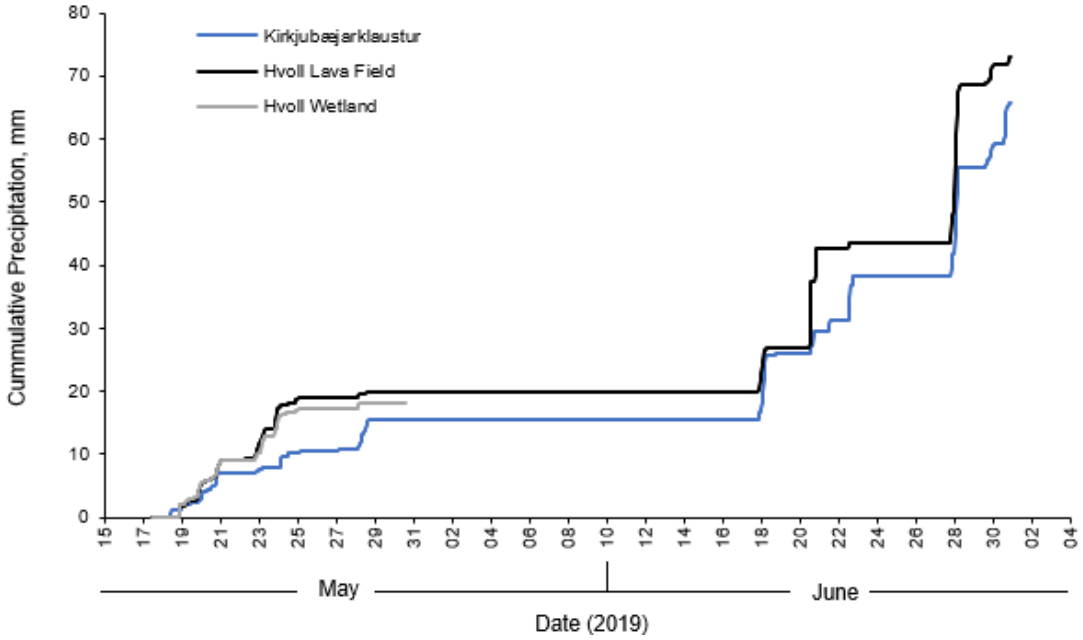

Figure 5.3 Cumulative precipitation of hourly total rainfall for Kirkjubæjarklaustur (blue line), Hvoll lava field (black line), and Hvoll wetland (grey line) between 19 May and 30 June 2019. The rainfall data for Kirkjubæjarklaustur were obtained from the IMO (2019).

Over the entire study period (1 July 2018–30 September 2019) the highest total precipitation measured in a single hour was 8.1 mm on 2 July 2018, 7.4 mm on 14 August 2019, and 7.3 mm on 25 August 2019 (Figure 1.2). Kirkjubæjarklaustur and Hvoll both experienced an abnormally dry summer in 2019. No precipitation was recorded for 19 consecutive days (30 May–17 June 2018). The total

precipitation measured in June 2018 (51.4 mm), and June 2019 (50.3 mm) was approximately 80 mm lower than the 30-year average (131 mm). A 30 year-average of precipitation at the IMO Kirkjubæjarklaustur station from 1961–1990 indicated that historically, October is the rainiest month, with August, September, and January being the next largest contributors to yearly rainfall (Table 5.2). From 2017 to 2019, monthly rainfall has shifted to extremes, with 21 out of 33 months having a total rainfall falling outside of the 30-year average range (115.1–184.7 mm) (Table 5.2). In 2017–2019, March, June and August were dryer than the historic average, while April was wetter. For the period when water temperature and water level loggers were installed at the Hvoll study site (19 May and 30 September, 2019), all months were 35.7% drier than the historical average except for September (171.1 mm), which was 21.6% wetter than the historical average (140.7 mm). The largest rainfall events (where events were separated by at least 24 hours without rainfall) occurred toward the end of the study period. On 25 August, 37.3 mm of rain fell in a single day. Over the next 7 days, a total of 63.5 mm of precipitation fell. In September, the rainiest days were the 9th (28.2 mm), 14th (28 mm), 18th (19.9 mm), and 20th (29.2 mm).

Table 5.2 Monthly total precipitation, mm measured by the IMO Kirkjubæjarklaustur weather station. The 30-year average (1961–1990) for each month and hourly data from 2017–2019 were obtained from the Icelandic Meteorological Office (IMO) (2019).

	Total Precipitation, mm												
Year	Jan	Feb	Mar	Apr	May	Jun	Jul	Aug	Sep	Oct	Nov	Dec	Yearly Total
2017	143.5	237.0	78.7	197.3	83.1	69.5	131.5	98.6	250.5	79.0	77.5	91.2	1537.5
2018	131.0	152.9	54.0	116.3	232.0	51.4	110.0	111.9	111.4	218.1	139.8	205.8	1634.6
2019	114.0	113.5	95.8	172.2	83.3	50.3*	87.2	120.3	171.1	99.9	105.6	175.2	1388.4
30-year avg (1961-1990)	145.0	130.4	130.6	115.1	117.6	131.0	120.8	158.7	140.7	184.8	136.5	133.1	1644.30

* Total precipitation measured at Hvoll in June 2019 was 52.2 mm

5.2.2 Air Temperature

The air temperature at Hvoll study site followed a similar trend ($R^2 = 0.96$) as air temperature at Kirkjubæjarklaustur, Iceland. The daily average temperature at Hvoll (measured by atmospheric HOBO sensor in the wetland) from 19 May to 1 October 2019, was 4.2°C warmer than in Kirkjubæjarklaustur.

Within the study period (1 July 2018–30 September 2019) July was the warmest month (12.7°C in 2018 and 13.2°C in 2019) measured at Hvoll (Table 5.3). The 3 hottest days measured at Hvoll occurred on 12 June 2019 (17.2°C), 28 June 2019 (17.8°C), and 7 July 2019 (17.3°C). January was the coldest (-1.0°C) month in the study period. During the study period, 61 days had an average temperature below 0°C, with the first occurring on 26 October 2018 and the last on 1 April 2019.

Hvoll and Kirkjubæjarklaustur average monthly air temperatures are comparable to the 30-year average (1961–1990) for the IMO Kirkjubæjarklaustur station (Table 6.3). Within the study period (July 2018 to October 2019), the average air temperature at Kirkjubæjarklaustur in November 2018 (4.0°C) was 2.9°C warmer and April (5.8°C) was 2.8°C warmer than the 30-year averages for these months. The winter of 2018–2019 was warmer and wetter than the 30-year average while the summer months in 2018 and 2019 were warmer and drier than the 30-year average.

Table 5.3 Average monthly air temperature, °C, for Hvoll and Kirkjubæjarklaustur. All Kirkjubæjarklaustur values are from data obtained from the IMO (2019).

		Average Air Temperature (°C)												
	Year	Jan	Feb	Mar	Apr	May	Jun	Jul	Aug	Sep	Oct	Nov	Dec	Yearly Average
Hvoll	2018							12.7	11.5	7.5	3.7	2.9	0.6	
	2019	-1.0	0.5	1.0	6.0	7.3	12.5	13.2	11.6	9.1				
Kirkjubæj.	2018	-0.7	0.0	1.6	3.9	6.5	10.5	11.3	10.7	7.0	3.8	4.0	1.6	5.0
	2019	-0.4	0.9	0.9	5.8	6.1	10.4	11.9	10.5	8.7	4.5	1.0	0.5	6.1
	30 year avg (1961-1990)	-0.4	0.2	0.7	3.2	6.5	9.4	11.2	10.4	7.5	4.5	1.1	-0.4	4.5

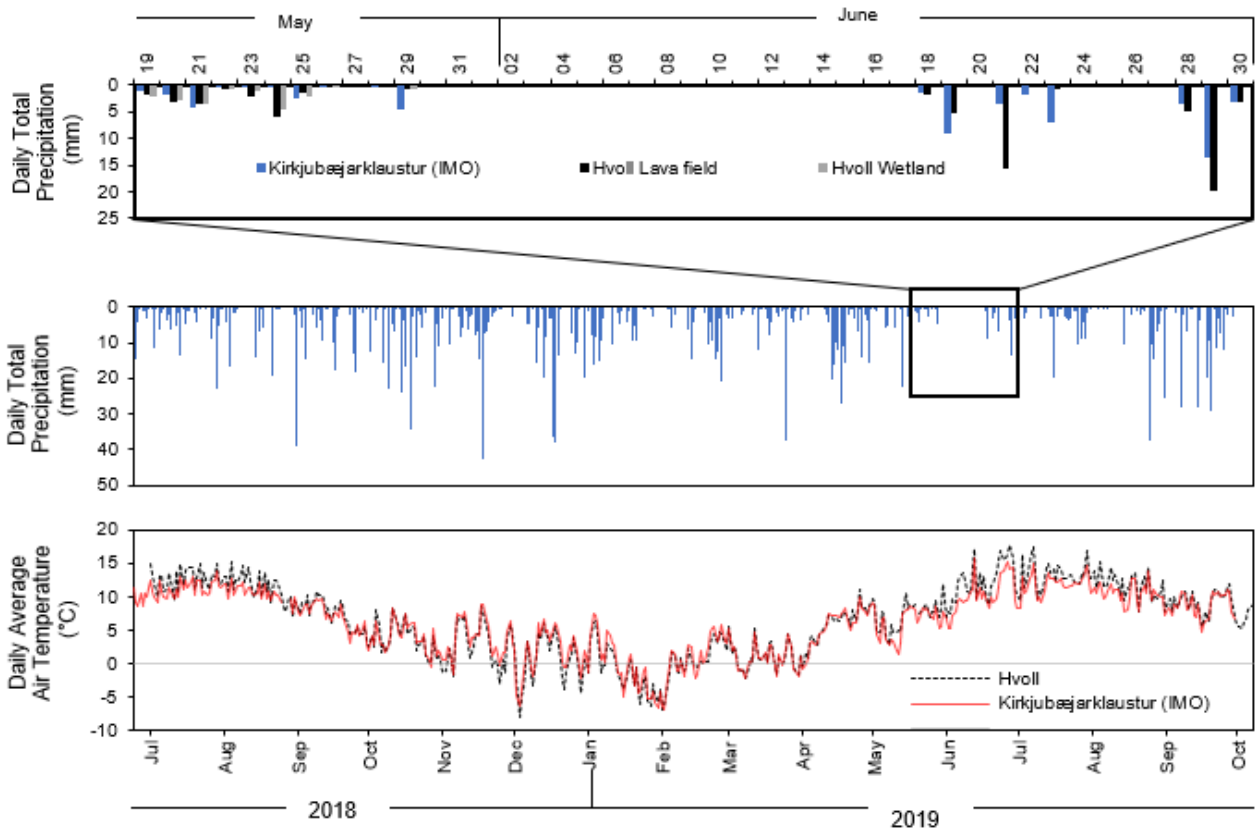

Figure 5.4 Daily total precipitation and average air temperature measured at the Hvoll study site and at the IMO weather station in Kirkjubæjarklaustur, Iceland. The top graph shows a zoomed in time frame where precipitation was measured by rain gauges at the Hvoll study site in Southeast Iceland. The Hvoll lava field rain gauge collected data from 19–31 May 2019. The Hvoll wetland rain gauge collected viable data from 19 May to 31 June 2019. Kirkjubæjarklaustur precipitation and air temperature data were obtained from the IMO (2019) for 1 July 2018 to 30 September 2019. Hvoll air temperature data were collected from 1 July 2018 to 7 October 2019.

5.3 Spring Water Discharge

Spot measurements of stream velocity were taken from streams emerging from the six main study springs between 20–30 May 2019 and used to calculate discharge. Water levels provided a lower-cost method to provide information on the periodicity of spring discharge patterns and response to hydroclimatic events while we were unable to be at the study site.

5.3.1 Spring Discharge

The spread of the data allowed three clearly defined categories of discharge to be identified: Low discharge springs ($0 < Q \leq 25$ L/s), Medium discharge springs ($0 < Q \leq 50$ L/s), and High discharge springs ($Q > 50$ L/s) (Figure 5.5). An ANOVA test indicated that there was a significant difference ($F_{(2, 110)} = 2074$, $p < 0.001$) in the discharge values of these groupings. A Tukey HSD test indicated that High discharge (*Mean* = 73.1 L/s, *SD* = 8.6), Medium discharge (*Mean* = 37.5 L/s, *SD* = 3.7, and Low discharge (*Mean* = 4.61 L/s, *SD*=1.5), averages were significantly different from one another.

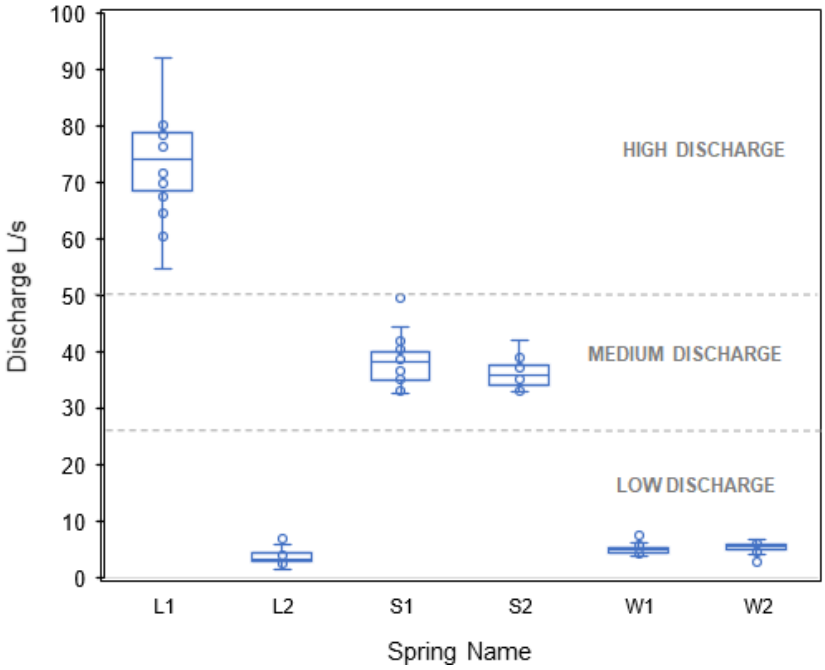

Figure 5.5 Boxplot showing the spread of discharge (L/s) calculated for the six main study springs at the Hvoll study site, 20–30 May 2019. L1 and L2 were located in the lava field/wetland, S1 and S2 were located at the border of the sandur, and W1 and W2 were located in the wetland.

The spring with the largest pore width (L1) had the highest discharge. The maximum discharge measured at L1 was 92.1 L/s. Medium sized sandur springs, S1and S2, had maximum discharge values of 48.6 and 42.7 L/s, respectively. The lowest discharge springs were L2, W1, and W2, and they had maximum discharge values of 7.0 L/s, 8.0 L/s and 6.9 L/s, respectively. The springs with higher discharge values also had a wider range in calculated discharge (Table 5.4). According to the classification of springs based on annual average discharge rate introduced by Meinzer, (1923), the low discharge springs are fifth magnitude (1 to 10 L/s) springs, and the medium and high discharge springs in this study are fourth magnitude springs (10 to 100 L/s). However, it should be noted that the discharge data from the current study is only from 10 days in May and cannot be a true representation of annual average discharge.

Table 5.4 Summary of maximum, minimum, and range of discharge (L/s) measured at the streams emerging from six different springs across the Hvoll study site, 20–30 May 2019.

	L1	L2	S1	S2	W1*	W2*
Max discharge L/s	92.1	7.0	49.5	42.1	8.0	6.9
Min discharge L/s	54.6	1.4	32.8	33.1	4.0	2.7
Discharge range L/s	37.5	5.6	16.7	9.0	4.0	4.2

* fed by multiple small springs

Four episodes of rainfall occurred during the May 2019 field period. Episode 1, from 19 May 1800 h to 21 May 0100 h delivered 4.8 mm of precipitation to Kirkjubæjarklaustur and 6.4 mm precipitation to Hvoll. Cluster 2, from 22 May 0700 h to 23 May 0800 h delivered 4.8 mm of precipitation to Hvoll, and only 0.6 mm to Kirkjubæjarklaustur. Episode 3, from 23 May 1900 h to 24 May 1400 h had 2.6 mm of precipitation at Kirkjubæjarklaustur and 4.2 mm of precipitation at Hvoll. Finally, Episode 4, from 28 May 0400 h to 28 May 1600 h had 4.6 mm of precipitation at Kirkjubæjarklaustur and 0.8 mm of precipitation at Hvoll.

The largest spring, L1, showed the greatest change in discharge over time. There was a 32.5% increase in discharge measured at L1 39.6 hours after the peak in the Episode 1 rainfall. Discharge

remained high during the Episode 2 and 3 rainfall events. The lowest discharge (54.6 L/s) at L1 was measured 176 hours after the peak on 21 May. A 41.4% increase occurred between 30–31 May, 54.9 hours after the peak in Episode 4 rainfall.

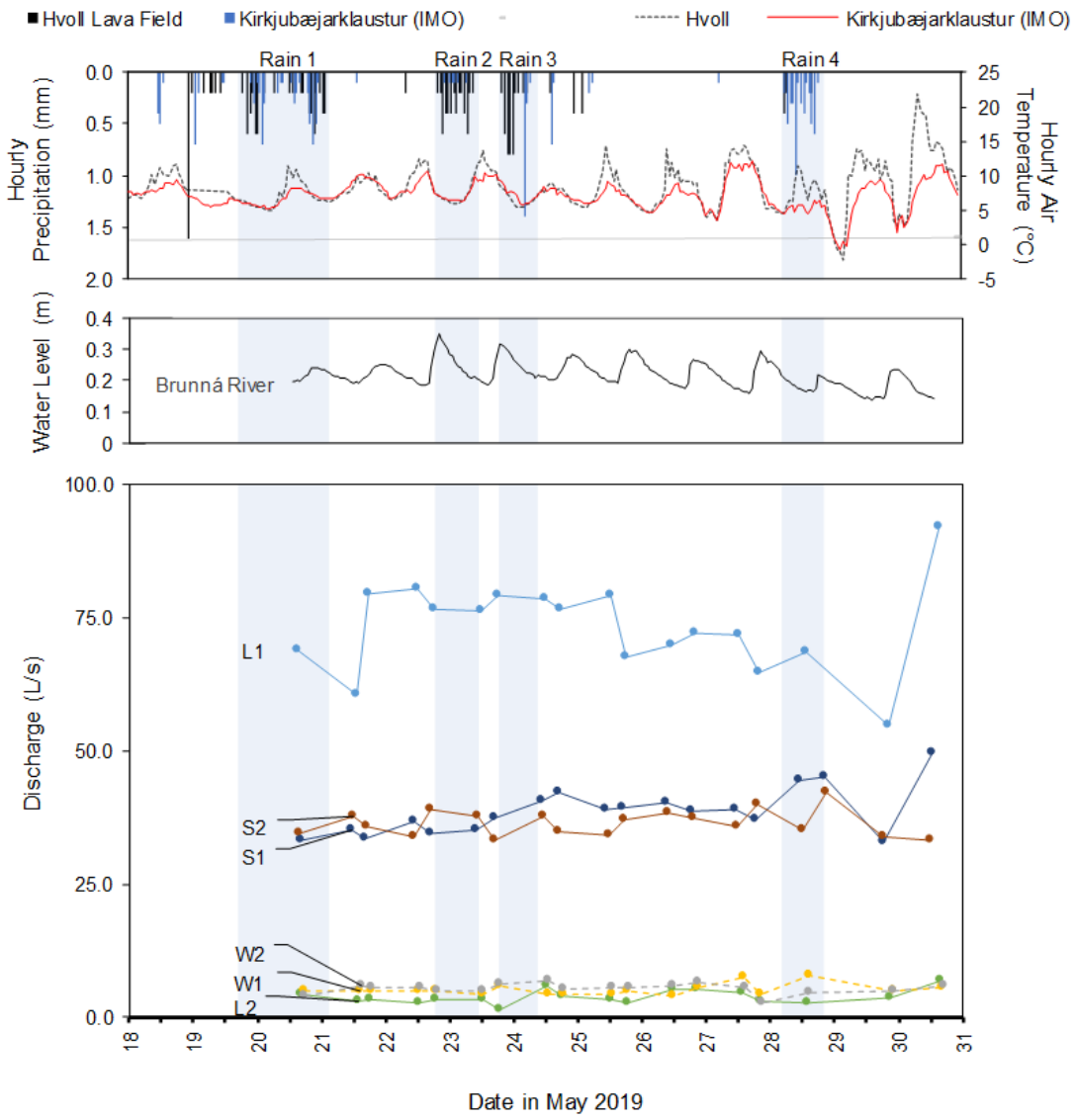

Figure 5.6 Discharge (L/s) calculated from velocity measurements taken across cross-sections of streams emerging from the 6 main study springs L1, L2, S1, S2, and W1, W2A (lower diagram). Also plotted are hourly air temperature (°C) and precipitation totals (mm) (top diagram), and Brunná River water levels (m) (middle diagram).

The small springs with low discharge had an average range in discharge between 5.6 L/s and 4.0 L/s. The highest two measurements of discharge at W2A occurred after the second and third rainfall events. No change was observed 25–31 May except for a low of 2.7 L/s measured on 28 May. The highest discharge (8.0 L/s) at W1 occurred on 28 May. The second highest discharge of 7.6 L/s was measured at 1355 h on 27 May. All other velocity measurements were between 4.0 and 5.7 L/s. The lowest discharge at W2 (2.7 L/s) was measured on 27 May at 2248 h. The two highest discharge values (6.9 and 6.3 L/s) were recorded on 24 May and 25 May, following the second and third rainfall episodes. S2 experienced a 16.6 % increase in discharge 12.9 hours after the peak in rainfall in Episode 4. S1 experienced a 17.3% increase in discharge 12.5 h after the peak in rainfall in Episode 4. The lowest discharge at S1 was measured on 29 May 29, 21.7 hours after the previous peak in discharge.

5.3.2 IMO River Discharge

A regression of hourly data from 20–30 May 2019 revealed that Djúpá River discharge was the best predictor of Brunná River water levels ($R^2 = 0.70$). This was expected because both rivers receive inputs from the same glacial margin (Síðujökull). All IMO rivers increased in discharge following rainfall events (Figure 5.6). Djúpá had the steepest recession limbs following rainfall and returned to near-base flow conditions within 1–4 days. July and August precipitation events resulted in a higher peak in discharge than events earlier in the year. The spring fed river, Þverárvatn, took 1–5 days to return to near baseflow conditions. Gierlandsá had a more gradual recession limb, (especially in April), taking 5 to 10 days to return to baseflow conditions.

Different trends in baseflow (inputs from groundwater) were observed for each river. Baseflow calculated for the glacial-fed river, Djúpá, had a similar trend as Kirkjubæjarklaustur daily average air temperature ($R^2 = 0.64$). At air temperatures below 5°C, there was a weak relationship between air temperature and discharge. Similarly, MacDonald et al (2016), found that river discharge in a glacier-fed river near Virkisjökull (63.95° N, 16.81° W) was highest when weekly air temperatures were above 7°C.

Over 50% of the recharge to proglacial groundwater springs at Virkisjökull, comes from glacial meltwater (Dochartaigh et al., 2019) .

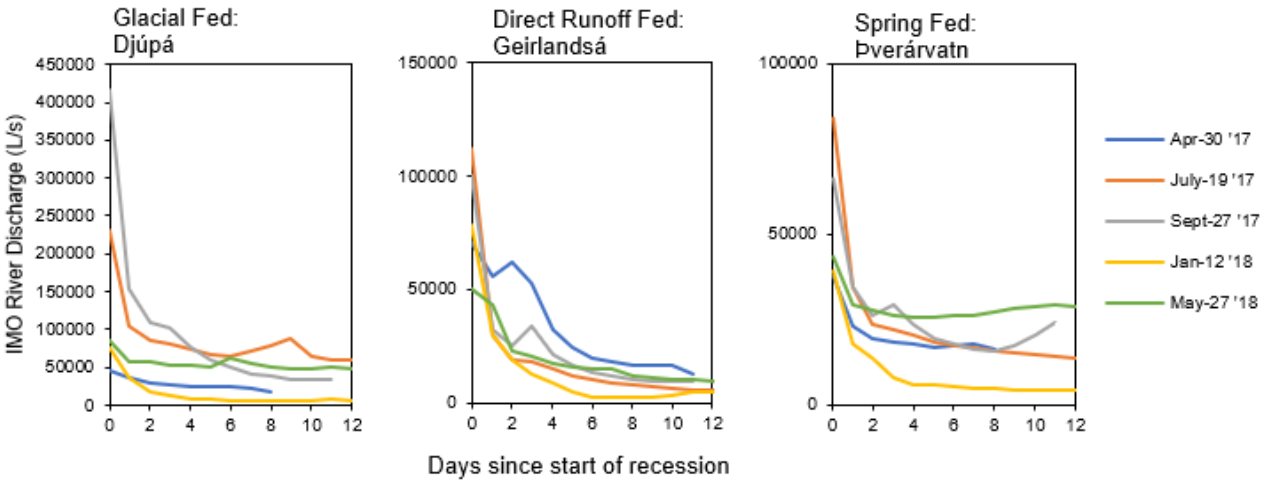

Figure 5.7 Plot of IMO daily average river discharge up to 12 days following the peak in in discharge. Recession periods are assumed to end when the discharge reaches a plateau. New peaks in rainfall did not occur during each recession period.

The summer peaks in discharge and baseflow at Djúpá and Skaftá indicate a similar influence of water contributions from ablation driven glacial melt (Figure 5.8). During winter months with an average temperature below 5°C, the daily discharge and calculated baseflow at Djúpá was at its lowest and experienced little variation. A similar trend could be expected for the Brunná River. It should be noted that if the Brunná River receives a larger volume of input from groundwater discharge, seasonal patterns in discharge may be dampened, as was seen with the Skaftá River (Figure 5.8). The Skaftá River is predicted to receive 80% of its discharge from groundwater recharged by Vatnajökull subglacial waters (Flowers et al., 2003). The larger catchment basin with more storage, resistance, and longer flow paths, causes subglacial groundwater to be slower and have a dampened response than surface runoff flows (Finger et al., 2013).

Increases in discharge at the direct-run off river, Gierlandsá, corresponded with periods of heavy and/or prolonged rainfall and spring melt. Between January 2017 and October 2019, the highest average

monthly discharge at Gierlandsá was 29,629 L/s, in April 2019. This was 8.2 times higher than the lowest average monthly discharge measured in June 2019 (3627 L/s). Gierlandsá, had low discharge during the summer (June to September) and winter months (December to February) when rainfall was low or falls as snow. Similar seasonal trends have been shown for runoff rivers in east and northwest Iceland (Jónsdóttir & Uvo, 2009).

Like the other rivers, the spring-fed river, Þverárvatn, had peaks in discharge following rainfall events. Monthly discharge was calculated from hourly discharge from January 2017 to November 2018. Discharge was highest in June and May, and lower during the winter months. The highest (83617 L/s) daily average discharge occurred on 19 July 2017, following a heavy rainfall event. The other rivers also showed a large spike in discharge on this day (Figure 5.8). The calculated discharge allowed separation of groundwater component of discharge from other sources such as runoff. The spring-fed river had peaks in baseflow in early June 2017 and 2018. The lowest baseflow (2959 L/s) occurred on 6 January 2018. Spring baseflow at Þverárvatn begins to increase earlier than the other IMO rivers, steadily increasing from the January low, to a high of 20738 L/s on 8 June 2018 representing a 601% increase. Immediately after reaching this high, baseflow steadily declined, to a low of 5698 L/s on 28 August 2018. The seasonal trends in discharge and baseflow indicate that spring snow melt and rainfall, as well as fall rainfall are important drivers of surface flow and groundwater recharge (Figure 5.8).

The IMO discharge data indicate that groundwater springs in South Iceland might be expected to experience a climb in discharge in the spring months as aquifers are replenished by precipitation and snowmelt. Direct runoff experiences episodic increases in discharge during periods of heavy rain and snowmelt. However, wet soils or surfaces with low permeability are needed to limit infiltration and initiate runoff (Carey & Woo, 2001). Larger contributing catchments and subsurface routes with higher storage, and longer travel-times allow more sustained discharge for spring-fed rivers. A peak in spring discharge may be seen in early June, with the potential for another during heavy fall rains. Inflows or

recharge from the glacial-fed Brunná River are most likely to follow a similar trend as the Djúpá River, with discharge increasing with air temperatures and baseflow peaking at the beginning of August.

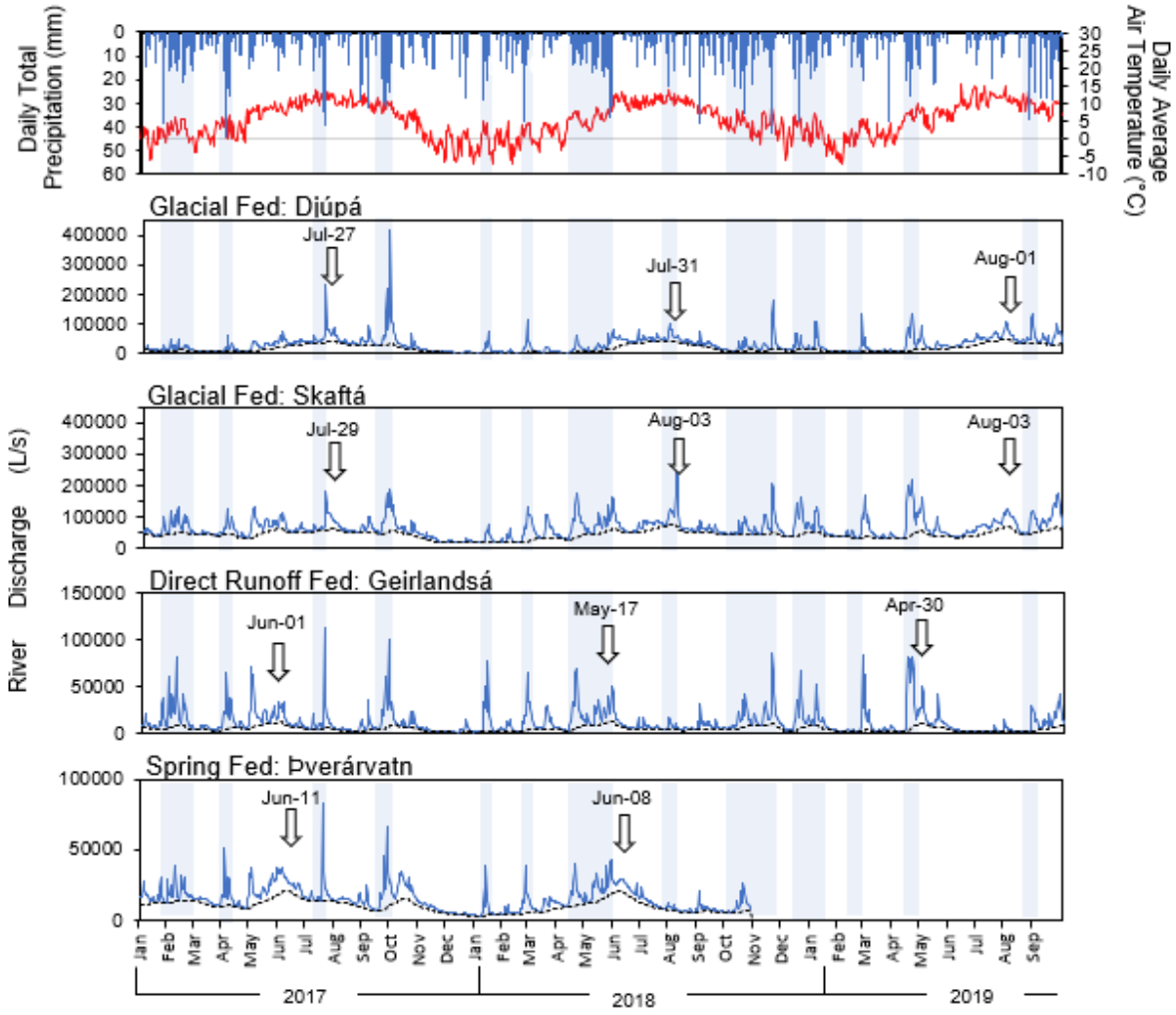

Figure 5.8 Discharge from two glacial rivers, a runoff river, and a spring-fed river. All data are from the IMO (2019). Air temperature and precipitation are for Kirkjubæjarklaustur, Iceland. Blue dotted line shows the daily average discharge and the black dotted line shows the baseflow based on the daily average discharge. Y axis range for direct runoff and spring fed rivers is smaller to allow visualization of trends. Arrows indicate dates of maximum calculated baseflow (groundwater contribution) for each year.

5.3.3 Hvoll Spring-fed River Water Levels

Two periods of water levels were recorded at Hvoll during this study: July 2018 to May 2019, and May 2019 to October 2019. The pattern of Hvoll spring water levels was plotted with IMO discharge data for two glacial rivers (the Djúpá and Skaftá), a runoff river (Gierlandsá), and the spring-fed river (Þverárvatn) (Figure 5.9 and Figure 5.10). This allowed visualization of similarities and differences in the timing of discharge and baseflow peaks in the study springs.

Between July 2018 and May 2019, water levels were recorded at two rivers in the wetland at Hvoll. Runoff Spring (located in the wetland near W2) had a peak in baseflow water levels on 15 September 2018. The W2 stream had a peak in baseflow the following day. The IMO river baseflows were receding on the 16 September 2018, with Djúpá, Skaftá, Gierlandsá, and Þverárvatn at 37%, 66%, 43%, and 29% of their baseflow peaks, respectively. From March to May 2019, Runoff Spring had an overall decline in water level while all IMO rivers were experiencing an increase in discharge (Figure 5.9).

W2 and Runoff Spring are both slow flowing, shallow streams. Air temperature was more important in influencing seasonal trends in baseflow at these locations than precipitation or glacier melt. Runoff Spring had an inverse relationship with air temperature, indicating that evaporation and saturation of the surrounding wetland may have played a role in modifying groundwater supply water to this location. W2 had a similar inverse relationship with temperature between 25 June and 14 January (Figure 5.9). But, water levels began to increase as early as 18 February 2019. This earlier increase in baseflow was similar to the trend seen for the spring-fed river Þverárvatn, which had a gradual increase in discharge starting in January and peaking mid-June in 2017 (Figure 5.8). In January 2017 and February 2019, daily temperatures averaged above 0°C. Groundwater recharge during this time would be from local snowmelt and rainfall. At Djúpá (Figure 5.8) and other glacial-fed rivers in Iceland, glacial discharge is low during the winter months and begins to spike in May (de Woul et al., 2006; Macdonald et al., 2016).

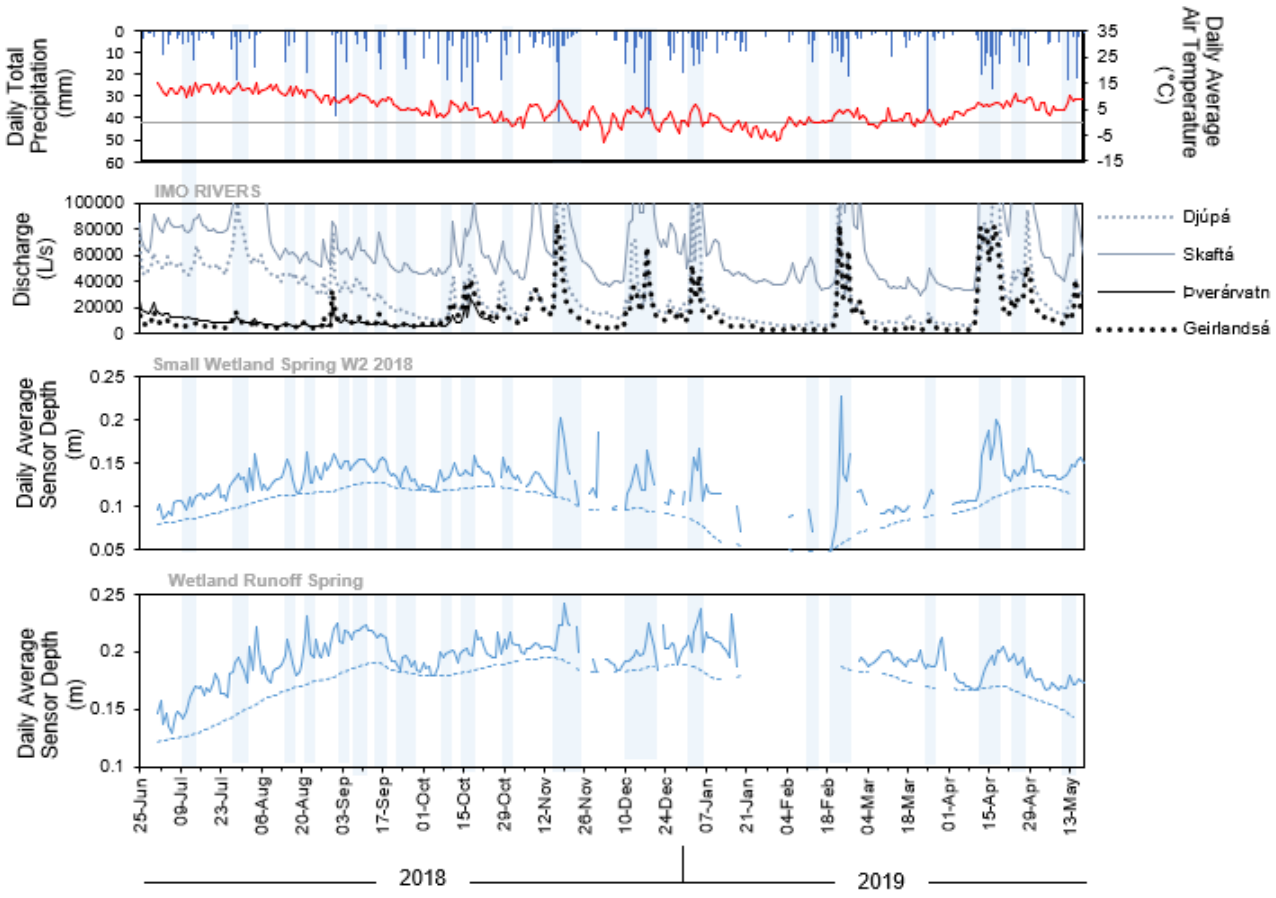

Figure 5.9 Daily average sensor depth for the streams emerging from wetland spring (W2) and from a river fed by a conduit replenished by runoff and overland flow. "Baseflow" water level calculated by EcoHydRology package in R, is shown by the blue dotted line in the bottom two graphs.

Water level and calculated baseflow both increased at W2 and Runoff Spring following rainfall events (Figure 5.9). The calculated percent increase due to recharge (PIR) helped identify where water level increases occurred while controlling for changes to the calculated baseflow water levels. An ANOVA test indicated that daily total precipitation category has a significant effect ($F_{(3,223)} = 4.043$, $p = 0.008$) on average water level PIR at the small wetland spring W2. Days with more than 10 mm of precipitation (*Mean* = 30%, *SD* = 25.3) resulted in a larger average PIR than was seen on days with no precipitation (*Mean* = 18.4%, *SD* = 18.5) as well as days with 0.1–1 mm of precipitation (*Mean* = 19.1%, *SD* = 8.8). In contrast, daily total precipitation category had no effect ($F_{(3,226)} = 2.16$, $p = 0.09$) on the

average PIR at Runoff Spring. A closer investigation of hourly responses to rainfall events revealed that increases in water level do not always occur on the same day as a rainfall event (Figure 5.10).

The recession limbs for different rain events indicated that both springs showed variation in the response to isolated rain events, with some events creating a spike in water levels while others did not (Figure 5.10). Following the 21 August 2018 rain event, both springs had a peak in water level, 25 hours after the peak in rainfall. On 17 November 2018, 42.5 mm of precipitation fell at Kirkjubæjarklaustur in a single day. Six hours after the peak in rainfall, W2 water levels reached a peak that was 21% higher than pre-event levels. Runoff Spring reached a maximum after 45 hours.

The runoff spring is located at a lower elevation than W2. If these springs were fed by a high local water-table, the lower elevation spring would be expected to reach its peak first. If W2 is fed by a high water table, it does not intersect the runoff spring. Runoff Spring may be fed by a combination of groundwater and overflow from higher elevation streams. The nearby streams must reach a level that exceeds their banks before overflow can occur, causing a delay in water level peak measured at Runoff Spring. Additionally, soil properties such as saturation and porosity can influence the timing and amount of runoff water that reaches the Runoff Spring (Carey & Woo, 2001). During wet periods (September 2018 and April 2019), water levels at Runoff Spring remained high between rainfall events. Water stored in soils may travel downslope, gradually delivering water to the Runoff Spring. The development and loss of flow pathways with soil wetting and drying may also contribute to the gradual recession limb during wet periods (Carey & Woo, 2001).

Groundwater in Iceland can be replenished quickly following rain events as rain quickly flows over glaciers and penetrates highly permeable young lava fields (Kiernan et al., 2003; Jónsdóttir, 2008). The 2-day recession limb at W2 was typical of the IMO glacial and spring-fed rivers (Figure 5.7).

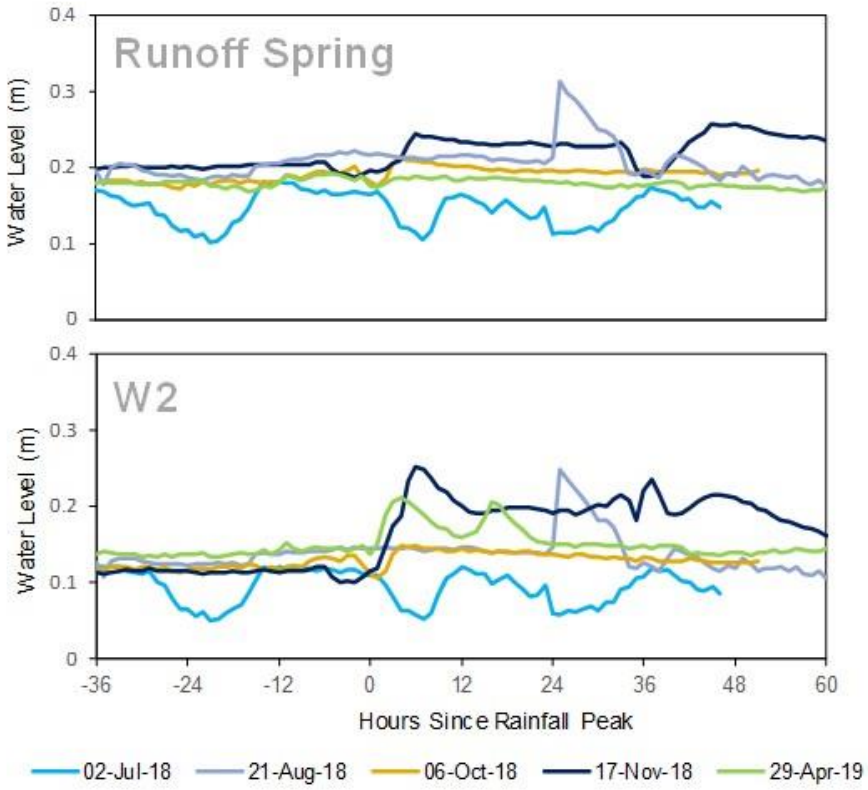

Figure 5.10 Water levels at the small wetland springs, Runoff Spring, and W2, are shown for four different rainfall events. If more than 1 mm of precipitation was delivered as part of a subsequent rainfall event, the recession limb was terminated.

Water level data were collected for a small wetland spring, W1, and a medium sandur spring, S1, and plotted with Hvoll air temperature and Kirkjubaejarklaustur precipitation data from 20 May to 29 September 2019 (Figure 5.11). The water level at the medium sandur spring S1 never went lower than the lip of the spring (0.53 m above the data logger). The threshold for flooding at the stream emerging from the small wetland spring, W1, needed a water level above 0.25 m to exceed the bank heights, and was not exceeded. Flow was maintained at both locations.

The daily average (Figure 5.11) and hourly (Figure 5.12) water level data showed that S1 had a more rapid and higher amplitude peak and recession limb following precipitation events than W1. On 26 July 2019 10.4 mm of precipitation fell at Kirkjubæjarklaustur, and an additional 23.7 mm fell over the next 4 days. An initial peak in S1 water levels was measured 22 hours after the peak in rainfall, and a second occurred on 29 July, 77 hours after the peak in rainfall. This second peak may have been caused

by inflow of water from the Brunná River. On 29 July, an average temperature of 17°C was measured at Hvoll and increases in discharge were measured at glacial-fed rivers Skaftá and Djúpá. The further in-land spring, W1, did not experience a similar peak but maintained its levels at an average of 7% above pre-rain levels between 16 to 30 July. This was a particularly rainy period, with a total of 73.3 mm of precipitation measured at Kirkjubæjarklaustur.

Both W1 and S1 had an increase in water levels on 26 August. A total of 37.3 mm of precipitation was recorded at the Kirkjubæjarklaustur weather station on 25 August. Over the next 6 days, an additional 63.5 mm of precipitation fell. S1 hourly water levels peaked at 82% above pre-event levels on 27 August, 36 hours after the peak in rainfall. Again, W1 did not experience a distinct peak in water level (Figure 5.12). W1 water levels through the week averaged 18% higher than 24 August daily average water level.

From 18–20 September 2019, a total of 58.8 mm of precipitation fell at Kirkjubæjarklaustur. On 23 September, S1 had a daily average water level 45% above pre-event (17 September) levels. W1 had a more gradual response. On 18 September, W1 daily average water levels jumped to 13% above pre-event levels, then gradually climbed to 31% above pre-event levels by 26 September. In comparison, the glacial fed river Djúpá had a peak in discharge on 23 September, and the runoff river, Gierlandsá, had a peak in discharge on 25 September 2019.

These events indicate that the wetland spring has a relatively stable discharge. Compared to S1 and the IMO rivers, W1 had a delayed and dampened response to precipitation events. The medium sandur spring, S1, had a more rapid response, to precipitation, especially following precipitation events in the late summer and early autumn, when glacial melt is at a peak. The nearby glacial-fed Djúpá river had peaks in discharge that corresponded with those at S1, and the Brunná River would have had a similar response. No spikes in water temperature were observed at S1 during these times (see section 5.4.1), suggesting that flooding or backflow from the Brunná river did not play a role in the increased water levels measured at S1. However, the water level logger may have been installed too deeply to pick up

temperature changes from mixing of surface inflows. The S1 spring appears to be a ceiling spring from a lava tube (Figure 5.2E). These conduits have low resistance and are able to rapidly transport large volumes of water (Kiernan et al., 2003).

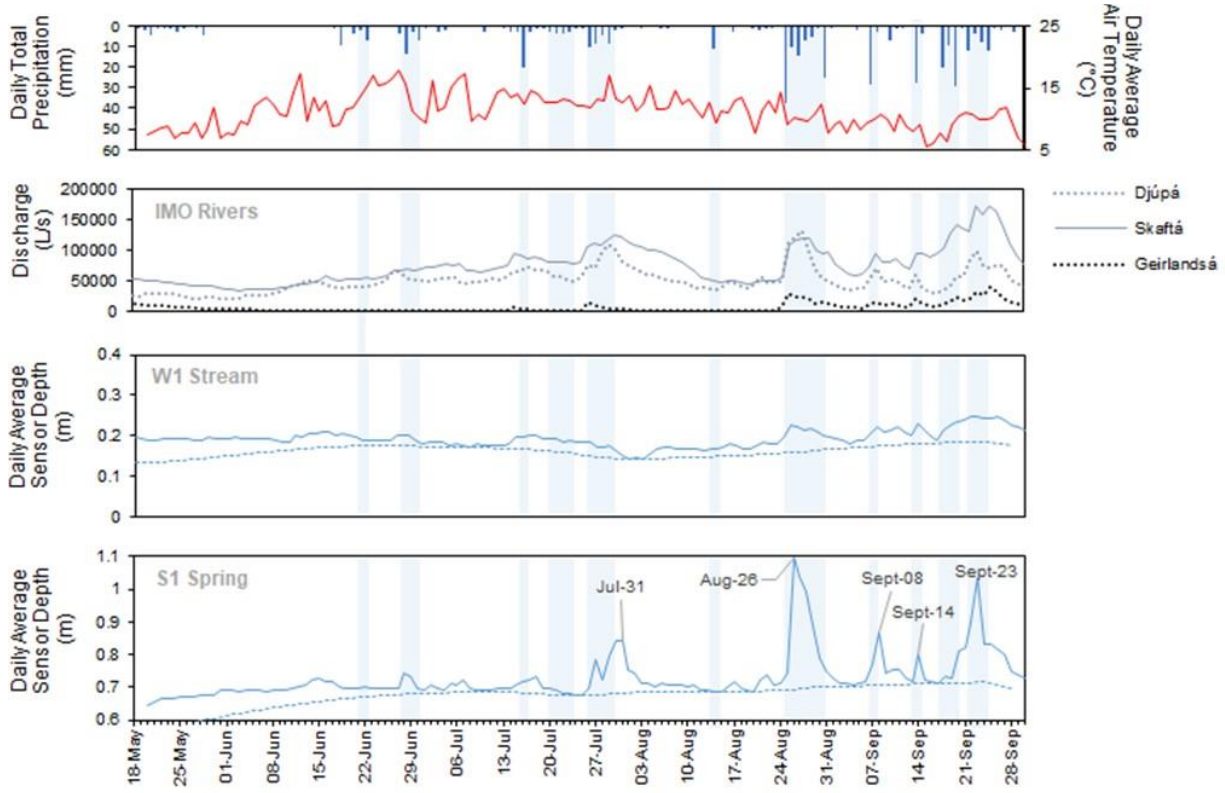

Figure 5.11 Daily average water levels for the stream emerging from the W1 wetland spring for the S1 sandur spring pore.

An ANOVA test indicated that the daily total precipitation has a significant effect ($F_{(3,128)}$ =5.2, p = 0.0019) on average water level percent increase due to recharge (PIR) at the medium sandur spring S1. Days with more than 10 mm of precipitation (*Mean* = 15.7%, *SD* = 17.5) resulted in a larger average PIR than days with no precipitation (*Mean* = 6.3%, *SD* = 4.2). Similarly, total precipitation category had a significant effect ($F_{(3,128)}$ = 5.7, p = 0.0011) on the average PIR at the stream emerging from the small wetland spring W1. Like S1, days with more than 10 mm of precipitation (*Mean* = 24.7%, *SD* = 9.4) resulted in a larger average PIR than was seen on days with no precipitation (*Mean* = 17.2%, *SD* = 9.9).

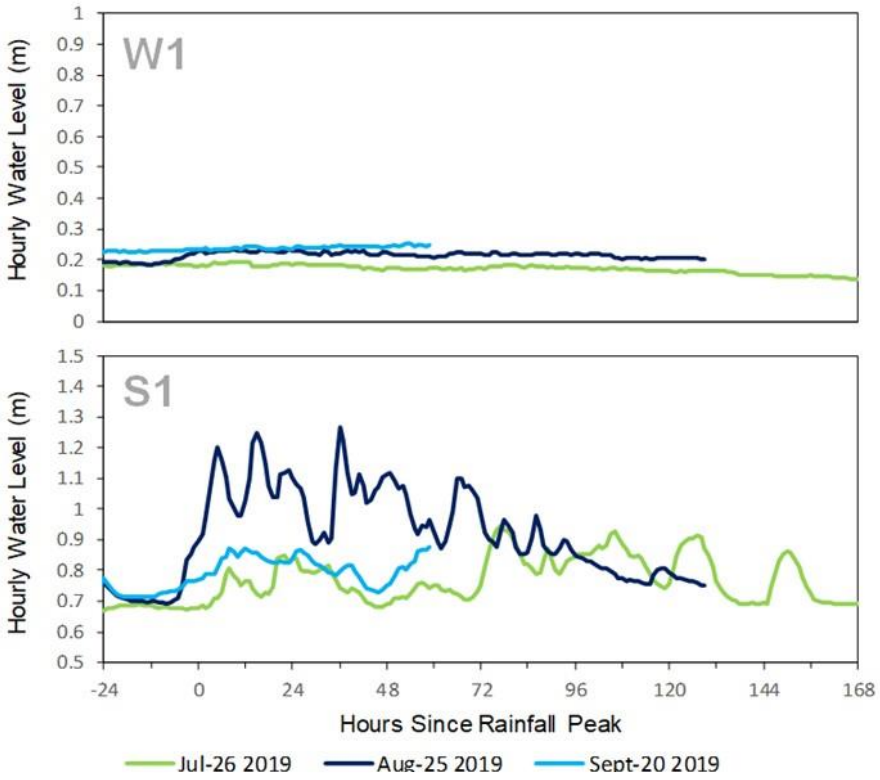

Figure 5.12 Response of springs to different rainfall events. The peak in rainfall occurs at 0 hours on the x-axis. The curves were terminated when another rainfall event occurred or after 7 days.

Table 5.5 Results of Student *t*-tests (assuming equal variances) for the percent increase due to recharge (PIR) compared between the stream emerging from the small wetland spring W2 and the runoff spring. PIR values between the medium sandur spring S1 and the stream emerging from a small wetland spring W1, were also compared.

	Daily Total Precipitation Category							
Spring	0 mm		0.01-1.0 mm		1.01 -10.0 mm		> 10.0 mm	
	Mean PIR	*p*	Mean PIR	*p*	Mean PIR	*p*	Mean PIR	*p*
W2	20.9	<0.001	19.1	0.0018	23.2	<0.001	30.0	<0.001
run	12.8		13.2		14.5		13.9	
S1	6.3	<0.001	9.0	<0.001	9.2	<0.001	15.7	0.10
W1	17.2		23.7		20.0		24.7	

Although the absolute value of water level increase was higher for S1, two-sample Student *t*-tests indicated that relative to their baseflows, W1 had a higher increase when less than 10 mm of total precipitation fell (Table 5). This is not surprising, given that water levels at W1 took longer than S1 to return to baseflow levels following precipitation events.

The daily maximum levels occurred from 1900 h to 0100 h at S1 and between 2200 h and 0400 h at W1. Between 19 May and 30 September 2019, the daily maximum water levels occurred outside of the typical time range 24 times for S1, and 29 times for W1. Many of the outlying points occurred up to 3 days after a day that received more the 10 mm of precipitation, accounting for 75% of S1 outliers, and 41% of W1 outliers. Daily minimum levels occurred most often between 0600 h and 1200 h for S1 and between 0900 h and 1700 h for W1. Air temperatures reached a maximum closer to midday. The timing of the daily maximum and minimum water levels do not correspond to the diurnal trend in latent heat flux (maximum: 1300 to 1400, minimum: 0000 to 0300) estimated at Hvoll in July and August, 2016 (Scheffel & Young, submitted). Thus, local evaporative losses do not explain the diurnal trend, as was expected for flowing streams where the source (groundwater) is not exposed to incoming radiation.

The diurnal variation in water level can be an indicator of influence from glacial melt (Tristram et al., 2015). Diurnal variation in water level were plotted for periods without rain in May, July, and August. At S1, there was almost no variation in diurnal water level in May 2019. Diurnal amplitude increased over the summer, reaching a high in mid-August, 2019 (Figure 5.11). Macdonald et al., (2016) observed a similar trend for a river fed by glacial melt from Falljökull, Southeast Iceland. Later in the spring and summer, diurnal trends were observed due to the diurnal trend of glacial ablation, causing melt during the day. At Hvoll, the peak in diurnal water level was not observed until later in the day as it would have taken time for water to travel from the glacial margins to the location of the S1 spring. The waters most likely travelled by the Brunná River and contributed to the spring by backflow of surface water or shallow, sub-surface flows. Well transects placed 40 cm below the ground surface have previously shown this process at Hvoll (sandur to wetland water transfer) (see Scheffel & Young, submitted).

In contrast, the present study showed that W1, a spring closer to the center of the wetland, had little diurnal or monthly variation in water level (Figure 5.13). Groundwater streams in Iceland often have low diurnal variation in flow (Crossman et al., 2011). Diurnal trends tend to be dampened for water stored and transported deeper in a sediment vertical profile (Tristram et al., 2015) or through groundwater aquifers (Jónsdóttir & Uvo, 2009).

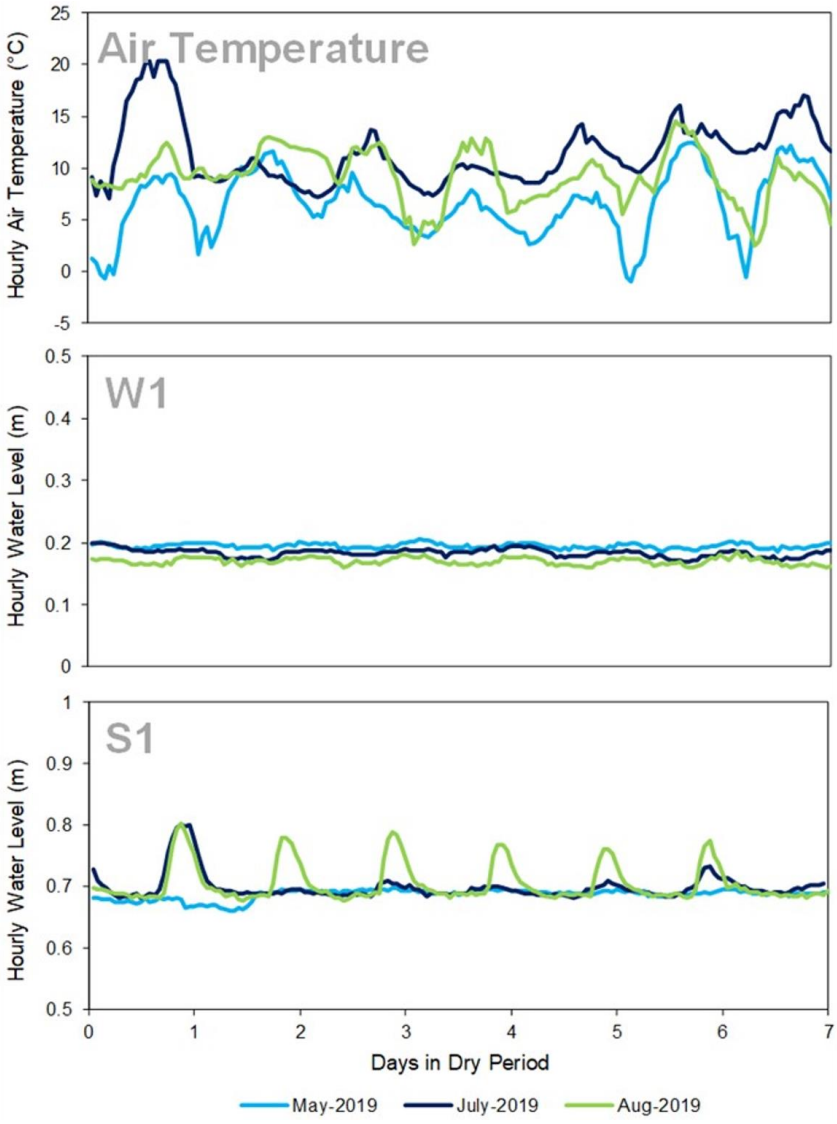

Figure 5.13 Water level in the week during dry periods (negligible rainfall) from May, July, and August 2019. The top graph shows water levels for W1 and the bottom graph shows water levels for S1. At least two days without rain occurred before the start of the data shown above. Air temperature recorded at the

Hvoll field site are shown to illustrate the difference in timing of peaks and troughs in air temperatures and water levels.

5.4 Water Quality

5.4.1 Water Temperature

For the period of 19 May–30 September 2019, the average water temperature for springs ranged from 4.0 to 5.0°C. The lowest average temperature was measured at S1, followed by S2, S3, S4, S5, Oxbow spring, L3, L1, W2, W1, L2. The small Sandur spring, S6, was the exception, having an average temperature of 7.3°C (*SD* = 1.2). This spring had a near-stagnant flow and was observed receiving backflow from the Brunná River on 7 October 2019. This was also the only spring to experience periodic drying during dry spells throughout the summer of 2019.

The medium sized Sandur springs had the coldest water temperature with the least variation in the study. S1 and S2 had average temperatures of 4.0°C (*SD* = 0.1) and 4.30°C (*SD* = 0.2), respectively. S3 had an average temperature of 4.4°C (*SD* = 0.2). The medium sized Sandur springs had no daily variation in water temperature on most days (S1 had a daily average range of 0.0°C, while S2 and S3 were 0.3 and 0.2°C, respectively). This is typical of groundwater fed streams, which show weak diurnal variation and little thermal responses to hydrometeorological events (Brown & Hannah, 2008).

The temperature of springs was expected to increase following precipitation events due to increased inputs from local runoff and groundwater recharge. Figure 5.14 shows the daily average temperature of all gauged streams between 29 May and 30 September 2019. The S4, S5, L1, and the logger before the Oxbow spring all had gradual increases in temperature peaking around 3–12 June. There was a climb in air temperature during this period, with a mean peak of 17.3°C on 12 June. This indicates an influence of air temperature on the spring water (temperature logger) warming. These same springs also had an increase in temperature between 28 June and 6 July, when daily average Hvoll air temperatures were 17.3°C and 16.6°C, respectively.

Another noticeable peak in water temperature occurred on 23 September 2019 for Sandur springs S2, S3, S4, S5, S6. This followed a heavy rainfall event that peaked on 20 September, when 29.2 mm of precipitation fell at Kirkjubæjarklaustur. All Sandur springs except for S1 experienced a 36-39% increase in water temperature compared to pre-rainfall temperatures. There was a spike in water level recorded at S1 on 23 September, suggesting possible flooding from the Brunná River. Scheffel & Young (submitted) found that Brunná River water levels range from 5 to 9°C. Mixing of Brunná and spring waters at the surface could explain the spike in the Sandur springs. The water logger at S1 was 0.5 meters below the lip of the pore, and the upwelling of large volumes of groundwater may have prevented mixing of Brunná River waters at this depth.

On 22 September 2019, there was a spike in temperature measured at the logger downstream of the Oxbow spring, but not upstream of it. The Oxbow spring is located at the bottom of the slope at the edge of the lava field. L3 is also located on a slope at the edge of the lava field, and a slight increase in water temperature was also seen during this period. These springs may receive runoff flow during heavy rainfall but this could not be directly observed during this study.

Some springs were more sensitive to precipitation than others, and the effect of different categories of total daily precipitation (0 mm, 0.1–1 mm, 1.1–10 mm, and > 10 mm) on daily average water temperature was analyzed for the six main study springs.

There was a significant effect of rainfall on daily average water temperature at the wetland springs W1:($F_{(1,188)} = 7.1$, $p < 0.01$) and W2 ($F_{(3,129)} = 3.4$, $p = 0.02$). A Tukey HSD test revealed that days with over 10 mm of precipitation resulted in a change in water temperature for both W1 and W2. The average water temperature for W1 increased from 4.9°C ($SD = 0.4$) on dry days, to 5.3°C ($SD = 0.2$) when more than 10 mm of daily total precipitation fell. Likewise, the average water temperature for W2 increased from 4.9°C ($SD = 0.3$) on dry days, to 5.2°C ($SD = 0.2$) when more than 10 mm of daily total precipitation fell. Changes in water temperature following rainfall events are an indication of inputs from rainfall runoff (Hamdan et al., 2016).

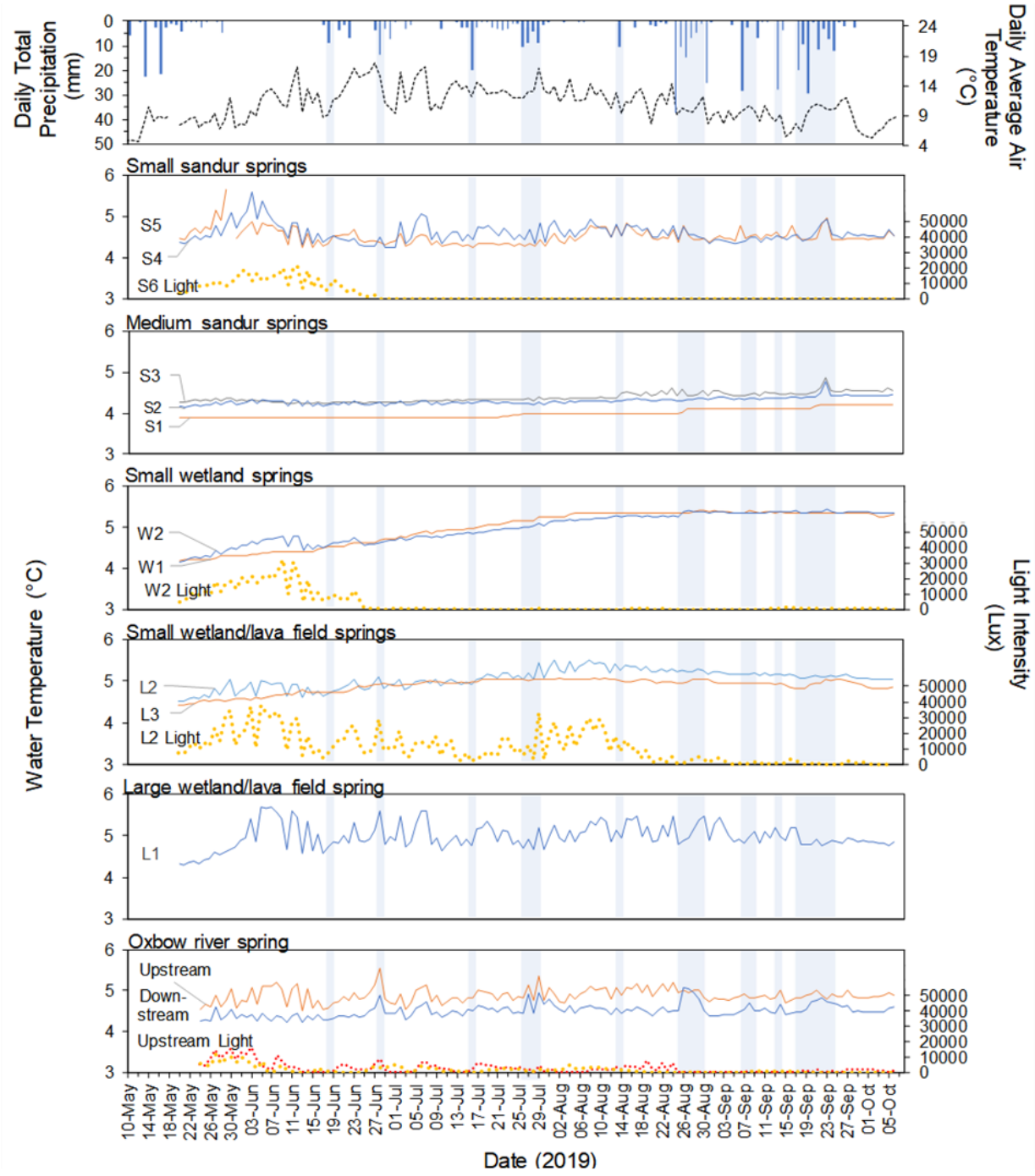

Figure 5.14 Daily average temperature measured at streams emerging from 10 springs across the study area, inside the pore of one spring (L1), and on either side of a spring in a stream. S6 is not shown. Days with total precipitation over 10 mm are highlighted by light-blue bars. Daily average temperature is from Hvoll, and daily total precipitation is from Kirkjubæjarklaustur, Iceland IMO station.

However, in this case, the higher temperatures observed on days with more rain may be explained by a large proportion of days with over 10 mm of rain occurring later in the season when water temperatures were higher. Both W1 and W2 had a gradual increase in water temperature over time, with May being over 1°C cooler than August and September (Figure 5.14).

Water temperatures for small springs in the wetland located closer to the lava field did not show any significant change in average temperature with rainfall (L2: $F_{(3,129)} = 0.83$, $p = 0.48$; L3: $F_{(3,129)} = 2.66$, $p = 0.051$). Water temperature for the large spring, L1, near the lava field was affected by rainfall ($F_{(3,128)} = 7.1$, $p < 0.01$). For rain categories; 0.01–1 mm (*Mean* = 4.9, *SD* = 0.3). 1.01–10 mm (*Mean* = 4.9, *SD* = 0.3) and > 10 mm (*Mean* = 4.9, *SD* = 0.2) daily total rainfall resulted in cooler average water temperatures compared to days with no rain (*Mean* = 5.1, *SD* = 0.3). At the beginning of a rain event, raindrops are several degrees cooler than the ambient air but within 1°C of the ambient air after the peak in rainfall (Byers et al., 1949). At Hvoll, time periods (hours) with rainfall averaged 11.4°C (*SD* = 4.6) between 19 May and 1 October 2019. Therefore, inputs from local rainfall and runoff might be expected to cause an increase or little change in water temperatures. No significant change was seen in average air temperatures measured at Hvoll when compared across precipitation groupings ($F_{(3,129)} = 1.68$, $p = 0.18$). L1's lower water temperatures on days with rainfall may therefore be an indication of older groundwater being pushed out following aquifer recharge.

Sandur water temperatures were not influenced by precipitation. The ANOVA tests found no significant difference between mean water temperature for the different rain categories tested on S2, S3, S4, and S5. The medium sandur spring, S1, appeared to be influenced by precipitation ($F_{(3,129)} = 4.32$, $p = 0.006$), with temperature increasing from an average of 4.0°C (*SD* = 0.08) during dry days, and 4.1°C (*SD* = 0.1) when more than 10 mm of precipitation falls in Kirkjubæjarklaustur. However, a closer look at the data (Figure 5.14) revealed that there are many days with rain but no corresponding increase in temperature. Overall, this spring had very stable temperatures across the study period (Figure 5.15).

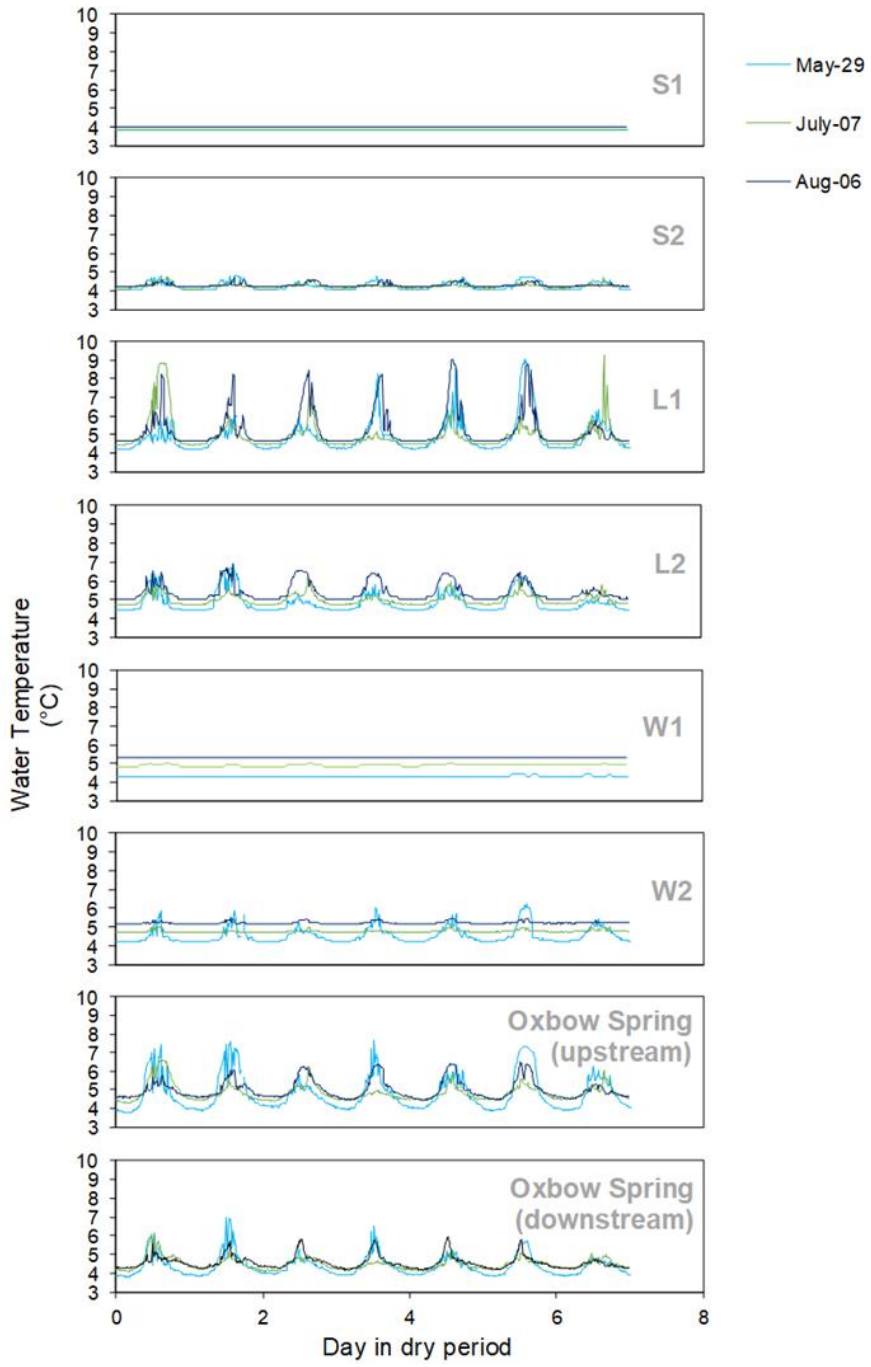

Figure 5.15 Diurnal variation in water temperature for three different dry periods in Spring and Summer 2019 measured at the six main study springs (S1, S2, L1, L2, W1, W2) and upstream and downstream of the Oxbow spring. Rain had not fallen for at least two days before the start of each dry period. The loggers at S1 and W1 were installed perpendicular to the water surface, while all other locations had the logger installed facing upward, toward the water surface. Diurnal variation can be an indicator of warming from incoming solar radiation or diurnal pattern of inflows from other sources.

At S1, hourly temperatures were recorded from 19 May to 7 October 2019, and 3.9°C made up 46.6% of the observations, 4.0°C made up 23.8%, and 4.1°C and 4.2°C made up the other 29.5%. These temperatures increased steadily over time, not episodically in response to precipitation. However, because more rain events occurred in September, when water temperatures were already elevated, a misleading correlation between rainfall and daily average water temperature was identified.

The water levels for S1 showed a gradual increase in diurnal change from May to August 2019 (Figure 5.13). When water temperature was plotted for the same period, no diurnal variation was observed (Figure 5.15). No seasonal change in diurnal water level (Figure 5.13) or water temperature (Figure 5.15) was identified for W1. The diurnal variation at L1, L2, S2 and the Oxbow spring loggers also showed little seasonal variation in diurnal temperature change (Figure 5.15). Diurnal variation before the Oxbow spring was higher than after this spring, suggesting a moderating effect of the spring on water temperatures in the Oxbow stream.

Temperature loggers that also collected light data indicated that daily peaks in water temperature are related to peaks in incoming light intensity. A linear regression indicated that 78.9% of the variation in daily maximum temperatures at the small Lava field spring L2 could be explained by the daily maximum light intensity. Daily range in light intensity could explain 88.5% of the variation in daily range in temperatures at L2. For the logger upstream of the Oxbow spring, 60.7% of the daily range in water temperature could be explained by the daily range in light intensity. Daily range in light intensity dropped off after 19 August 2019 for both the upstream logger and the L2 spring.

At the small Wetland spring, W2, light intensity dropped off by 25 June 2019. Before 25 June, light intensity averaged 13927 lux. A visit to the field site on 7 October revealed a large algal growth had formed on top of the logger. Thin layers of algae coated the other loggers, and long threads of algae floated on the stream surfaces of near springs with low flow (Figure 5.16). After 25 June, light intensity at W2 averaged 217 lux. Water temperatures that were measured by HOBO U20 pressure transducers had the lowest range in temperatures: the medium Sandur spring S1 had a daily average range which was

negligible and the small Wetland spring S1 had a daily average range of 0.1°C. In contrast, the logger at the large Lava field spring L1 had the highest average daily range of 2.0°C. The high discharge at L1 appeared to keep the logger free of algae.

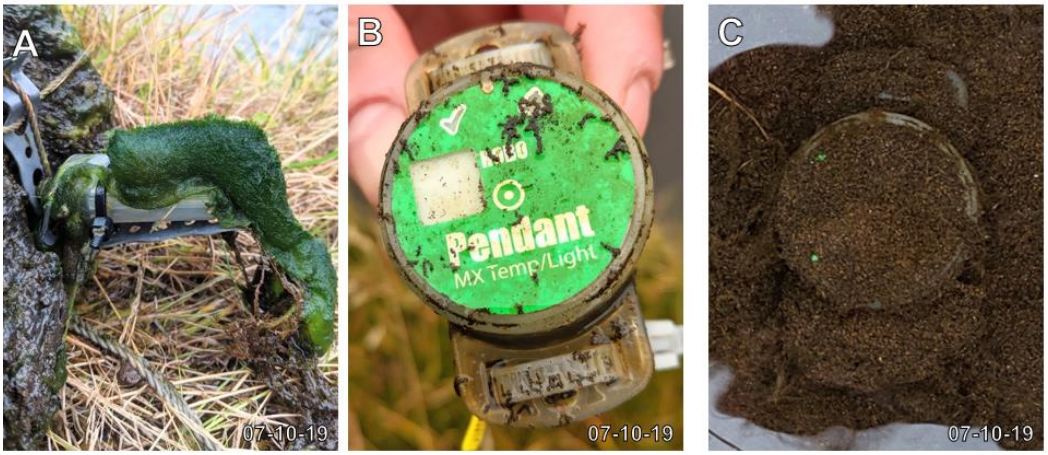

Figure 5.16 Light sensors for A. W2, B. Upstream of the Oxbow spring, and C. Downstream of the Oxbow spring. The light sensor at W2 had a large algae growth, observed on 10 October 2019. At the Oxbow spring, the upstream logger was relatively clear of debris, while the downstream logger was covered by sediment.

5.4.2 Water Chemistry

Electric conductivity (EC) for the springs at the study site ranged from an average of 47.1–50.7 µS/cm (Table 6). This is low in comparison to the EC typically reported for springs and spring-fed rivers across Iceland, which can be between 54 and 214 µS/cm (Gíslason et al., 1998; Levy, 2015). Fresh glacial waters have an EC between 10–20 µS/cm and rain water in the study had an EC of 13.4 µS/cm), but interactions with soils and rock causes EC to increase overtime. The Brunná River water chemistry had a conductivity of 36.4 µS/cm, which was within the range (28–50 µS/cm) previously reported for glacial rivers in Southeast Iceland (Gíslason et al., 1998) . The EC of the Brunná River dropped following rain events, indicating inputs from precipitation runoff. EC was stable for the springs throughout the study period (Figure 5.17).

Table 5.6 Water chemistry values measured between 20–30 May 2019 at the Hvoll study site. All water chemistry values are averages except for pH which is the mode.

Location	Temp (°C)	pH	EC (µS/cm)	Salinity (ppt)
Brunná River	7.2	6.5	36.4	0.016
Rain	12.2	6.2	13.4	0.005
Lava field 1	4.2	6.5	47.6	0.021
Lava field 2	4.2	6.4	48.9	0.022
Sandur 1	4.1	6.6	47.1	0.021
Sandur 2	4.1	6.7	47.9	0.022
Wetland 1	4.4	6.1	50.0	0.022
Wetland 2	4.2	6.1	50.7	0.023

The pH of springs at the study site were slightly acidic, ranging from 6.1 to 6.6 (Table 6). Cold water springs across Iceland have pH values between 7.4 and 9.3 (Guðmundsdóttir et al., 2019). Cold water springs with an acidic pH have not been reported for Iceland. Studies have shown that water may have a more acidic pH if (non-explosive) volcanic ash and positive ion salts are present (Gislason et al., 2011). However, the salinity of all springs was ~ 0.02 ppt, indicating fresh water. Runoff rivers on tertiary basalt formations of the Eastfjords have a pH range of 6.1–7.2 (Gíslason et al., 1998).

If springs were fed by runoff, a change in water chemistry would be expected following precipitation events. From 20–30 May 2019, temperature, EC, and salinity were stable for the main study springs (Figure 5.17). The mode pH values for the small Wetland springs, W1(6.1) and W2 (6.1), was lower than for rain (6.2). On 30 and 27 May 2019, the warmest days of the water chemistry study period, the Wetland springs W1 and W2 had a dip in pH. The two Sandur springs S1 and S2 had an increase in pH 24 hours after the 28 May rainfall event. This is a curious response as rainwater has a lower pH and the Brunná River has a similar pH compared to the Sandur springs.

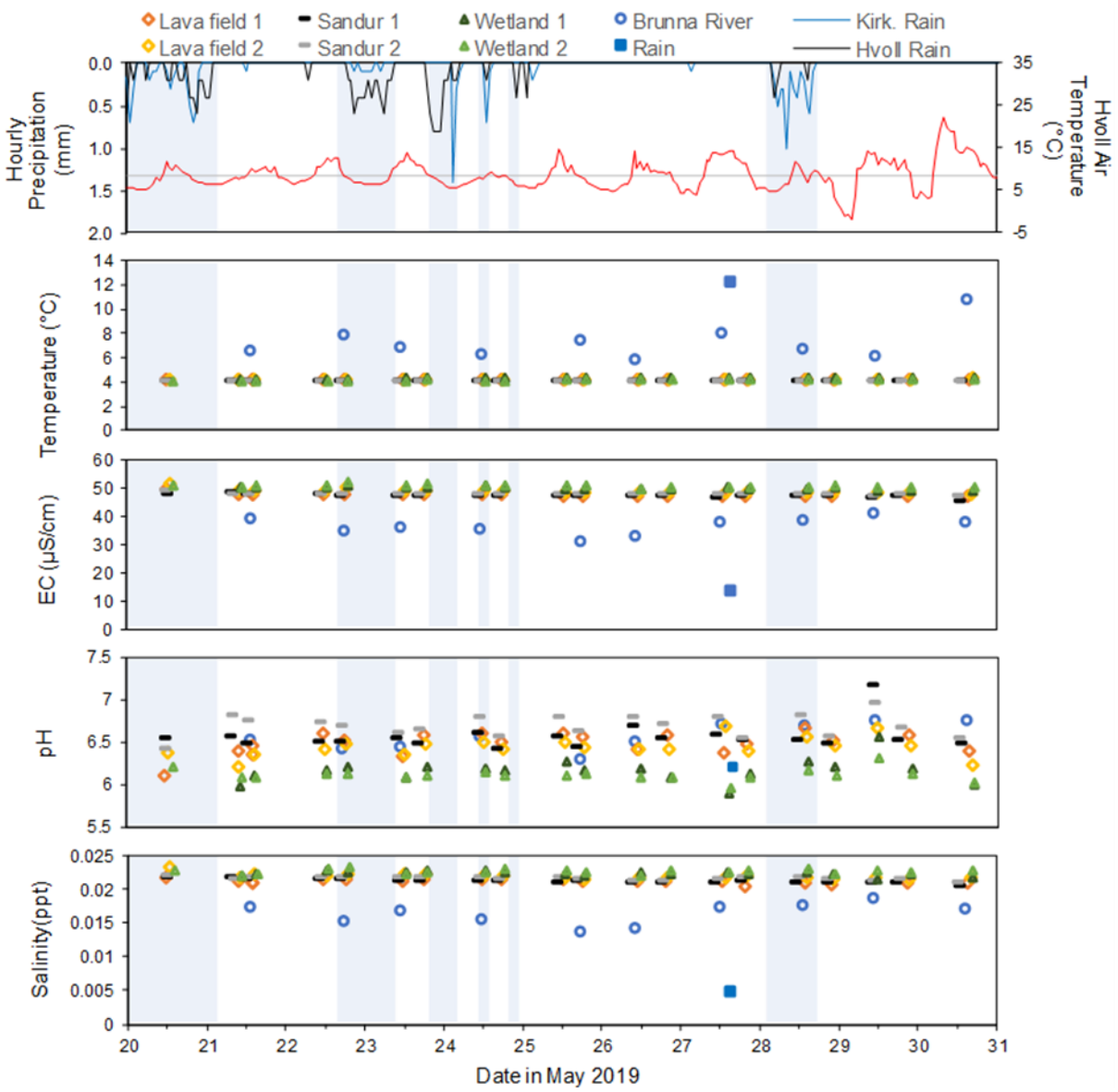

Figure 5.17 Plot of various water chemistry variables (temperature, electrical conductivity, pH, and salinity) measured at six different springs (W1, W2, S1, S2, L1, L2) across the study site between 20 May 2019 and 30 May 2019. Water chemistry data for the Brunná River (blue circles) are also shown. Water chemistry for precipitation captured by the rain collector between 19 May and 27 May 2019 and measured on 27 May is indicated by blue squares.

5.4.3 Stable Water Isotope Analysis

The stable water isotope signatures for the six main study springs and the Brunná River were plotted in graphs to compare the $\delta^{18}O$ and $\delta^{2}H$ compositions between samples taken across time and under different conditions (wet or dry) (Figure 5.17 and Figure 5.18). The 6 study springs and Brunná River plotted lower on the LMWL than the rainwater from the study.

The springs had a narrow range in isotopic signatures ($\delta^{18}O$: -66.47 to -64.83, - $\delta^{2}H$: -9.80 to -9.54). In comparison to other studies of stable isotopic signatures in Iceland, these values were most similar to groundwater and spring water from the lower sandur of the Virkisá catchment in Southeast Iceland, although the springs in the present study plotted higher above the LMWL (Macdonald et al., 2016).

In May, the Brunná River had a similar isotopic signature as the springs which clustered around $\delta^{18}O$ -65.70 and $\delta^{2}H$ -9.56 (Figure 5.19). On 7 October 2019 the Brunná River had a higher isotopic depletion, plotting lower on the LMWL than all other points in the study. The fall isotopic signature for the Brunná River is situated within the range reported by Macdonald et al. (2016) for glacier meltwater. This indicates that in May, spring water may be the main contributor to Brunná River water levels, but as glacier melt increased through the summer months, meltwater provided a larger proportion of the flow. This is typical for glacier-fed rivers in Iceland (Macdonald et al., 2016).

The Brunná River, Lava field springs L1 and L2, as well as the Wetland spring W1 plotted below the LMWL on 27 May 2019 (Figure 5.18). Groundwater stored and transported through basaltic rock can experience chemical reactions with the rocks that elevates $\delta^{18}O$ but not $\delta^{2}H$ (although elevated temperatures may be required for this reaction to occur) (Kristmannsdóttir & Ármannsson, 2004). Many of the points also fell slightly above the LMWL. This may be caused by $\delta^{2}H$ enrichment or $\delta^{18}O$ depletion.

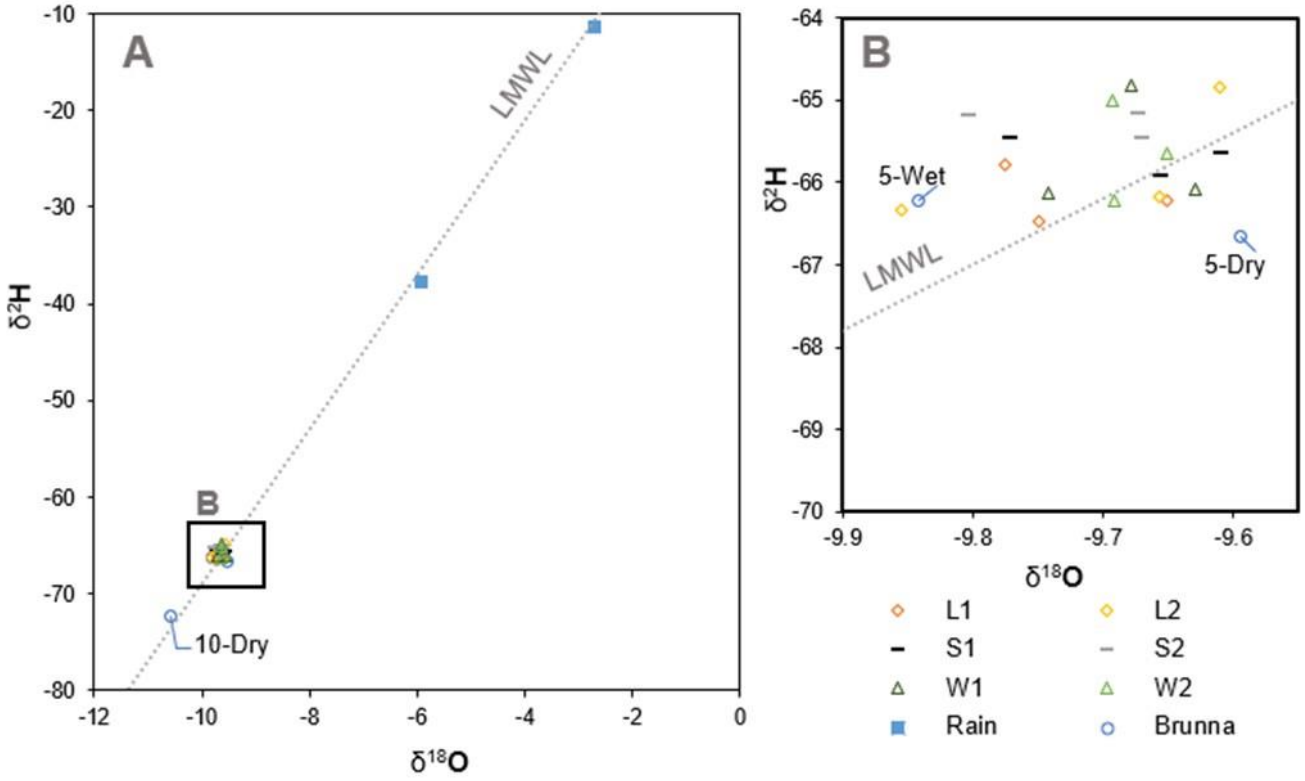

Figure 5.18 Isotopic composition of waters sampled from six springs, the Brunná River and rain water at the Hvoll study site. A. shows all points. B is enlarged to show the spread of datapoints that clustered around -66, -9.7. Refer to Appendix A for individual plots.

A two sample Student *t*-test of spring stable isotope signatures indicated that precipitation causes a significant increase in δ^2H but not in $\delta^{18}O$ (δ^2H: $p = 0.002$, $\delta^{18}O$: $p = 0.30$). The δ^2H signature for the study springs shifted from an average of -66.9 (*SD* = 0.4) under dry conditions to slightly more enriched: -65.2 (*SD* = 0.4) on the day following rainfall. There was a significant ($p = 0.002$) depletion in δ^2H from May (*Mean* = -65.5, *SD* = 0.5) to October (*Mean* = -66.1, *SD* = 0.3). Increased δ^2H can be caused by H_2S exchange or the hydration of silicates (Serno et al., 2017).

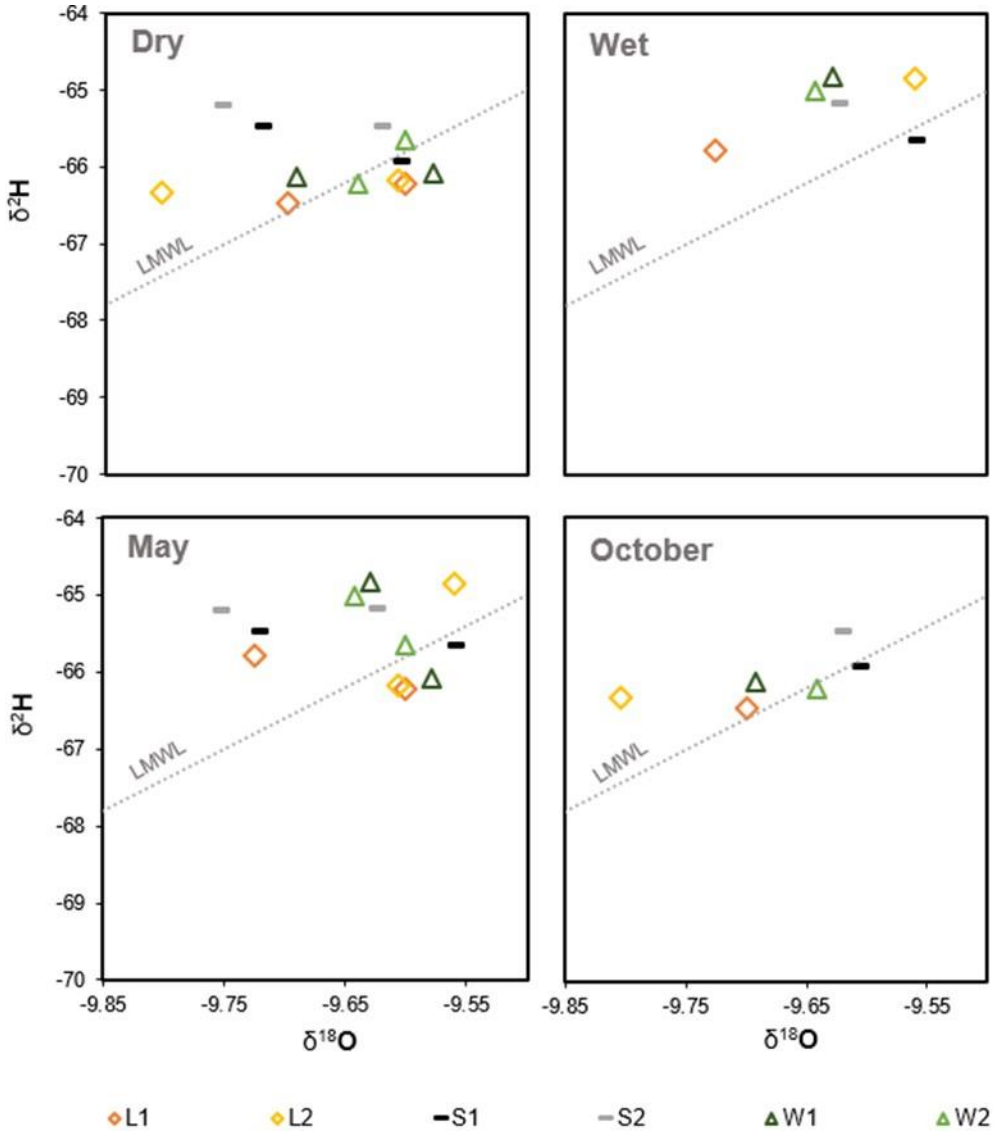

Figure 5.19 Oxygen and Hydrogen isotope composition of waters sampled from springs W1, W2, S1, S2, W1, and W2, and the Brunná River. Top left graph shows isotopic signatures for samples taken under dry conditions (27 May and 7 October 2019), Top right graph shows isotopic signatures for samples taken on 21 May 2019, following a day of rain. The bottom left shows isotopic signatures from all samples taken in May 2019 and the bottom right shows isotopic signatures for all samples taken in October 2019.

SECTION SIX: DISCUSSION

6.1 Introduction

This study investigated the hydrological function of springs in a landscape that is the intersection between a sandur, wetland, and a lava field in Southeast Iceland. Most of the springs in this study did not show a strong seasonal or episodic change in water level, temperature, or quality. The stability of groundwater and spring-fed river temperature (Brown & Hannah, 2008; Kaandorp et al., 2019), discharge (Jónsdóttir & Uvo, 2009), and water levels (Crossman et al., 2011) has been well documented by previous studies. In contrast, glacier fed rivers show stronger diurnal and seasonal variation (Brown et al., 2006; Crossman et al., 2011). At the study site, diurnal trends were seen at the glacial-fed Brunná River, and seasonal trends were observed for Djúpá River, and Skaftá River discharge. The episodic and diurnal trend in water level measured at one of the Sandur springs, S1, provided evidence of a hydrological linkage to the neighbouring Brunná River. This is in agreement with previous research at the Hvoll study site that identified subsurface water flows moving across a hydrological gradient from the sandur to the neighbouring wetland (Scheffel & Young, submitted). All study springs and the May Brunná River water samples had a stable isotope signature similar to lower sandur groundwater and spring water found in other studies (Macdonald et al., 2016).

6.2 Spring Formation

The geomorphology of the springs observed in the field provided some insight into the types of springs at the study site. The locations of springs all occurred near slopes at the edge of the Núpahruan lava field and in the wetland. Most of the springs in the wetland and the small springs in the sandur emerged through interstitial spaces in rubbly lavas, where spaces in the surrounding rock were filled with soil or sandur sediments. The small springs formed flowing streams. According to Springer & Stevens (2009) classification of springs, these springs would be termed rheocrene springs, and the rivers they feed may be called springbrooks, or springruns. Cold-water, rheocrene springs have been previously reported in Southeast Iceland by Guðmundsdóttir et al. (2019).

Springs in Iceland commonly occur along the margins of lava fields and the routes for their storage and transmission through lava fields has been previously discussed by Kiernan et al. (2003). The porosity of basaltic lava is low and this generates surface flows during precipitation events. Surface flows and falling precipitation can penetrate deeper layers of the lava field through openings such as cooling contraction cracks, joints, fissures, and lava rise pits (Kiernan et al., 2003). Water may then be stored or transferred through lateral and horizontal networks of these voids, as well as through interstitial spaces, lava tubes, and gaps that form between successive lava flows. Ash, debris, and alluvial and aeolian sediment may be deposited between successive lava flows and work their way into interstitial spaces over time, influencing the hydraulic conductivity and storage capacity of the substance (Kiernan et al., 2003). Older lavas often have lower permeabilities caused by processes of mineralization, compaction, and introduction of sediment, which occur over a long timeframe (Gíslason et al., 1996). The differences in permeabilities and hydraulic conductivities of different age lavas, and layers of sediments can create semi-confined conditions for water in aquifers.

Water in semi-confined and confined aquifers can be pushed out at lower elevations by hydrostatic pressure (Kresic & Stevanovic, 2010). Studies of basaltic springs in the Cascades of Oregon show that springs emerge at contacts between basalt and sedimentary deposits due to the difference in their permeability (Manga, 1998; Burns et al., 2015). At the Hvoll study site, differences in permeability would exist between and within different aged lava flows, along with various sediments. For example, the infiltration of water through the sand and gravel of the sandur at the study site is 40 cm/hr (9.6 m/day) and much lower (up to 3.4 cm/hr or 0.816 m/day) when layers of compacted ash are present (Scheffel & Young, submitted). Springs at the edges of lava flows also form where aquifers within and between successive lava flows become exposed by erosion or the termination of the layers above (Burns et al., 2015).

The water chemistry and stable isotope analysis in this study provide some indication of the size and conditions of the aquifer that feeds the springs. Cold, groundwater springs across Iceland have been

reported with pH values from 7.4 to 10 (Gudjonsson, 1990; Guðmundsdóttir et al., 2019). Groundwater that has experienced long-term interactions with the basaltic bedrock in Iceland tend to have more alkaline pH values as high as 9–10 (Gudjonsson, 1990). However, the waters at the study site, in May 2019, were slightly acidic, ranging from 6.1–6.5. Acidic spring water has not been previously reported for cold, fresh, groundwater springs in Iceland. Interactions with volcanic ash where proton salts are high may reduce the pH of water (Gislason et al., 2011). Strong and frequent winds in this region can erode and carry ash from Skeiðarársandur, creating sandstorms in this region (Arnalds et al., 2016; Scheffel & Young, submitted). Some of the ash is likely deposited on the lava fields, and over time, washed into the crevasses where rainwater flows (Arnalds et al., 2016). The pH data points to an aquifer where water has a short residence time but there is a higher interaction with volcanic ash, in comparison to other Icelandic springs.

The stable water temperatures throughout the summer months suggest that the springs are fed by older groundwater. All springs, except S6, fell within a temperature range of 4.0 and 5.0°C between May and October 2019. This is the same range of temperatures of groundwater springs in southwest Iceland observed by Muanza (2016) and falls within the 3 to 6°C range known for Icelandic groundwater (Sigurdsson & Einarsson, 1988). Stable temperatures that are close to the annual average air temperature, are reflections of large aquifers with long residence times (Manga, 1999). Springs at the study site had temperature ranges less than 2°C between May and September 2019. Air temperatures at Hvoll averaged 5.0°C in 2018, and spring water temperatures ranged from 4.0°C to 5.0°C on average. Electric conductivity (47.6 to 50.7 μS/cm) was also low compared to spring-fed rivers in previous studies (Gíslason et al., 1998). This agrees with the pH data in indicating that the water has had less time to interact with the bedrock in this region (Gudjonsson, 1990).

The spring water chemistry (temperature, EC, and salinity) was stable throughout changes in precipitation and air temperature 20–30 May 2019. Groundwater-fed streams have stable water chemistry through time, while runoff -fed streams experience increases in temperature and decreases in EC and

salinity following rainfall events due to inputs of warmer, fresher rainwater. The increase in pH observed for the Sandur springs following the 28 May 2019 rainfall event is an indication that older groundwater was pushed out of the aquifer following recharge by the rainfall runoff. Rainwater that recharges an aquifer can result in discharge of older groundwater by pressure propagation (Figure 6.1). Old water is stored deeper in aquifers (Kresic & Stevanovic, 2010). The pressure from new inputs of water may have forced the older groundwater out of the springs with deeper connections to the aquifer, such as the medium sized springs.

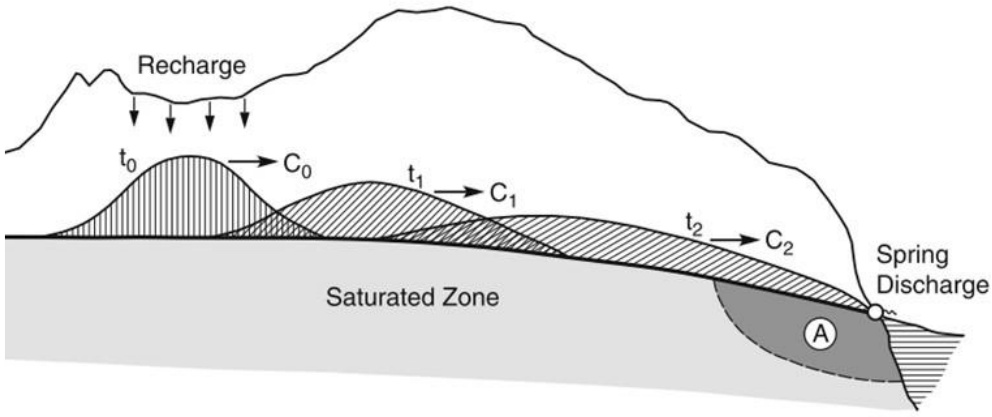

Figure 6.1 Pressure propagation following a recharge event, where a groundwater "wave" is propelled forward. The velocity, C_n of the wave is shown across time t_n, where $C_n > C_n > C_n$ due to the hydraulic gradient. The wave travels the slope of the saturated zone, and discharges at the spring. A volume of older groundwater, close to the spring, will be under pressure and discharge from the spring. Source Kresic & Stevanovic (2010), modified from Yevjevich, (1981).

At least one of the Sandur springs, S1, appeared to be a ceiling spring from a lava tube. The end of the tube is visible in Figure 5.1H. Lava tubes, are able to transport large volumes of water, rapidly through the landscape (Kiernan et al., 2003). However, the constant water temperature following rainfall events further supports that this spring is fed primarily by deeper groundwater. The ceiling spring may have formed overtime as water travelling through the tunnel scoured the sides of the tube and caused erosion of the walls. Being close to a walking trail, it is possible that human activity may have weakened

its structure. Both S3 and S6 springs became larger from May 2019 to October 2019. Some structural collapse occurred around the locations where the small rocks with temperature loggers were placed. By October 2019, bed collapse was also beginning to occur at S2, where we stood for the May 2019 velocity tests.

Springs can often be found at the edges of alluvial fans as erosion carves out the edges of the river terrace (Kresic & Stevanovic, 2010). The formation of these springs may have been accelerated by the collapse of the old lava rock below the sandur, as many springs were found with rocks near their openings. These rocks may have been deposited along the edges of the sandur during jökulhlaup floods. Many of the springs found along the edge of the spring were covered by large rocks. The collapse of the structure below may open new pathways for water to flow freely, where hard packed sediments and rock were previously.

The medium Sandur springs had the most stable water level and temperatures in the study, but all springs had a similar water chemistry and stable water isotope signature. This suggest that the springs are likely fed by the same, or closely connected aquifers, with a residence time that is long enough for rainwater to cool to 4–5°C but not so long that reactions with basaltic rock are able to raise the pH (Figure 6.2).

Local runoff and subsurface flows may play a role in the seepage springs at the study site. The Oxbow spring was a seepage spring at the bottom of a steep, eroded streambank at the edge of the lava field. The temperature of the water after the spring was consistently cooler than the upstream logger. On 22 September 2019, following a period of heavy rainfall, a spike in water temperature was observed downstream of the spring but not upstream, indicating that local runoff may feed this spring during periods of heavy precipitation. The runoff likely flows through/under the lava field and is pushed to the surface where the bank is cut low enough to intersect the below-ground flow-path. Additionally, diurnal water level changes measured at S1 support Scheffel & Young's (submitted) findings from 2016, for shallow sub-surface flows moving down a hydrological gradient from the sandur towards the wetland.

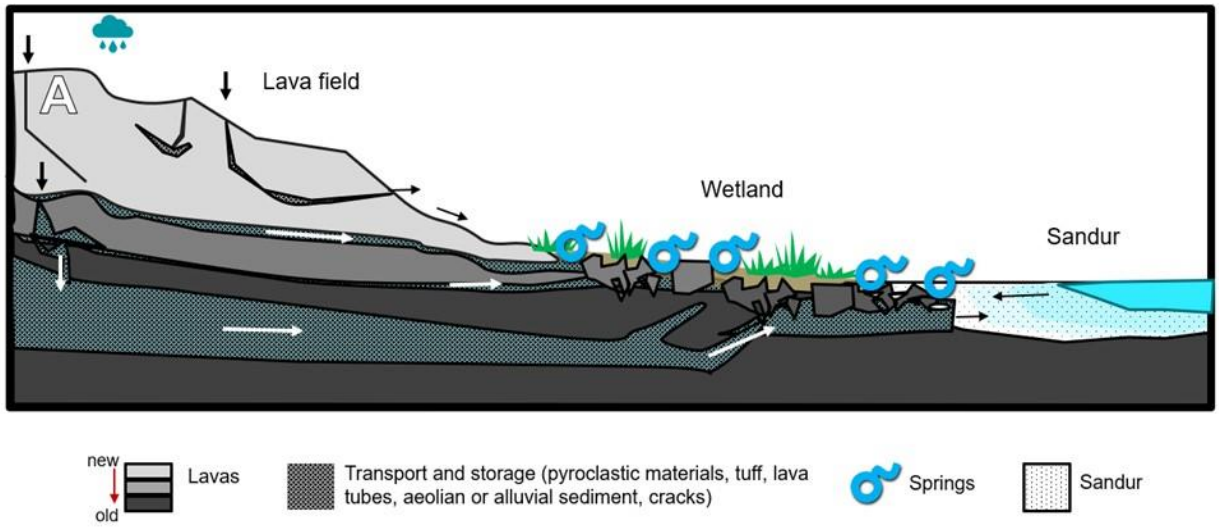

Figure 6.2 A conceptual diagram showing the proposed mechanism of spring discharge at the study site in Southeast Iceland. A. At the study site, water comes to the surface by gravity, as water flowing through high permeability routes such as cracks in rocks, or pyroclastic material, tuff, aeolian or alluvial sediments are deposited between successive lava flows. Water may be forced to the surface from lower elevations when the high permeability route reaches a low permeability barrier such as compacted ash (not pictured) or older, more compact lava layers at deeper levels.

6.3 Spring Contirbutions to the Landscape

The springs at the study site deliver cold (4.0–5.0°C), slightly acidic (pH 6.1–6.7), fresh (0.02 ppt) groundwater to the surface. The six springs, whose discharge was quantified in this study ranged from high discharge springs (over 50 L/s), to low discharge springs (0–25 L/s). The water temperatures reported were typical of cold water springs in Iceland, between 2.5 and 11.5°C (Guðmundsdóttir et al., 2019). As previously mentioned, the pH is more acidic here than other groundwater springs in Iceland.

The springs appeared to create a stable environment, as water chemistry and levels showed little variation. Most of the differences in temperature variation between springs could be explained by the logger's exposure to direct sunlight. For example, the large wetland/lava field spring L1 had the highest daily temperature range. The high discharge at this spring kept the area around the logger free of debris and algae. The logger was shallowly installed (0.1 m) and was likely influenced by incoming solar

radiation. Loggers that were covered by algae (W2, L2), installed perpendicular to the water surface (S1, W1), or covered by an overhang (L3), all had low to no diel variation in water temperatures.

Water temperature was monitored before and after a seepage spring in an Oxbow river at the study site. The light intensity data and field observations indicated that sediments were carried with the issuing spring waters, serving to cover the downstream logger and vegetation. The water from the spring mixed with upstream waters from the lava field river, and this had an overall moderating effect on water temperature, with lower diurnal temperature variations and dampened response to precipitation events. However, the presence of a stable environment and sediment substrate may allow bacteria communities to establish more easily (Guðmundsdóttir et al., 2019).

Due to the overall stable environment created by the springs, different ecological communities may exist. Here, the species upstream of the springs may vary from those downstream. In the wetland, long, green algae strands formed near the low-discharge springs, and iron oxidizing microbial mats formed in some areas along the spring-fed rivers and ponds (Figure 6.3 B). Iron-oxidizing microbial mats have been documented growing in calm, groundwater-fed streams in Iceland with a mean annual temperature below 5°C (Cockell et al., 2011). The spring type has a significant impact on the invertebrate communities that they support (Govoni, 2011). Spring-fed streams are likely important for the maintenance of the wetland, an important habitat for a variety of breeding birds, several of which were observed at the study site in July 2018 and May 2019 (Figure 6.3).

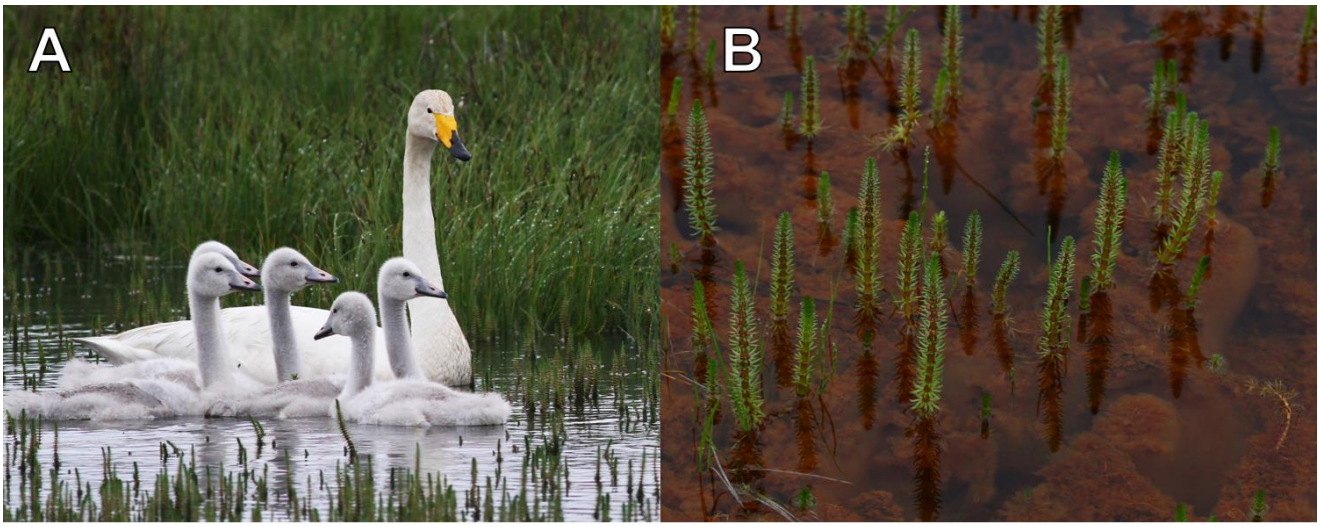

Figure 6.3 A. The spring-fed wetlands provide important habitat for birds such as Whooper swans (*Cygnus cygnus*). Slavonian (horned) Grebe (*Podiceps auritus*), red-throated divers (*Glavia stellata*) and at least one other species of waterfowl were observed breeding at the spring-fed wetlands of the study site in July 2018 and May 2019. B. The groundwater at Hvoll may be rich in iron, as iron-oxides arising from iron-oxidizing microbes were founded around stalks of aquatic vegetation growing in spring-fed streams.

6.4 Seasonal and Episodic Changes in Spring Discharge

The seasonal and episodic changes in stream hydrology are important to understand, in order to predict future trends with changes in climate. For the glacial fed river, Djúpá, 64% of the variation in baseflow was shown to be explained by the variation in daily average air temperature. Djúpá was the best predictor of Brunná River discharge. As a glacial-fed river, Brunná will be impacted by changes in glacial melt. The stable isotope analysis in this study indicated that glacial meltwaters become a greater proportion of the Brunná River's discharge in the autumn. In the winter and spring, before glacial melt has begun, a larger proportion of glacial-fed river flow comes from groundwater (Macdonald et al., 2016). This explains the similarity in water chemistry and stable isotope signatures between the Brunná River and the study springs measured in May 2019.

Changes in discharge for each spring over 10 days in May 2019 could not be clearly linked to rainfall or air temperatures. Long term data on spring discharge would be required to determine the stability of flow regimes on a seasonal and annual scale. Unfortunately, logger errors prevented a full year

of water level data from being collected, so winter levels cannot be commented on. The data from the present study show that water levels in the wetland and sandur are maintained through the spring, summer and fall, with little variation in water level or temperature. This continued supply of fresh groundwater is important for the maintenance of the wetland in this area. Occasional spikes in water level measured at S1 corresponded with spikes in discharge at glacial-fed river Djúpá. This, along with the increasing diurnal amplitude as summer progressed suggested that the sandur springs may receive inflows and floodwaters from the Brunná River.

Iceland has a Low Arctic climate with increases in precipitation and summer temperatures expected for Southern Iceland. Models of glacial mass loss due to climate change predict that southern Vatnajökull will lose 1200 km^3 by the year 2205 (Aoalgeirsdóttir et al., 2006). Glacial-fed rivers such as the Brunná River will have an initial increase in discharge as summer melt increases with increasing air temperatures. At a certain point, the discharge will begin to drop, as the glaciers become depleted (Milner et al., 2009). In contrast, spring-fed systems, fed largely by rainfall runoff, may become/remain an important source of water to hydrological systems in Iceland.

The wetlands at Hvoll were shown to maintain a positive water balance, with inputs coming from precipitation, subsurface flows, and spring-fed streams in 2017 (Scheffel & Young, submitted). During 24 hours of a jökulhlaup, and heavy precipitation events in 2015 and 2016, sizeable spikes in water level at the Brunná River were observed (Scheffel & Young, submitted). However, an increase in water levels in the wetland was not observed until the following day and subsurface flows from the sandur to the wetland likely played a role in this delayed response. In the present study, the time of water level peaks at S1 occurred up to 2 days following days with more than 1 mm of precipitation. It is suggested that it could take up to 2 days for rainwater to travel through groundwater flow paths and reach the spring, or for the increased pressure in the aquifer to propagate to the spring. Subsurface flow from the sandur to the wetland is supported by hydraulic gradient data, where water levels were higher in the sandur than the wetland (Scheffel & Young, submitted). During this study, increases in sandur spring water levels did not

correspond with increases in water temperature at any of the medium sized Sandur springs, except for on 23 September 2019 when all Sandur springs except S1 had a spike in water temperature following a period of heavy precipitation and possibly elevated flood waters from the Brunná River. Inflows from the warmer Brunná River occurred closer to the surface, and with limited mixing. This prevented temperature changes from being detected at the depth (0.5 m) of the S1 logger. If air temperatures increase in the future, shifts in glacial melt may influence the frequency of flood water moving down the Brunná River.

Climate models show varied predictions of future precipitation patterns across Iceland but generally agree that precipitation will increase with increases in air temperature (Aðalgeirsdóttir et al., 2006; Gosseling, 2017). This may result in higher water levels in the wetland triggered by spring-fed streams whose aquifers are recharged by rainfall. An increased probability of days with over 10 mm of precipitation is also expected (Gosseling, 2017). During some days in this study with more than 10 mm of precipitation, we observed significant increases in water level at the Wetland spring W1 and the Sandur spring S1. In the future, a higher number of days receiving heavy rainfall will result in an overall higher baseflow and spikes in wetland water levels.

Groundwater-fed springs will become important sources of water as air temperatures increase because they are less vulnerable to the forces of evaporation. Runoff Spring was (partially) recharged by runoff and had decreases in water levels corresponding with increases in air temperature. Elevated air temperatures likely resulted in an increase in evaporation and dampened overflow runoff feeding the Runoff spring. The Wetland spring W2 did not show a similar trend. Water from a groundwater spring like W2 would not be influenced by evaporation, as water is stored and transported beneath the ground surface.

Jökulhlaups at the Brunná River could not be identified with certainty over the course of the study. However, previous jökulhlaup events on 4 October 2015 and 20 June 2016 have resulted in increases in turbidity and water levels in the Brunná River where it passes by the study site (Scheffel & Young, submitted). Streams fed by the groundwater springs did not appear to have a similar increase in

turbidity (Figure 6.4). Increases in discharge may be expected for springs following precipitation-related jökulhlaup events, as more than 10 mm of precipitation caused significant increases in water level for the S1 and W1 springs gauged at the study site. Constant temperature data from S1 suggests that these increases would be from aquifer recharge rather than subsurface flow of water from the Brunná River to the spring pores.

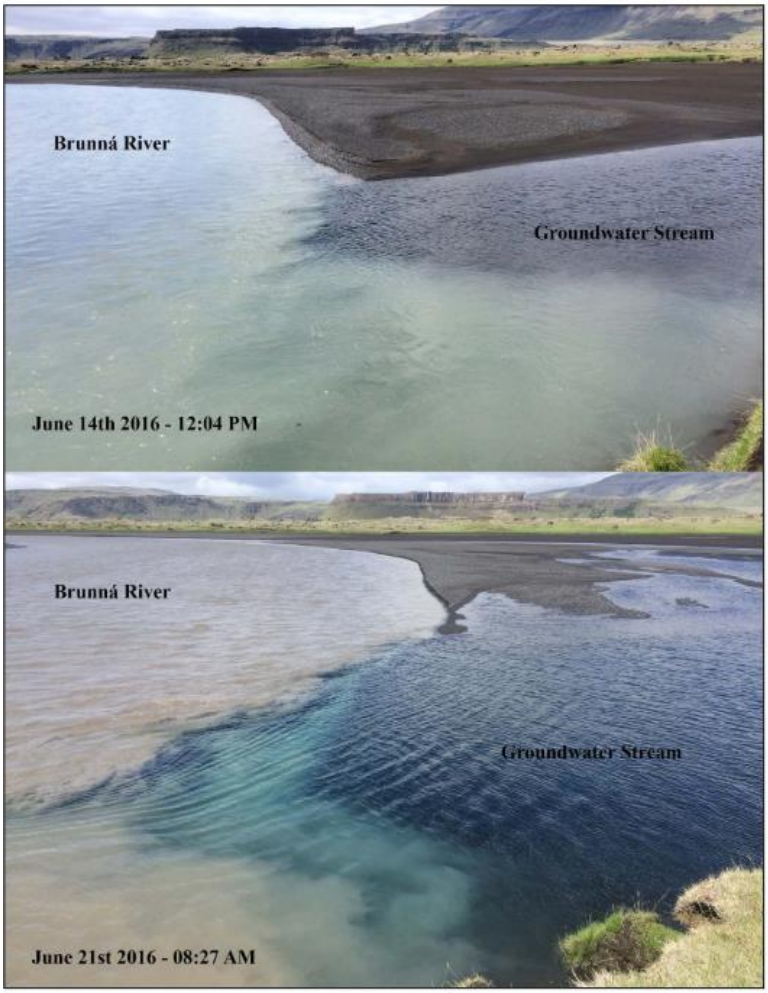

Figure 6.4 Two images taken at the study site, where the streams fed by the sandur springs (labelled as "Groundwater Stream", joins with the Brunná River. The top photograph shows this location before a sandstorm event that occurred on 19 June 2016. The sandstorm was followed by a rise in water levels in the Brunná River, and an increase in turbidity, as can be seen in the bottom photograph. The water from the groundwater stream has much lower turbidity than the Brunná River. The difference in turbidity is markedly visible following the sandstorm event. Photographs from Scheffel & Young (submittted).

6.5 Study Limitations

Caution should be used when interpreting the results from the temperature loggers in this study, as water temperature measured by the loggers was correlated with incoming light intensity. While the logger would have absorbed some of the incoming light over time, the water, having just emerged from the ground would not have had time to be warmed by the incoming rays. Therefore, daily averages and ranges of water temperature were likely overestimated. Additionally, loggers covered by sediment or thick layers of algae likely had dampened diel temperature variations. As temperature loggers were installed at different depths, the ability for light to reach and warm the deep loggers was diminished. Also, loggers installed quite deep within the spring pore may not be able to sense temperature changes from inflows occurring above the depth of the sensor. For more accurate representations of spring water temperature, temperature loggers should be installed at the orifice of the spring. Due to the loss of winter data from the W2 and runoff spring water level loggers, a full year of data was not obtained for the springs at the study site. No conclusions about winter or annual water levels or temperatures could be made.

The water chemistry values should be investigated again in the future. The low pH for rainwater (median 6.2) measured at the study site is an indication that the probe may have required recalibration. The probes were not recalibrated following the flight to Iceland.

SECTION SEVEN: CONCLUSIONS AND FUTURE WORK

The aim of this study was to determine the role of springs in a sandur-lava field-wetland complex in Southeast Iceland. Field observations of springs morphology and, stability of spring discharge and water quality provided insight into the types of springs found at the study site. Water chemistry and stable isotope data, along with local precipitation and air temperature data were used to draw conclusions about spring contributions to the sandur-lava field-wetland complex, on a seasonal and episodic basis. The main findings of this study can be summarized as follows:

1. Springs at the study site are fed by groundwater, where the aquifer is deep enough that rainfall results in pressure propagation and discharge of older groundwater rather than rapid discharge of newly infiltrated rainwater.
2. Groundwater-fed springs ranged in temperature from 4.0–5.0°C from May to September 2019. In May 2019, the waters were fresh, with a pH (6.1–6.7) that is more acidic than other cold springs reported in Iceland. This may indicate that springs at this location are fed by waters with a shorter residence time than springs in other regions of Iceland. Interactions with frequent tephra (ash/dust) deposits may have also contributed to lower pH values.
3. The discharge from groundwater springs was relatively stable. A significant effect of days with more than 10 mm of precipitation was observed for water levels and temperatures of many of the springs. Between May and September 2019, the water temperature was stable for springs where loggers were not exposed to sunlight. Spring water chemistry did not change following rainfall. Spikes in water level at the sandur springs were observed following rainfall and potential flooding of the Brunná River. However, corresponding temperature data had no or a small increase in temperature.

To obtain a full picture of the mode of transport of rainwater to the springs, future studies should aim to quantify the permeability of the lava fields in Southeast Iceland. Drilling tests may be required to investigate the depths and permeability of layers of the lava field, and the presence of sediment layers. Long-term studies of groundwater springs in Southeast Iceland will be required to better understand the seasonal and annual variability in spring hydrology, and their vulnerability to climate change.

SECTION EIGHT: REFERENCES

Aðalgeirsdóttir, G., Jóhannesson, T., Björnsson, H., Pálsson, F., & Sigurosson, O. (2006). Response of Hofsjökull and southern Vatnajökull, Iceland, to climate change. *Journal of Geophysical Research: Earth Surface*, *111*(3), 1–15. https://doi.org/10.1029/2005JF000388

Anderson, M. P. (2005). Heat as a ground water tracer. *Ground Water*, *43*(6), 951–968. https://doi.org/10.1111/j.1745-6584.2005.00052.x

Aoalgeirsdóttir, G., Jóhannesson, T., Björnsson, H., Pálsson, F., & Sigurosson, O. (2006). Response of Hofsjökull and southern Vatnajökull, Iceland, to climate change. *Journal of Geophysical Research: Earth Surface*, *111*(3), 1–15. https://doi.org/10.1029/2005JF000388

Arnalds, O., Dagsson-Waldhauserova, P., & Olafsson, H. (2016). The Icelandic volcanic aeolian environment: Processes and impacts-A review. *Aeolian Research*, *20*, 176–195. https://doi.org/10.1016/j.aeolia.2016.01.004

Arnold, J. G., & Allen, P. M. (1999). Automated methods for estimating baseflow and ground water recharge from streamflow records. *Journal of the American Water Resources Association*, *35*(2), 411–424. https://doi.org/10.1111/j.1752-1688.1999.tb03599.x

Arnold, J. G., Allen, P. M., Muttiah, R., & Bernhardt, G. (1995). Automated base flow separation and recession analysis techniques. *Ground Water*, *33*(6), 1010–1018. https://doi.org/10.1111/j.1745-6584.1995.tb00046.x

Björnsson, H. (2002). Subglacial lakes and jökulhlaups in Iceland. *Global and Planetary Change*, *35*, 255–271. www.elsevier.com/locate/gloplacha

Björnsson, H., & Pálsson, F. (2008). Icelandic glaciers. *Jökull*, *58*(58), 365–386.

Björnsson, H., Pálsson, F., Gudmundsson, S., Magnússon, E., Adalgeirsdóttir, G., Jóhannesson, T., Berthier, E., Sigurdsson, O., & Thorsteinsson, T. (2013). Contribution of Icelandic ice caps to sea level rise: Trends and variability since the Little Ice Age. *Geophysical Research Letters*, *40*, 1546–1550. https://doi.org/10.1002/grl.50278

Brown, L. E., & Hannah, D. M. (2008). Spatial heterogeneuty and water temperature across an apline river basin. *Hydrological Processes*, *22*, 954–967. https://doi.org/10.1002/hyp

Brown, L. E., Hannah, D. M., Milner, A. M., Soulsby, C., Hodson, A. J., & Brewer, M. J. (2006). Water source dynamics in a glacierized alpine river basin (Taillon-Gabiétous, French Pyrénées). *Water Resources Research*, *42*(8). https://doi.org/10.1029/2005WR004268

Bryan, K. (1919). Classification of Springs. *The Journal of Geology*, *27*(7), 522–561.

Burns, E R, Williams, C. F., Ingebritsen, S. E., Voss, C. I., Spane, F. A., & Deangelo, J. (2015). Understanding heat and groundwater flow through continental flood basalt provinces: insights gained from alternative models of permeability/depth relationships for the Columbia Plateau, USA. *Geofluids*, *15*, 120–138. https://doi.org/10.1111/gfl.12095

Burns, Erick R., Zhu, Y., Zhan, H., Manga, M., Williams, C. F., Ingebritsen, S. E., & Dunham, J. B. (2017). Thermal effect of climate change on groundwater-fed ecosystems. *Water Resources Research*, *53*(4), 3341–3351. https://doi.org/10.1002/2016WR020007

Byers, H. R., Moses, H., & Harney, P. J. (1949). Measurement of rain temperature. *Journal of Meteorlogy*, *6*, 51–11. https://doi.org/10.16309/j.cnki.issn.1007-1776.2003.03.004

Carey, S. K., & Woo, M.-K. K. (2001). Slope runoff processes and flow generation in a subarctic, subalpine catchment. *Journal of Hydrology*, *253*(1–4), 110–129. https://doi.org/10.1016/S0022-1694(01)00478-4

Cockell, C. S., Kelly, L. C., Summers, S., & Marteinsson, V. Þ. (2011). Following the kinetics: iron-oxidizing microbial mats in cold Icelalndic volcanic habitats and their rock-associated carbonaceous signature. *Astrobiology*, *11*(7), 679–694.

Craig, H. (1961). Isotopic variations in meteoric waters. *Science, New Series*, *133*(3465), 1702–1703. https://doi.org/10.1126/science.133.3465.1702

Crochet, P., Jóhannesson, T., Jónsson, T., Sigurðsson, O., Björnsson, H., Pálsson, F., & Barstad, I. (2007). Estimating the spatial distribution of precipitation in Iceland using a linear model of orographic precipitation. *Journal of Hydrometeorology*, *8*, 1285–1306. https://doi.org/10.1175/2007JHM795.1

Crossman, J., Bradley, C., Boomer, I., & Milner, A. (2011). Water flow dynamics of groundwater-fed streams and their ecological significance in a glacierized catchment. *Arctic, Antarctic, and Alpine Research*, *43*(3), 364–379. https://doi.org/10.1657/1938-4246-43.3.364

de Woul, M., Hock, R., Braun, M., Thorsteinsson, T., Jóhannesson, T., & Halldórsdóttir, S. (2006). Firn layer impact on glacial runoff: A case study at Hofsjökull, Iceland. *Hydrological Processes*, *20*(10), 2171–2185. https://doi.org/10.1002/hyp.6201

Dochartaigh, B. Ó. B., Macdonald, A. M., Black, A. R., Everest, J., Wilson, P., George Darling, W., Jones, L., & Raines, M. (2019). Groundwater-glacier meltwater interaction in proglacial aquifers. *Hydrology and Earth System Sciences*, *23*(11), 4527–4539. https://doi.org/10.5194/hess-23-4527-2019

Duller, R. A., Warner, N. H., Mcgonigle, C., Angelis, S. De, Russell, A. J., & Mountney, N. P. (2014). Landscape reaction, response, and recovery following the catastrophic 1918 Katla jökulhlaup, southern Iceland. *Geophycial Research Letters*, *41*, 4214–4221. https://doi.org/10.1002/2014GL060090.Received

Einarsson, M. Á. (1984). Climate of Iceland. In *van Loon* (pp. 673–697). Elsevier. https://doi.org/10.1002/qj.49702511010

Fattorini, S., Borges, P. A. V., Fiasca, B., & Galassi, D. M. P. (2016). Trapped in the web of water: Groundwater-fed springs are island-like ecosystems for the meiofauna. *Ecology and Evolution*, *6*(23), 8389–8401. https://doi.org/10.1002/ece3.2535

Faybishenko, B., Bodvarsson, G. S., & Salve, R. (2003). On the physics of unstable infiltration, seepage, and gravity drainage in partially saturated tuffs. *Journal of Contaminant Hydrology*, *62–63*, 63–87. https://doi.org/10.1016/S0169-7722(02)00175-4

Finger, D., Hugentobler, A., Huss, M., Voinesco, A., Wernli, H., Fischer, D., Weber, E., Jeannin, P. Y., Kauzlaric, M., Wirz, A., Vennemann, T., Hüsler, F., Schädler, B., Weingartner, R., Husler, F., Schadler, B., & Weingartner, R. (2013). Identification of glacial meltwater runoff in a karstic environment and its implication for present and future water availability. *Hydrological Earth System Scie*, *12*(8), 3261–3277. https://doi.org/10.1029/2004JF000200

Flowers, G. E., Björnsson, H., Pálsson, F., Bjo, H., Rnsson, «, Pa¨lsson, F., & Pa¨lsson, P. (2003). New insights into the subglacial and periglacial hydrology of Vatnajokull, Iceland, from a distributed physical model. *Journal of Glaciology*, *49*(165), 257–270. https://doi.org/10.3189/172756503781830827

Freeze, R. A. (1974). Streamflow generation. *Reviews of Geophysics*, *12*(4), 627. https://doi.org/10.1029/RG012i004p00627

Gíslason, G. M., Ólafsson, J. S., & Adalsteinsson, H. (1998). Animal communities in Icelandic rivers in relation to catchment characteristics and water chemistry: preliminary results. *Nordic Hydrology*, *29*(2), 129–148. https://doi.org/10.2166/nh.1998.0008

Gíslason, S. D. S. R., Arnórsson, S., & Ármannsson, H. (1996). Chemical weathering of basalt in Southwest Iceland: Effects of runoff, age of rocks and vegetative/glacial cover. *American Journal of Science*, *296*(8), 837–907. https://doi.org/10.2475/ajs.296.8.837

Gislason, S. R., Hassenkam, T., Nedel, S., Bovet, N., Eiriksdottir, E. S., Alfredsson, H. A., Hem, C. P., Balogh, Z. I., Dideriksen, K., Oskarsson, N., Sigfusson, B., Larsen, G., & Stipp, S. L. S. (2011). Characterization of Eyjafjallajökull volcanic ash particles and a protocol for rapid risk assessment. *Proceedings of the National Academy of Sciences of the United States of America*, *108*(18), 7307–7312. https://doi.org/10.1073/pnas.1015053108

Gosseling, M. (2017). *CORDEX climate trends for Iceland in the 21st century*. https://en.vedur.is/media/vedurstofan-utgafa-2017/VI_2017_009.pdf

Gudjonsson, S. (1990). Classification of Icelandic watersheds and rivers to explain life history strategies of Atlantic salmon. *Ph.D. Thesis. Oregon State University, Corvallis, Oregon.*, 136. http://ir.library.oregonstate.edu/xmlui/bitstream/handle/1957/37370/GudjonssonSigurdur1991.pdf?sequence=1

Guðmundsdóttir, R., Kreiling, A. K., Kristjánsson, B. K., Marteinsson, V. Þ., & Pálsson, S. (2019). Bacterial diversity in Icelandic cold spring sources and in relation to the groundwater amphipod Crangonyx islandicus. *PLoS ONE*, *14*(10), 1–21. https://doi.org/10.1371/journal.pone.0222527

Guilbaud, M. N., Self, S., Thordarson, T., & Blake, S. (2005). Morphology, surface structures, and emplacement of lavas produced by Laki, A.D. 1783-1784. *Special Paper of the Geological Society of America*, *396*(January 2015), 81–102. https://doi.org/10.1130/0-8137-2396-5.81

Hamdan, I., Wiegand, B., Toll, M., & Sauter, M. (2016). Spring response to precipitation events using δ18O and δ2H in the Tanour catchment, NW Jordan. *Isotopes in Environmental and Health Studies*, *52*(6), 682–693. https://doi.org/10.1080/10256016.2016.1159205

Herschy, R. (1993). The velocity-area method. *Flow Measurement and Instrumentation*, *4*(1), 7–10. https://doi.org/10.1016/0955-5986(93)90004-3

Hurrell, J. W., Kushnir, Y., Ottersen, G., & Visbeck, M. (2003). An overview of the North Atlantic oscillation. In *The North Atlantic Oscillation: Climatic Significance and Environmental Impact*. https://doi.org/10.1029/GM134

IMO. (2019). *The Icelandic Meteorological Office. Delivery of data from the Hydrological database, no. 2019-11-04/01*.

IMO. (2018, September 13). *The August glacial outburst - one of the larger jökulhlaups to have affected Skaftá in recent decades*. (Icelandic Meteorological Office). https://en.vedur.is/about-imo/news/the-august-glacial-outburst-one-of-the-larger-jokulhlaups-to-have-affected-skafta-in-recent-decades

Jansson, R., Laudon, H., Johansson, E., & Augspurger, C. (2007). The importance of groundwater discharge for plant species number in riparian zones. *Ecology*, *88*(1), 131–139. https://doi.org/10.1890/0012-9658(2007)88[131:TIOGDF]2.0.CO;2

Jefferson, A., Grant, G., & Rose, T. (2006). Influence of volcanic history on groundwater patterns on the

west slope of the Oregon High Cascades. *Water Resources Research*, *42*(12), 1–15. https://doi.org/10.1029/2005WR004812

Jóhannesson, T., Aðalgeirsdóttir, G., Björnsson, H., Crochet, P., Elíasson, E. B., Guðmundsson, S., Jónsdóttir, J. F., Ólafsson, H., Pálsson, F., Rögnvaldsson, Ó., Sigurðsson, O., Snorrason, Á., Sveinsson, Ó. G. B., & Thorsteinsson, T. (2007). Effect of climate change on hydrology and hydro-resources in Iceland. In *Earth*.

Jónsdóttir, J. F. (2008). A runoff map based on numerically simulated precipitation and a projection of future runoff in Iceland. In *Hydrological Sciences Journal* (Vol. 53, Issue 1).

Jónsdóttir, & Uvo, C. B. (2009). Long-term variability in precipitation and streamflow in Iceland and relations to atmospheric circulation. *International Journal of Climatology*, *29*, 1369–1380. https://doi.org/10.1002/joc.1781

Jónsson, S. (1999). Temperature time series from Icelandic coastal stations. *Rit Fiskideildar*, *16*(November), 59–68.

Kaandorp, V. P., Doornenbal, P. J., Kooi, H., Peter Broers, H., & de Louw, P. G. B. (2019). Temperature buffering by groundwater in ecologically valuable lowland streams under current and future climate conditions. *Journal of Hydrology X*, *3*, 100031. https://doi.org/10.1016/j.hydroa.2019.100031

Ketilsson, J., Óskarsdóttir, S. M., Claesson, A., & Collett, N. J. (2017). the Kerauga Cave and Lækjarbotnaveita in South Iceland – Groundwater Safety and Hydrogeology. *Journal of Water Security*, *3*(1), 1–11. https://doi.org/10.15544/jws.2017.001

Kiernan, K., Wood, C., & Middleton, G. (2003). Aquifer structure and contamination risk in lava flows: Insights from Iceland and Australia. *Environmental Geology*, *43*(7), 852–865. https://doi.org/10.1007/s00254-002-0707-8

Kjartansson, G. (1945). Íslenskar vatnsfallategundir (classification of Icelandic streams). *Náttúrufræðingurinn*, *15*, 113–126

Kløve, B., Kvitsand, H. M. L., Pitkänen, T., Gunnarsdottir, M. J., Gaut, S., Gardarsson, S. M., Rossi, P. M., & Miettinen, I. (2017). Overview of groundwater sources and water-supply systems, and associated microbial pollution, in Finland, Norway and Iceland. *Hydrogeology Journal*, *25*(4), 1033–1044. https://doi.org/10.1007/s10040-017-1552-x

Kresic, N., & Stevanovic, Z. (2010). *Groundwater Hydrology of Springs*. Elsevier Inc.

Kristmannsdóttir, H., & Ármannsson, H. (2004). Groundwater in the Lake Myvatn area, northern Iceland: Chemistry, origin and interaction. *Aquatic Ecology*, *38*(2), 115–128.https://doi.org/10.1023/B:AECO.0000032067.47495.71

Levy, A, Robinson, Z., Krause, S., & Waller, R. (2012). *The impact of glacial fluctuations on the shallow proglacial groundwater systems of two SE Icelandic glaciers* . *14*(2011), 2012

Levy, Amir, Robinson, Z., Krause, S., Waller, R., & Weatherill, J. (2015). Long-term variability of proglacial groundwater-fed hydrological systems in an area of glacier retreat, Skeiarársandur, Iceland. *Earth Surface Processes and Landforms*, *40*(7), 981–994. https://doi.org/10.1002/esp.3696

Liljedahl, A. K., Gädeke, A., O'Neel, S., Gatesman, T. A., & Douglas, T. A. (2017). Glacierized headwater streams as aquifer recharge corridors, subarctic Alaska. *Geophysical Research Letters*, *44*(13), 6876–6885. https://doi.org/10.1002/2017GL073834

Macdonald, A. M., Black, A. R., Ó Dochartaigh, B. E., Everest, J., Darling, W. G., Flett, V., & Peach, D.

W. (2016). Using stable isotopes and continuous meltwater river monitoring to investigate the hydrology of a rapidly retreating Icelandic outlet glacier. *Annals of Glaciology*, *57*(72), 151–158. https://doi.org/10.1017/aog.2016.22

Manga, M. (1999). On the timescales characterizing groundwater discharge at springs. *Journal of Hydrology*, *219*(1–2), 56–69. https://doi.org/10.1016/S0022-1694(99)00044-X

Manga, M. (1998). Advective heat transport by low-temperature discharge in the Oregon Cascades. *Geology*, *26*(9), 799–802. https://doi.org/10.1130/0091-7613(1998)026<0799:AHTBLT>2.3.CO;2

Mazor, E. (1990). *Applied chemical and isotopic groundwater hydrology*. (Third Edit). Open University Press.

McDonnell, J. J., McGuire, K., Aggarwal, P., Beven, K. J., Biondi, D., Destouni, G., Dunn, S., James, A., Kirchner, J., Kraft, P., Lyon, S., Maloszewski, P., Newman, B., Pfister, L., Rinaldo, A., Rodhe, A., Sayama, T., Seibert, J., Solomon, K., … Wrede, S. (2010). How old is streamwater? Open questions in catchment transit time conceptualization, modelling and analysis. *Hydrological Processes*, *24*, 1745–1754. https://doi.org/10.1002/hyp.7796

McDonnell, J. J., Sivapalan, M., Vaché, K., Dunn, S., Grant, G., Haggerty, R., Hinz, C., Hooper, R., Kirchner, J., Roderick, M. L., Selker, J., & Weiler, M. (2007). Moving beyond heterogeneity and process complexity: A new vision for watershed hydrology. *Water Resources Research*, *43*(7), 1–6. https://doi.org/10.1029/2006WR005467

McNamara, J. P., Kane, D. L., & Hinzman, L. D. (1998). An analysis of streamflow hydrology in the Kuparuk River Basin, Arctic Alaska: A nested watershed approach. *Journal of Hydrology*, *206*(1–2), 39–57. https://doi.org/10.1016/S0022-1694(98)00083-3

Meinzer, O. E. (1923). *The occurrence of ground water in the United States with a discussion of principles*. U.S. Geological Survey Water-Supply Paper 489.

Mercier, D. (2008). Paraglacial and paraperiglacial landsystems: concepts, temporal scales and spatial distribution. *Géomorphologie : Relief, Processus, Environnement*, *14*(4), 223–233. https://doi.org/10.4000/geomorphologie.7396

Milner, A. M., Brown, L. E., & Hannah, D. M. (2009). Hydroecological response of river systems to shrinking glaciers. *Hydrological Processes*, *23*, 62–77. https://doi.org/10.1002/hyp

Morgenstern, U., Daughney, C. J., Leonard, G., Gordon, D., Donath, F. M., & Reeves, R. (2015). Using groundwater age and hydrochemistry to understand sources and dynamics of nutrient contamination through the catchment into Lake Rotorua, New Zealand. *Hydrology and Earth System Sciences*, *19*(2), 803–822. https://doi.org/10.5194/hess-19-803-2015

Muanza, P. K. (2016). Geothermal Mapping in Middalur Field , Hengill Area ,. *Proceedings, 6th African Rift Geothermal Conference Addis Ababa, Ethiopia, 2nd-4th November 2016.*, *November*

Nathan, R. J., & McMahon, T. A. (1990). Evaluation of automated techniques for base flow and recession analyses. *Water Resources Research*, *26*(7), 1465–1473

Old, G. H., Lawler, D. M., & Snorrason, Á. (2005). Discharge and suspended sediment dynamics during two jökulhlaups in the Skaftá river, Iceland. *Earth Surface Processes and Landforms*, *30*(11), 1441–1460. https://doi.org/10.1002/esp.1216

Óskarsson, G. J., Gudmundsdottir, A., & Sigurdsson, T. (2009). Variation in spatial distribution and migration of Icelandic summer-spawning herring. *ICES Journal of Marine Science*, *66*(8), 1762–1767. https://doi.org/10.1093/icesjms/fsp116

R Core Team. (2019). *R: A language and environment for statistical computing*. R Foundation for Statistical Computing. https://www.r-project.org/

Robinson, Z. P., Fairchild, I. J., & Russell, A. J. (2009). Hydrogeological implications of glacial landscape evolution at Skeiðarársandur, SE Iceland. *Geomorphology*, *97*, 218–236. https://doi.org/10.1016/j.geomorph.2007.02.044

Rosenberry, D. O., & Hayashi, M. (2013). Assessing and measuring wetland hydrology. In A. JT & D. DA (Eds.), *Wetland techniques* (pp. 87–225). Springer.

RStudio Team. (2020). *R Studio: Integrated Development for R*. PBC. http://www.rstudio.com/

Scheffel, H.-A., & Young, K. L. (n.d.). The hydrology of a Sandur- Wetland in a volcanic environment, Southeast Iceland. *Submittd to Wetlands, July 2020*

Serno, S., Flude, S., Johnson, G., Mayer, B., Karolytė, R., Haszeldine, R. S., & Gilfillan, S. M. V. (2017). Oxygen isotopes as a tool to quantify reservoir-scale CO2 pore-space saturation. *International Journal of Greenhouse Gas Control*, *63*(June), 370–385. https://doi.org/10.1016/j.ijggc.2017.06.009

Sigurdsson, F., & Einarsson, K. (1988). Groundwater resources of Iceland -availability and demand. *Jokull*, *38*, 35–54.

Sigurdsson, O., & Stefansson, V. (2002). Porosity structure of icelandic basalt. *Proceedings of the Estonian Academy of Sciences*, *51*, 33–46.

Sklash, M. G., & Farvolden, R. N. (1979). The role of groundwater in storm runoff. *Journal of Hydrology*, *43*, 45–65.

Springer, A. E., & Stevens, L. E. (2009). Spheres of discharge of springs. *Hydrogeology Journal*, *17*(1), 83–93. https://doi.org/10.1007/s10040-008-0341-y

Stallman, R. W. (1965). Steady one-dimensional fluid flow in a semi-infinite porous medium with sinusoidal surface temperature. *Journal of Geophysical Research*, *70*(12), 2821–2827. https://doi.org/10.1029/jz070i012p02821

Sun, Y., Solomon, S., Dai, A., & Portmann, R. W. (2006). How often does it rain? *Journal of Climate*, *19*(6), 916–934. https://doi.org/10.1175/JCLI3672.1

Sveinbjörnsdóttir, Á. E., Heinemeier, J., & Arnórsson, S. (1995). Origin of 14C in Icelandic groundwater. *Proceedings of the 15th International 14C Conference*, *37*(2), 551–565

Tallaksen, L. (1995). A review of baseflow recession analysis. *Journal of Hydrology*, *165*(1–4), 349–370. https://doi.org/10.1016/0022-1694(95)92779-d

Thien, B. M. J., Kosakowski, G., & Kulik, D. A. (2015). Differential alteration of basaltic lava flows and hyaloclastites in Icelandic hydrothermal systems. *Geothermal Energy*, *3*(1). https://doi.org/10.1186/s40517-015-0031-7

Thordarson, T., & Larsen, G. (2007). Volcanism in Iceland in historical time: Volcano types, eruption styles and eruptive history. *Journal of Geodynamics*, *43*, 118–152. https://doi.org/10.1016/j.jog.2006.09.005

Todd, D. K. (1980). *Groundwater hydrology*. Wiley.

Tristram, D. A., Krause, S., Levy, A., Robinson, Z. P., Waller, R. I., & Weatherill, J. J. (2015). Identifying spatial and temporal dynamics of proglacial groundwater-surface-water exchange using combined temperature-tracing methods. *Freshwater Science*, *34*(1), 99–110.

https://doi.org/10.1086/679757

Veðurstofa Íslands, J. H., & Náttúrustofa Suðaustur. (2020). *Yfirlit um íslenska jökla í árslok 2019. Fréttabréf. Overview of Icelandic glaciers at the end of 2019*. https://www.vedur.is/media/loftslag/frettabref-joklar-newsletter-glaciers-iceland-2019-1-.pdf

Vincent, L. A., & Mekis, É. (2006). Changes in daily and extreme temperature and precipitation indices for Canada over the twentieth century. *Atmosphere - Ocean*, *44*(2), 177–193. https://doi.org/10.3137/ao.440205

Wang, H., Gao, J. E., Zhang, M.-J., Li, X.-H., Zhang, S.-L., & Jia, L.-Z. (2015). Effects of rainfall intensity on groundwater recharge based on simulated rainfall experiments and a groundwater flow model. *Catena*, *127*, 80–91. https://doi.org/10.1016/j.catena.2014.12.014

Wittmann, M., Zwaaftink, C. D. G., Schmidt, L. S., Gumundsson, S., Pálsson, F., Arnalds, O., Björnsson, H., Thorsteinsson, T., & Stohl, A. (2017). Impact of dust deposition on the albedo of Vatnajökull ice cap, Iceland. *Cryosphere*, *11*(2), 741–754. https://doi.org/10.5194/tc-11-741-2017

Woo, M. K. (2012). Chapter 3: Groundwater. In *Permafrost Hydrology* (pp. 73–118). Springer. https://doi.org/10.1007/978-3-642-23462-0

SECTION NINE: APPENDIX

9.1 Appendix A: Specifications for Hanna H1981934 Multimeter Probe

Parameters	Range	Resolution	Accuracy
Temperature	-5 to 55°C	0.01°C	± 0.15°C
pH and mV	0.00 to 14.00 pH; -600.00 to 600.00 mV	0.01 pH 0.1 mV	± 0.02 pH ± 0.5 mV
Electric conductivity	0 to 200 mS/cm	auto-ranging: 1 µS/cm from 0 to 9999 µS/cm; 0.01 mS/cm from 10.00 to 99.99 mS/cm; 0.1 mS/cm from 100.0 to 400.0 mS/cm; auto-ranging (fixed mS/cm): 0.001 mS/cm from 0.000 to 9.999 mS/cm; 0.01 from 100.0 to 400.0 mS/cm ; manual: 1 µS/cm; 0.001 mS/cm; 0.01	± 1% of reading or ± 1 µS/cm, whichever is greater
Salinity	0.00 to 70.00 PSU	0.01 PSU	± 2% of reading or ± 0.01 PSU, whichever is greater